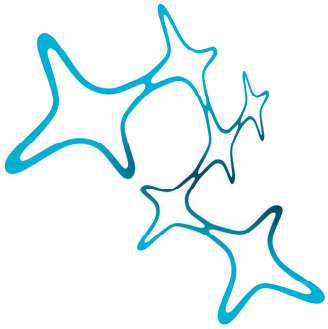

Graduate School of
Systemic Neurosciences
LMU Munich

ACTIVITY-DEPENDENT CHANGES IN A NEURONAL CIRCUIT IMPORTANT FOR SOUND LOCALIZATION

Dissertation

of the

Graduate School of Systemic Neurosciences

of

Ludwig-Maximilians-University Munich

Submitted by

Benjamin Haßfurth

Munich, May 2010

Supervisor:	PD Dr. Ursula Koch
Second expert appraiser:	Prof. Benedikt Grothe
Day of the oral defense:	31.08.2010

Für meine Familie

TABLE OF CONTENTS

SUMMARY

Aside from recognizing and distinguishing sound patterns, the ability to localize sounds in the horizontal plane is an essential component of the mammalian auditory system. It facilitates approaching potential mating partners and allows avoiding predators.

The superior olivary complex (SOC) within the auditory brainstem is the first site of binaural interaction and its major projections and inputs are well investigated. The adult input pattern, however, is not set from the beginning but changes over the period of development. Mammals including humans experience different stages and conditions of hearing during auditory development. The human brain for instance has to perform a transition after birth from the perception of sound waves transmitted in amniotic fluid to the perception of airborne sounds. Furthermore, small mammals like rodents, which are common model organisms for auditory research, perceive airborne sounds for the first time some days after birth, when their ear canals open. The basic neuronal projections and the intrinsic properties of neurons, such as the expression of specific ion channels, are already established and adjusted in the SOC during the perinatal period of partial deafness. An additional refinement of inputs and further adaptations of intrinsic characteristics occur with the onset of hearing in response to the new acoustic environment. It is likely that with ongoing maturation well-established inputs within the sound localization network need these adaptations to balance anatomical changes such as an increasing head size. In addition, short-term adjustments of synaptic inputs in the adult auditory system are equally necessary for a faithful representation of auditory space. A recent study suggests that these short-term adaptations are partially represented at the auditory brainstem level.

The question of how intrinsic properties change during auditory development, to what extent auditory experience is involved in these changes and the functional implications of these changes on the sound localization circuitry is only partially answered. I used the hyperpolarization-activated and cyclic nucleotide-gated cation channels (HCN channels), which are a key determinant of the intrinsic properties of auditory brainstem neurons, as a target to study the influence of auditory experience on the intrinsic properties of neurons in the auditory brainstem.

Another important question still under discussion is how neurons in the auditory brainstem might fine-tune their firing behavior to cope optimally with an altered acoustic environment. Recent data suggest that auditory processing is also affected by modulatory mechanisms at the brainstem level, which for instance change the input strength and thus alter the spike output of these neurons. One possible candidate is the metabotropic $GABA_B$ receptor ($GABA_BR$) which has been shown to be abundant in the adult auditory brainstem, although GABAergic projections are scarce in the mature auditory brainstem.

These questions were investigated by performing whole-cell patch-clamp recordings of SOC neurons from Mongolian gerbils at different developmental stages in the acute brain slice preparation. Specific currents and receptors were isolated using pharmacological means. Immmunohistochemical results additionally supported physiological findings.

In the first study, I investigated the developmental regulation of HCN channels in the SOC and their underlying depolarizing current I_h, which has been shown to regulate the excitability of neurons and to enhance the temporally precise analysis of binaural acoustic cues. I characterized the developmental changes of I_h in neurons of the lateral superior olive (LSO) and the medial nucleus of the trapezoid body (MNTB), which in the adult animals show different HCN subunit composition. I showed that right after hearing onset there was a strong increase of I_h in the LSO and just a minor increase in the MNTB. In addition, the open probability of HCN channels was shifted towards more positive voltages in both nuclei and the activation time constants accelerated during the first days of auditory experience. These results implicate that I_h is actively regulated by sensory input activity. I tested this hypothesis by inducing auditory deprivation which was achieved by surgically removing the cochlea in gerbils before hearing onset. The effect was opposite in neurons of the MNTB and the LSO. Whereas in LSO neurons auditory deprivation resulted in increased I_h amplitude, MNTB neurons displayed a moderate decrease in I_h. These results suggest that auditory experience differentially changes the amount of HCN channels dependent on the subunit composition or possibly alters intracellular cAMP levels, thereby shifting the voltage dependence of I_h. This regulatory mechanism might thus maintain adequate excitability levels within the SOC.

A second study was carried out to investigate the role of $GABA_B$Rs in the medial superior olive (MSO). Upon activation, these metabotropic receptors are known to decrease the release probability of neurotransmitters at the presynapse thereby altering excitatory and inhibitory currents at the postsynaptic site. Neurons in the MSO analyze interaural time differences (ITDs) by comparing the relative timing of the excitatory inputs from the two ears using a coincidence mechanism. In addition, these neurons receive a precisely timed inhibitory input from each ear which shifts ITDs in the physiological relevant range. Since the major inhibitory input changes its transmitter type from mixed GABA/glycinergic to only glycinergic after hearing onset it was now interesting to examine the mediated effects of $GABA_B$Rs, which have been shown to be abundant in the prehearing and adult MSO of gerbils. Furthermore, revealing the precise expression pattern of $GABA_B$Rs and their influence on excitatory and inhibitory currents in the MSO during auditory development should provide further evidence of their functional relevance. Performing pharmacological experiments I could now demonstrate that the activation of $GABA_B$Rs before hearing onset decreases the current of excitatory inputs stronger than that of inhibitory inputs whereas a switch is performed after hearing onset and inhibitory currents are stronger decreased

compared to excitatory currents. In a similar way, also the expression pattern of $GABA_BRs$ changes before and after hearing onset as revealed by immunohistochemistry. Since the main inhibitory inputs to the adult MSO are purely glycinergic, it was commonly assumed that $GABA_BRs$ occupy only a minor role in the mature auditory brainstem. Contradictory to this, it was possible to activate presynaptic $GABA_BRs$ by synaptic stimulation even in adult animals and to observe a profound decrease of inhibitory current in MSO neurons. These results suggest GABAergic projections of yet unknown origin targeting the MSO. It is therefore quite likely that $GABA_BRs$ modulate and possibly improve the localization of low frequency sounds even in adult mammals.

Summarized, the outcome of this thesis contributes to a better understanding of the developmental adaptation in the auditory system and demonstrates that the orderly specification of intrinsic properties within the SOC is dependent on auditory experience. Moreover, I show that even in mature animals the synaptic strength of MSO inputs can be modulated by synaptic GABA release. This should emphasize the importance of modulatory mechanisms and could be the basis for future studies concerning the field of sound localization.

ZUSAMMENFASSUNG

Neben dem Erkennen und Unterscheiden von Klangbildern ist die Fähigkeit Schall in der horizontalen Ebene zu lokalisieren ein wesentlicher Bestandteil des auditorischen Systems von Säugetieren. So wird hierdurch die Annäherung an mögliche Paarungspartner erleichtert oder das Meiden von Raubtieren ermöglicht.

Der obere Olivenkomplex (SOC) im auditorischen Hirnstamm ist die erste Stelle binauraler Wechselwirkung und die Hauptprojektionen innerhalb dieses Komplexes sind hinreichend untersucht. Das adulte Muster der Eingänge ist jedoch zu Anfang noch nicht endgültig festgelegt und ändert sich im weiteren Verlauf der Entwicklung. Säugetiere, einschließlich des Menschen, durchlaufen während ihrer auditorischen Entwicklung verschiedene Stadien und Zustände des Hörens. So muss das menschliche Gehirn beispielsweise nach der Geburt eine Umstellung der Schallwahrnehmung in Fruchtwasser hin zur Schallwahrnehmung in Luft vollziehen. Des Weiteren nehmen kleine Säuger, wie Nagetiere (übliche Modellorganismen für die Hörforschung), luftübertragenen Schall erst einige Tage nach der Geburt mit dem Öffnen ihrer Gehörgänge wahr. Die grundlegenden Projektionen und intrinsischen neuronalen Eigenschaften, wie z.B. die Expression spezifischer Ionenkanäle, sind bereits während des geburtsnahen Zeitraums teilweiser Taubheit im SOC ausgebildet und angepasst. Mit Hörbeginn finden eine zusätzliche Verfeinerung des Eingangsmusters und weitere Anpassungen intrinsischer Eigenschaften als Antwort auf eine neue akustische Umgebung statt. Es ist durchaus möglich, dass vorhandene Eingänge innerhalb des Schaltkreises zur Schalllokalisierung diese Angleichungen mit fortschreitender Reifung benötigen, um anatomische Veränderungen wie einen zunehmenden Kopfumfang auszugleichen. Darüber hinaus sind kurzfristige Anpassungen synaptischer Eingänge des adulten auditorischen Systems gleichermaßen notwendig, um eine zuverlässige Darstellung des auditorischen Raumes wiederzugeben. In einer kürzlich veröffentlichten Studie wurde vorgeschlagen, dass diese kurzfristigen Anpassungen teilweise auf Ebene des auditorischen Hirnstammes wieder zu finden ist.

Die Fragen, wie sich intrinsische Eigenschaften während der auditorischen Entwicklung verändern, in welchem Ausmaß auditorische Erfahrung daran beteiligt ist und die Frage nach der funktionellen Bedeutung dieser Änderungen für den Schaltkreis zur Schalllokalisierung sind nur teilweise beantwortet.

Ich verwendete die Hyperpolarisations-aktivierten Zyklonukleotid-gesteuerten Kationenkanäle (HCN Kanäle), die ein bestimmender Faktor der intrinsischen Eigenschaften auditorischer Hirnstamm-Neurone sind, als Ansatzpunkt, um den Einfluss auditorischer Erfahrung auf ebendiese Eigenschaften von Neuronen des auditorischen Hirnstammes zu untersuchen.

Eine weitere und immer noch diskutierte Frage ist, wie Neurone des auditorischen Hirnstammes ihr Antwortverhalten feinabstimmen könnten, um eine veränderte akustische Umgebung optimal zu verarbeiten. Neueste Daten lassen vermuten, dass die Verarbeitung auditorischer Signale auch durch modulatorische Mechanismen auf Ebene des Hirnstammes beeinflusst wird. Diese Mechanismen können beispielsweise die Stärke der Eingänge und somit das Ausgangssignal auditorischer Neurone verändern. Ein möglicher Kandidat hierfür ist der metabotrope $GABA_B$ Rezeptor ($GABA_BRs$), der, wie bereits gezeigt wurde, reichhaltig im adulten auditorischen Hirnstamm exprimiert wird, obwohl GABAerge Projektionen im reifen auditorischen Hirnstamm kaum zu finden sind.

Diese Fragestellungen wurden an akuten Hirnschnittpräparationen mit Hilfe von Ganzzellableitung von SOC Neuronen Mongolischer Wüstenrennmäuse in unterschiedlichen Entwicklungsstadien durchgeführt. Spezifische Ströme und Rezeptoren wurden pharmakologisch isoliert und immunhistochemische Ergebnisse unterstützten die so erhaltenen physiologischen Erkenntnisse.

In der ersten Studie untersuchte ich die entwicklungsabhängige Regulierung von HCN Kanälen im SOC und den durch diese Kanäle vermittelten Strom I_h, der erwiesenermaßen die neuronale Erregbarkeit bestimmt und die zeitlich präzise Analyse von binauralen akustischen Signalen verstärkt. Ich charakterisierte entwicklungsbedingte Veränderungen von I_h in Neuronen der lateralen oberen Olive (LSO) und des medialen Nukleus des Trapezkörpers (MNTB), die in adulten Tieren eine unterschiedliche Zusammensetzung von HCN Untereinheiten aufweisen. Ich konnte zeigen, dass es direkt nach Hörbeginn einen starken Anstieg von I_h in der LSO und nur einen geringen Anstieg im MNTB gibt. Zusätzlich wurde die Öffnungswahrscheinlichkeit der HCN Kanäle beider Nuklei in Richtung positiverer Spannung verschoben und die Zeitkonstanten der Aktivierung beschleunigten sich während der ersten Tage der Hörerfahrung. Diese Ergebnisse implizieren, dass I_h durch sensorische Aktivität reguliert wird. Diese Hypothese testete ich durch das Herbeiführen auditorischer Deprivation, erzielt durch operative Entfernung der Cochlea in Wüstenrennmäusen vor Hörbeginn. Der zu beobachtende Effekt war gegensätzlich in Neuronen der LSO und des MNTB. Während auditorische Deprivation in LSO Neuronen in einem Anstieg der I_h Amplitude resultierte, zeigten Neurone des MNTB eine geringfügige Verringerung von I_h. Diese Ergebnisse lassen darauf schließen, dass auditorische Erfahrung entweder die Menge an HCN Kanälen unterschiedlich verändert, abhängig von der Zusammenstellung der Untereinheiten, oder möglicherweise intrazelluläre cAMP Konzentrationen abändert und dadurch die Spannungsabhängigkeit von I_h verschiebt. Dieser regulatorische Mechanismus könnte deshalb dafür verantwortlich sein, einen entsprechenden Grad an Erregbarkeit innerhalb des SOC beizubehalten.

Eine zweite Studie wurde durchgeführt, um die Rolle der $GABA_BRs$ in der medialen oberen Olive (MSO) zu untersuchen. Nach ihrer Aktivierung verringern diese metabotropen Rezeptoren die Wahrscheinlichkeit der Ausschüttung von Neurotransmittern an der Präsynapse und verändern dadurch erregende und hemmende Ströme an der Postsynapse. Neurone in der MSO analysieren interaurale Zeitunterschiede (ITDs) indem sie das zeitliche Aufeinandertreffen von erregenden Eingängen beider Ohren durch einen Koinzidenzmechanismus vergleichen. Ferner erhalten diese Neurone zeitlich präzise abgestimmte hemmende Eingänge von beiden Ohren, mit denen ITDs in den physiologisch relevanten Bereich verschoben werden. Da sich in den größten hemmenden Eingängen der vorherrschende Transmitter-Typ von gemischt GABA/glyzinerg zu rein glyzinerg nach Hörbeginn ändert, war es nun interessant, die durch $GABA_BRs$ vermittelten Effekte zu untersuchen. Reichhaltige $GABA_BR$ Expression wurde bereits sowohl in der MSO von Tieren vor Hörbeginn, wie auch in adulten Wüstenrennmäusen gezeigt. Allerdings sollte nun das genaue Expressionsmuster der $GABA_BRs$ und ihr Einfluss auf erregende und hemmende Ströme in der sich entwickelnden MSO untersucht werden, um dadurch weitere Hinweise auf ihre funktionelle Bedeutung zu erhalten. Durch pharmakologische Experimente konnte ich nun zeigen, dass die Aktivierung von $GABA_BRs$ vor Hörbeginn Ströme erregender Eingänge stärker verringert, als die hemmender Eingänge. Dieses Bild änderte sich nach Hörbeginn komplett, denn nun wurde die Amplitude hemmender Ströme stärker reduziert als die erregender Ströme. In ähnlicher Weise änderte sich auch das Expressionsmuster von $GABA_BRs$ vor und nach Hörbeginn, wie durch immunohistochemische Experimente deutlich gemacht werden konnte. Da die hemmenden Haupteingänge der adulten MSO rein glyzinerg sind, wurde allgemein angenommen, dass $GABA_BRs$ nur eine kleine Rolle im reifen auditorischen Hirnstamm einnehmen. Im Widerspruch dazu war es sogar in adulten Tieren möglich präsynaptische $GABA_BRs$ durch synaptische Stimulation zu aktivieren und eine signifikante Verringerung hemmender Ströme in MSO Neuronen zu beobachten. Diese Ergebnisse deuten auf bis jetzt noch unbekannte GABAerge Projektionen in der MSO hin. Es ist deshalb durchaus möglich, dass $GABA_BRs$ die Lokalisierung tief-frequenten Schalls selbst in adulten Tieren modulieren und möglicherweise sogar noch verbessern.

Zusammengefasst trägt das Ergebnis dieser Arbeit zu einem besseren Verständnis entwicklungsbedingter Anpassungen im auditorischen System bei und demonstriert, dass die geregelte Spezifizierung intrinsischer Eingänge innerhalb des SOC abhängig ist von auditorischer Erfahrung. Des Weiteren zeige ich, dass die synaptische Stärke von MSO Eingängen sogar in adulten Tieren durch synaptische GABA Ausschüttung moduliert werden kann. Dies soll die Bedeutung modulatorischer Mechanismen unterstreichen und könnte die Grundlage für weitere Studien auf dem Gebiet der Schalllokalisierung darstellen.

1 INTRODUCTION

1.1 The evolution of hearing

At the end of the Devonian period, 360 million years ago, hearing did not exist. Various aquatic vertebrate groups inhabited the ancient sea (Panthalassa) and the sheer perception of sound sources was a rather challenging issue for animals. In order to understand this difficulty, we first have to define sound and sound localization.

The American Heritage Dictionary of the English Language (Fourth Edition, Houghton Mifflin Company 2006) describes sound as a traveling wave which is an oscillation of pressure transmitted through a solid, liquid or gas, composed of frequencies within the range of hearing and of a level sufficiently strong to be heard. When we speak of sound localization, we mean the process of detecting the origin of a pressure variation in a given medium. It is now obvious that fish encounter problems detecting sounds in their natural environment. Since their tissue has approximately the same density as the surrounding medium, their bodies follow the amplitude of traveling sound waves in water. One could therefore regard fish as being acoustically transparent. Exploiting the environment for as much information as possible is beneficial and can be essential for any organism. Hence, these animals evolved an organ called the lateral line, which detects disturbances in streaming water produced, for example, by prey or enemies in the near-field (Denton and Gray 1982; Webb 1989). At that time, vertebrates already possessed an inner ear, which presumably was able to perceive outer vibrations to some degree by comparing hair cell deflections with the body position in space. It seems that the control of equilibrioception and proprioception was initially the major task of the inner ear. In this way it most likely supported the adequate function of the lateral line (Van Bergeijk 1966). The vertebrate conquest of land during the late Devonian period (Clack 1997) was the initial trigger to develop hearing as one of the most sophisticated biological sensory systems, which is capable of localizing both prey and predator, as well as selecting relevant mating partners.

When tetrapods first populated the landmass (Pangaea) about 360 million years ago, they conquered a completely new niche, with few predators and abundant space as well as food resources. However, compared with the open sea, the environment on land changed more rapidly forcing terrestrial animals to adapt constantly to altering conditions. In fact, during the next 100 million years, new species evolved which developed new types of locomotion, reproduced on land and were completely independent from an aquatic habitat. Since at that point the landmass became progressively more populated with species now competing for food and space, further adaptations were necessary. The refinement of sensory systems in

several animal species enabled them to improve their hunting or flight behavior and therefore opened the possibility to occupy entirely new niches. One milestone in this process was the evolution of tympanic middle ears which first occurred in parareptiles approximately 260 million years ago (Fig.1.1) and was documented recently in fossil finds (Muller and Tsuji 2007). The novel and outstanding feature of such ears was the tympanum (eardrum) which for the first time allowed perception of high frequency airborne sounds. The tympanum itself is a thin membrane that separates the external ear from the middle ear. It transmits sound from the air to an auditory ossicle, the columella, inside the middle ear from where the sound energy is then transferred to the inner ear for further auditory processing. The columella derived from the hyomandibula, a jaw suspension bone, which was adapted to relay deflections of the tympanic membrane to the inner ear.

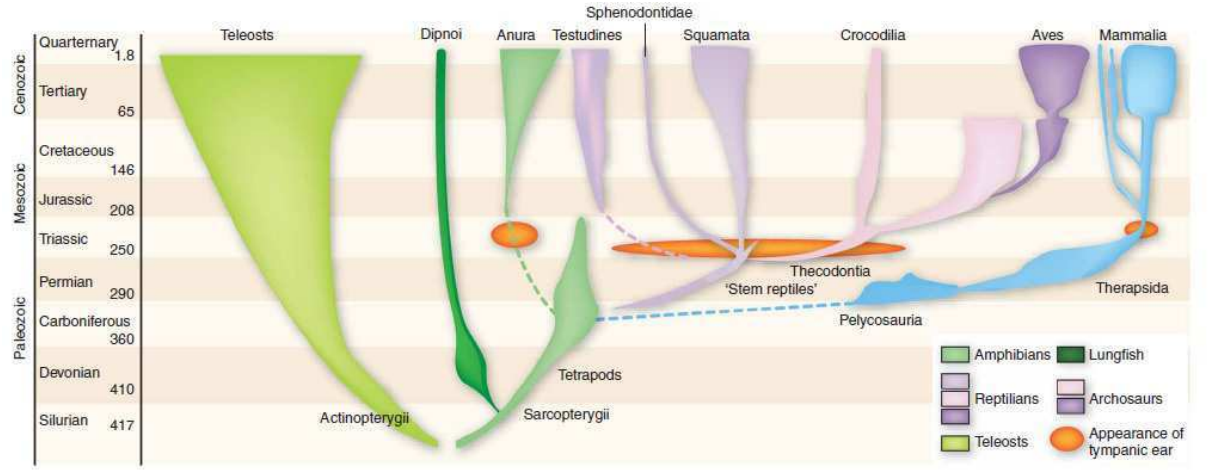

Figure 1.1: The evolution of vertebrate ears. During the transition from water to land, tympanic middle ears capable of receiving airborne sound evolved separately among the ancestors of modern frogs, turtles, lizards, archosaurs (birds and crocodilians) and mammals. Extinct forms (e.g. parareptiles), non-anuran amphibians, coelacanths and many actinopterygian groups are omitted from this diagram (Schnupp and Carr 2009 modified from Walker and Liem 1994).

Even though it was speculated that fish without a functional middle ear theoretically have also been able to perceive low frequency airborne sounds by actively decoding sound-induced vibrations of the skull in their inner ear, the necessity for a system able to acquire precise auditory input is obvious (Christensen-Dalsgaard and Carr 2008). Soon it turned out to be beneficial to discern a difference of self-emitted sounds, sounds from possible mating partners or noise that is produced by potential predators. Moreover, an elaborate auditory system including a functional middle ear was so beneficial that tympanic ears have emerged independently at least five more times, i.e. in the lines leading to amphibians, turtles, lepidosaurs, archosaurs and mammals (Allin 1975; Christensen-Dalsgaard and Carr 2008; Clack 1997; Grothe 2000; Manley 2000). The latter evolved three middle ear ossicles (malleus, incus and stapes) from the hyomandibula and adjacent jawbones. This trait makes mammals phylogenetically unique compared to all other vertebrate classes.

Anatomical adaptations for the perception of airborne sounds were already quite valuable, though one has to ask the following questions: Is the capability to be aware of the existence of a nearby sound source all there is to hearing? Would it not be much more advantageous to avoid or approach this sound source by detecting its precise origin? One aspect that has not been mentioned so far is the bilateralism of the auditory system. Indeed, without two spatially separated acoustic detectors, pinpointing sound sources would be by far less accurate, relying solely on monaural spectral cues provided by the directional filtering of sounds by outer ears (Schnupp and Carr 2009; Wightman and Kistler 1997). The bilateralism of the auditory system could be regarded as the crucial point for the evolution of directional hearing. Only this feature allowed for the computation of binaural spectral cues, making accurate sound localization possible.

1.2 Sound transmission in the ear

With the evolution of tympanic ears, mammalian vertebrates have acquired excellent sound localization mechanisms. In land-living animals such as the majority of mammals, airborne sounds represent the most important auditory signal. However, in order to be localized, a sound first of all has to be perceived. Thus, the mammalian auditory system holds many specialized features enabling animals to make optimal use of airborne sound signals.

Once airborne sound waves reach the peripheral mammalian ear (Fig.1.2) they impinge on the tympanic membrane, thereby transferring energy and causing vibration in the tympanum. However, as we have seen in chapter 1.1, the terrestrial auditory system evolved from an aquatic one which raises a serious issue. Since air, as the “carrier of sound” is a medium of low acoustic impedance and the inner ear as the “terminal of sound” is filled with a liquid lymph of high impedance, roughly 99.9% of the sound energy would be lost during the transmission of vibration between those two media. Thus, the middle ear accomplishes an impedance modification by a mechanical conversion of energy in the cavum tympani, a gas-filled cavity, to overcome this problem. Since the cavum tympani has the same impedance level as the extra-tympanic medium, it allows the sound-driven oscillation of the auditory ossicles via the tympanum without a great loss of energy. The sound-driven osscilations of the tympanic membrane in a medium of low impedance are picked up by the auditory ossicles. Using leverage effects they transfer the now mechanical energy onto a medium of high impedance, the inner ear’s endolymph. The stapes moves back and forth, transferring the vibration onto the oval window, one of two thin membranes separating the middle ear from the inner ear. As the endolymph is a liquid of high rigidity more strength is needed to

cause its vibration. This is, apart form the leverage effect, achieved by a difference in surface area between the small oval window and the large tympanic membrane. Based on the different surface area the relatively large amplitudes of tympanic vibration are minimized by the ossicles but simultaneously the strength of the ossicle deflection is higher (conservation of energy). This enforcement enables the deflection of the small oval window in the rigid and almost incompressible endolymph, thus creating pressure waves in the entire cochlea. The cochlea is a snail-shaped structure in the inner ear, which possesses specialized features to resolve and convert the frequency and intensity components within each sound signal for auditory perception (Kelly and Chen 2009). Yet, pressure wave transmission is only made possible by the second membrane, the round window. It moves out when the stapes pushes in and moves in when the stapes pulls out rendering movement of the rigid lymph possible.

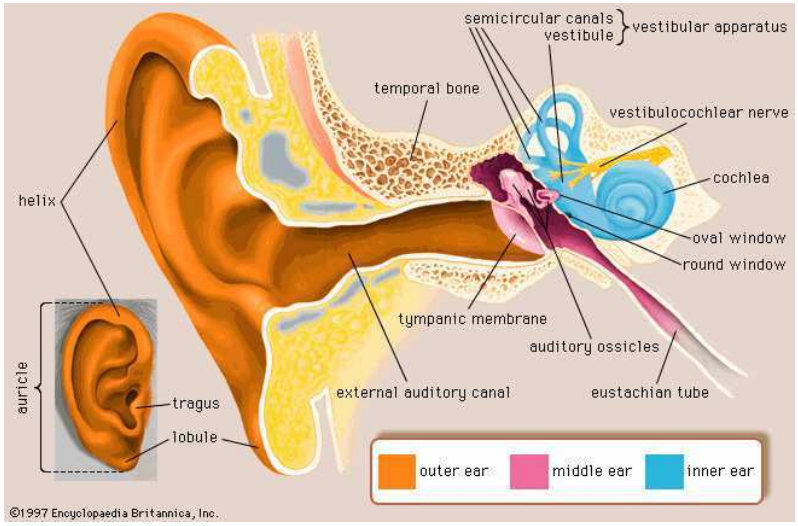

Figure 1.2: The mammalian ear. Sound travels through the ear canal at the outer ear and vibrates the tympanum in the middle ear. Vibrations are further transmitted, mediated by the ossicles in the gas-filled cavum tympani, to the cochlea in the inner ear. Another part of the inner ear is the vestibular system. Equilibrioception and proprioception are under the control of the vestibular apparatus. The Eustachian tube is important for maintaining an intact middle ear and connects the cavum tympani with the pharynx. With the additional pharyngeal gas volume, it can equalize pressure differences to prevent possible damage of the tympanum.

One of the characteristic features in the cochlea is the basilar membrane; a membrane that is situated inside the coiled cochlea, perpendicular to the oval window. The basilar membrane is stiff at its origin with decreasing rigidity towards the apical end. Its width decreases continuously and, accordingly, the stiffness of the membrane decreases about hundred-fold over its length. The whole membrane is embedded in fluid and as it vibrates, waves travel from the stiff part of the basilar membrane towards the softer part (Von Bekesy 1956a; b), increasing in amplitude with traveled distance. At this stage, the basilar membrane serves as a first frequency filter. As the pressure wave travels it does not move the basilar membrane much, but a burst of energy is suddenly released when the wave reaches the membrane's resonant point causing its maximal deflection. The resonant point itself is defined by the membrane's width and stiffness in comparison to the pressure wave's frequency, thus different sound frequencies differentially excite discrete regions in the cochlea, corresponding to a range from 0.1 to 20 kHz, e.g. in humans (Fettiplace and Hackney 2006). Low frequencies induce maximum deflection of the basilar membrane at the

basal part of the cochlea, high frequencies at the most apical part. At the resonant point, the released energy is strong enough to move cellular transducers in the organ of Corti, namely the stereocilia of the inner and outer hair cells (IHCs and OHCs, respectively), to generate electrical receptor potentials that represent the acoustic stimulus. Besides their opposing position in the cochlea, also functional differences have been described for both hair cell classes. Information about the acoustic environment (speech, music or other sounds in the outside world) is relayed primarily by the electrical signals of IHCs, whereas the main task of OHCs is to boost the stimulus by electromechanical feedback (Dallos 1992; Fettiplace and Hackney 2006). Again, we come across a feature in the auditory system of mammals which makes this animal class unique in evolutionary history, namely the separation of function between IHCs and OHCs (Fettiplace and Hackney 2006). Finally, the rising IHC and OHC receptor potentials produce chemically mediated excitation in the peripheral terminals of cochlear afferent neurons. The graded potentials of the hair cells are now converted into a binary “all-or-none” code based on the generation of action potentials (APs). Via the auditory nerve (VIIIth cranial nerve), these APs travel to the cochlear nucleus, the first station of the auditory central nervous system.

1.3 Auditory processing

The “standard model” of auditory processing begins with the frequency decomposition performed in the inner ear, which has already been outlined in chapter 1.2. The resulting spectro-temporal activity patterns of hair cells and auditory nerve fibers form a new representation of the incoming auditory stimulus (Nelken 2008). Henceforth, the mechanical and physical nature of the perceived sound wave is completely abolished and is translated into an ionic current code that is used through the ascending auditory pathway to convey information of enormous complexity (Fig.1.3).

At the level of the cochlear nucleus (CN) auditory nerve fibers split up to innervate three individual regions of the CN, the dorsal cochlear nucleus (DCN), the posteroventral cochlear nucleus (PVCN) and the anteroventral cochlear nucleus (AVCN) (Brawer et al. 1974). Each of these subdivisions has specific tasks. While neurons of the ventral cochlear nucleus aid in the localization of a sound stimulus on the horizontal axis, the DCN, probably via type IV neurons (Davis 2002), is involved in sound source localization in the vertical plane (May 2000). For this vertical localization, mammals use spectral cues, which are modifications in the spectra produced by the interactions of sound with the external ear (pinna) (Blauert 1996; Musicant et al. 1990; Oertel and Young 2004). The DCN integrates auditory with nonauditory

input and is thought to play a role in the orientation of the head toward sounds of interest and in the suppression of responses to self-generated sounds (May 2000; Shore 2005; Young et al. 1995; Zhao et al. 2009).
The PVCN projects to periolivary cell groups (Warr 1972; 1969) and strongly to contralateral upstream nuclei mainly involved in the transmission of monaural sound signaling. Nevertheless, studies showed that PVCN terminals also target nuclei important for binaural sound integration in the superior olivary complex (SOC) (Harrison and Irving 1964; Thompson and Thompson 1987).
Neurons of the AVCN primarily target auditory brainstem regions essential for binaural processing, and thus sound localization in the azimuthal plane (Cant and Casseday 1986; Smith et al. 1991; Smith et al. 1993). Therefore, the strongest projections of AVCN neurons terminate within the SOC and the medial nucleus of the trapezoid body (MNTB), transmitting a high-fidelity copy of the activity of the auditory nerve to these more central auditory brainstem nuclei (Brawer et al. 1974; Goldberg and Brownell 1973; Rose et al. 1974). Interestingly, a typical feature of a subset of neurons in the AVCN is their phase-locking response to auditory stimuli (Brugge et al. 1970; Smith et al. 1991) which is not observed in the DCN. In auditory physiology, phase-locking describes the phenomenon that auditory nerve fibers (and most auditory neurons involved in temporal coding) tend to fire an AP at a preferred phase of individual cycles of a pure tone (Galambos and Davis 1943; Kiang et al. 1965). This firing behavior encodes the temporal fine structure of auditory stimuli in a microsecond range with very high temporal precision (Koppl 1997).

Both the CN and the SOC directly innervate the nucleus of the lateral lemniscus (NLL), which comprises three spatially separated regions (dorsal, intermediate and ventral) (Adams 1979; Glendenning et al. 1981; Nordeen et al. 1983; Oliver 2000) and the inferior colliculus (IC) in the midbrain (Caird and Klinke 1987; Kuwada and Yin 1983; McAlpine et al. 1998; Nordeen et al. 1983; Zook and Casseday 1982). Basically, the NLL analyzes the temporal features of sound and forwards this information to the IC (Batra 2006; Benson and Cant 2008; Covey and Casseday 1991). However, since the NLL receives afferent inputs from the SOC and the CN, it was always regarded important for binaural signal processing (Brugge et al. 1970; Kelly et al. 1998; Kuwada et al. 2005; Markovitz and Pollak 1994; Siveke et al. 2006). Especially the dorsal part of the NLL (DNLL) is actively engaged in binaural processing and sound localization (Ito et al. 1996; Kelly et al. 1998). Another distinct role recently assigned to the DNLL is the so-called “precedence effect”, which describes a phenomenon that enables the auditory system to suppress echoes without eliminating their overall perception (Pecka et al. 2007; Pollak 1997). Essentially, echoes produced in a reverberant environment are perceived without being actually localized, thus the DNLL filters out information relevant for

sound localization without interfering with the perception of echoes. Key features for this task are reciprocal projections made between the ipsi- and contralateral DNLL.

The ventral part of the NLL (VNLL) is less well understood, but it has been suggested that it is important for the processing of monaural temporal features of sounds (Covey and Casseday 1991). Moreover, Ranjan Batra (2006) postulated recently that the VNLL converts the temporal code present at the level of the SOC in a rate code at the level of the IC (Joris et al. 2004; Langner and Schreiner 1988).

The function of the intermediate part of the NLL (INLL), on the other hand, is still not clear. Previous studies provide evidence that the INLL transmits ongoing information about the duration and intensity of a sound to the IC (Covey and Casseday 1991; Huffman et al. 1998a; b), however, more physiological studies need to be carried out in the INLL to disclose its major function.

All information gathered in the NLL, may it be monaural or binaural, is passed on to the IC which, unlike the NLL, is involved in refining information regarding the location of signals in the acoustic environment (Caspary et al. 2008; Pollak et al. 2003).

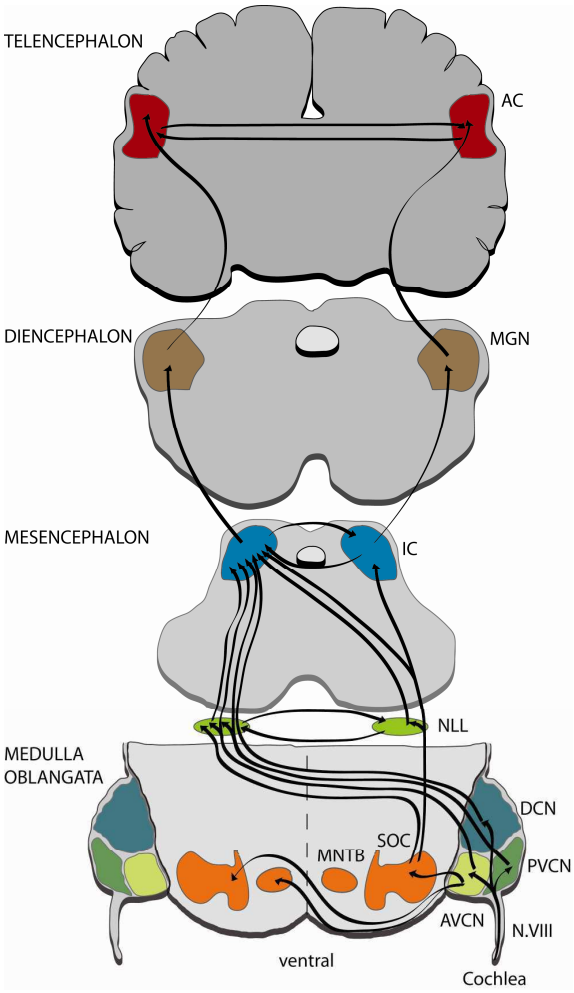

Figure 1.3: Stages of ascending auditory processing. Signals deriving from the cochlea are transmitted via the eighth nerve (N.VIII) to the cochlear nucleus (CN). Here, the auditory pathway splits up and targets all three subunits of the CN separately, namely the anteroventral cochlear nucleus (AVCN), the posteroventral cochlear nucleus (PVCN) and the dorsal cochlear nucleus (DCN). Each of these nuclei projects to the contralateral nucleus of the lateral lemniscus (NLL) as well as to the contralateral inferior colliculus (IC). Fibers of the AVCN additionally target the contralateral medial nucleus of the trapezoid body (MNTB), the superior olivary complex (SOC) and the superior periolivary nucleus (SPN, not shown). From the SOC ascending projections are made with the ipsilateral NLL and mainly with the dorsal region of the contralateral NLL, as well as with the ipsi- and contralateral IC. The NLL and the IC strongly interact with further connections to the respective nucleus opposite from the midline. From the level of the IC information is further transmitted to the medial geniculate nucleus (MGN), which in turn projects to the respective auditory cortex (AC). The ACs of both hemispheres are themselves linked by strong projections.
Depicted in this graph are the most relevant ascending auditory pathways although other important neural connections exist. Descending projections are entirely omitted. Also only one side of the auditory pathway is shown.

It is hardly appropriate to talk about the IC as one general nucleus. Similar to the NLL and CN, subdivisions can be distinguished (external and central part of the IC). Even though the IC comprises a diverse subset of cells (principal cells and interneurons) with different characteristic spiking patterns (Tan et al. 2007; Xie et al. 2008), its contribution to sound localization can be generalized as follows. Neurons in the IC more or less merge all incoming projections to generate an output function in which all principal localization cues are already evaluated. This includes computation of early monaural and binaural information deriving from the SOC as well as from the NLL. However, complex artificial stimuli like sinusoidally amplitude modulated sounds (SAMs) or sinusoidally frequency modulated sounds (SFMs) have been shown to be bandpass filtered at the level of the IC (Langner et al. 2002; Langner and Schreiner 1988; Rees and Moller 1983; 1987). Usually, SAMs and SFMs are well represented by precise phase-locked responses in the SOC and NLL at frequencies of up to 500Hz (Grothe 1994; Huffman et al. 1998b; Joris and Yin 1995), thereby reflected by a temporal code at the level of the auditory brainstem. The signal embedded in the initial temporal code is further processed as a rate code at the level of the IC. This conversion decreases the relevance of the precise spike-timing and puts more emphasis on the overall frequency of action potentials. Specialized neurons in the IC tuned to narrow ranges of modulation frequencies pick this signal up and further refine the auditory output pattern (Casseday et al. 1997; Rees and Moller 1983; Schuller 1979). The increasing selectivity for periodicity suggests active neuronal filter mechanisms even at the level of the IC (Koch and Grothe 1998). Since almost all acoustic signals mammals perceive in their natural environment are temporally modulated in their amplitude and frequency, this feature is highly significant. Neurons in the central nucleus of the IC also exhibit directional sensitivity when tested with spectrally rich sounds (Aitkin and Martin 1990; Aitkin and Martin 1987; Delgutte et al. 1999). Whereas some neurons require binaural stimulation to achieve spatial selectivity, other neurons exhibit this property under monaural conditions.

Apart from mutual interactions that are implemented via neuronal projections between the two ICs, the output signal of the inferior colliculus is conveyed further to the medial geniculate nucleus (MGN) within the thalamic area. From here, efferent fibers ascend to the auditory cortex (AC). These thalamocortical projections are known to constitute a network since they are topographically arranged and largely reciprocal (single MGN divisions project to several AC areas, which in turn each project to multiple MGN targets) (Winer and Lee 2007). Several MGN divisions also project to the amygdala, a group of nuclei forming part of the limbic system and therefore involved in memory and emotion processing, to establish auditory-limbic interactions (Shinonaga et al. 1994). These connections have been shown to be essential for autonomic learning based on auditory cues (LeDoux et al. 1986). Interestingly enough, all AC areas receive MGN input (Huang and Winer 2000), thus

thalamic connections may synchronize auditory, attentional, and limbic processes. The MGN and the AC form a feedback-loop as shown by Suga (1994), however, the role of this loop is still under discussion. While Suga and colleagues propose a contribution to cortical plasticity for the thalamo-cortico-thalamo loop (Gao and Suga 1998; 2000; Suga and Ma 2003) others entirely omit these projections in their model for plasticity in the AC (Weinberger 2004). In general the MGN is related doubtless to activity forwarded to the AC.

Compared to subcortical structures, rather complex auditory information processing takes place at the level of the auditory cortex (Nelken and Bar-Yosef 2008). The AC is the acoustically responsive part of the neocortex and represents the highest level of processing in the ascending auditory pathway. This is also true for the process of sound localization in the azimuthal plane. Jenkins and Merzenich (1984) demonstrated an essential role for the AC in the normal localization of brief sounds. Behavioral testing in cats following lesions indicated that the primary auditory cortex, a subfield of the AC, is probably sufficient for normal binaural azimuthal sound localization behavior. In some studies, AC damage interfered with auditory phenomena known as interaural level difference (ILD) and interaural time difference (ITD) perception (Bisiach et al. 1984; Yamada et al. 1996). ILDs as well as ITDs are encoded in the SOC, and represent the first stage of binaural sound localization processing. Hence, it is most interesting to shed more light on the mechanisms of ILD and ITD detection.

1.4 The superior olivary complex - interaural level differences and interaural time differences

The importance of sound localization for terrestrial mammals was mentioned in chapter 1.1. In the following, the specific features of sound localization in the horizontal plane (azimuth) regarding the superior olivary complex are going to be described.

Natural sounds consist of several frequencies though of course not all frequencies are necessarily embedded in every sound pattern. This perhaps trivial statement nevertheless has fundamental relevance for the localization of sound sources. The characteristic wavelengths of sounds vary with the sound's frequency. Consequently, to localize the broadest range of frequencies possible, two at least partially independent mechanisms have evolved in the auditory system. One system covers high frequencies, defined as sound waves with a wavelength smaller than the head diameter. The other system localizes sounds of low frequencies with wavelengths larger than the head diameter. The phenomenon of

utilizing two separate localization cues dependent on the frequency was first postulated by Lord Rayleigh under the name “The duplex theory of sound localization” (Rayleigh 1907). The first acoustic cue underlying the sound localization system for high frequency sounds are interaural level differences (ILDs) created by the head’s acoustic shadow. This means that the skull attenuates high frequency sound waves emitted left or right of the head, resulting in differences of sound pressure levels between the two ears (Fig.1.4). The lateral superior olive (LSO), a nucleus in the SOC, then further processes these level differences by comparing two inputs; an ipsilateral excitatory input from spherical bushy cells (SBCs) in the AVCN and a contralateral inhibitory input deriving from MNTB neurons (Brawer et al. 1974; Cant and Casseday 1986; Webster and Trune 1982; Wu and Oertel 1984) (Fig.1.4). The output rate of LSO is thus described by a subtractive function of the ipsilateral excitatory and contralateral inhibitory inputs. In other words, the more a sound is shadowed by the head the weaker the spike output of the contralateral LSO is going to be (Boudreau and Tsuchitani 1968; Tsuchitani and Boudreau 1969). Each LSO neuron holds its own minimal ILD at which complete suppression or complete saturation of the response rate occurs, but whether the integrated overall neuron population of both LSOs codes for the location of a sound source dependent on the spike-frequency (population-rate code) or whether a defined group of sharply tuned neurons within one LSO represents the spatial position of an object (labeled-line-code) remains an unanswered question to date. The resulting output signal is then passed on to the NLL and IC for further processing.

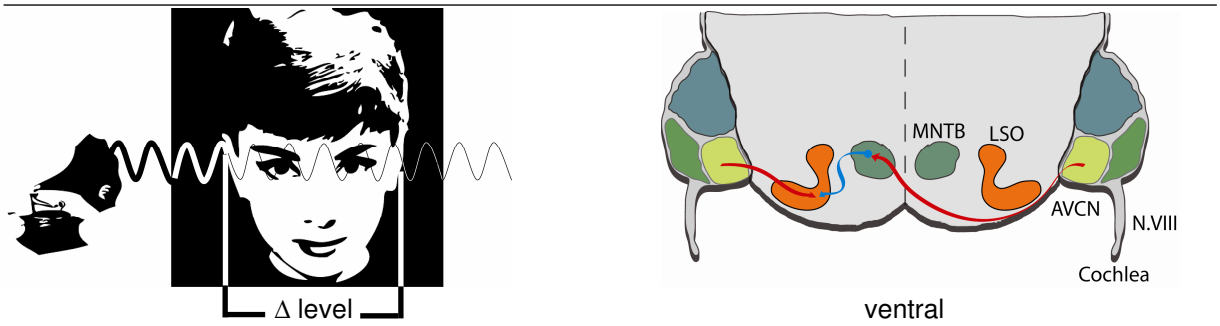

Figure 1.4: Interaural level differences (ILDs) are processed by neurons in the lateral superior olive (LSO). The skull dampens a high frequency sound deriving from the right or left side of the listener. The incoming sound signal is transferred by the eighth nerve and reaches the LSO via the AVCN and/or MNTB. By summing these two inputs up, the LSO codes for sound pressure level difference (Δ level in dB) between the two ears. On the ipsilateral side, excitatory projections directly innervate neurons in the LSO, whereas from the contralateral side excitatory projections first innervate neurons in the MNTB, which then send inhibitory afferents to the LSO. Together, both inputs to the LSO generate an output function that codes for the position of the sound source. (red arrows: excitation, blue arrows: inhibition)

In contrast to high frequency sound, low frequency sound waves travel longer distances, thus animals with spatially large behavioral ranges like carnivores, ungulates or primates, and animals living in an open space like the desert are more dependent on localizing the sources of low frequency sound emission (Grothe 2000). Therefore, certain animal classes evolved a second binaural sound localization mechanism to localize signals relying solely on the

different arrival time of sound waves at each ear; the interaural time differences (ITDs) (Goldberg and Brown 1968; Spitzer and Semple 1995; Yin and Chan 1990). Unlike high frequency sound waves, which are always attenuated by the head before being perceived by the contralateral ear, low frequency sound waves do not experience significant sound pressure level changes between the two ears. This statement, however, was demonstrated wrong for very close low-frequency sounds (distance for humans: 1-2m). Within this range, significant near-field ILDs are produced, which can be utilized to localize low frequency sound sources (Shinn-Cunningham et al. 2000). On the other hand, ITDs can also be conveyed by the envelopes of high-frequency sounds and thus elicit similar responses as the fine structure of low frequency sounds alone as observed by *in vivo* recordings from neurons of the guinea pig IC (Griffin et al. 2005). This study agrees with results reported at the same time indicating that low frequency LSO neurons are sensitive to ITDs (Tollin and Yin 2005). These two findings contradict the strict dichotomy of the “duplex theory” but will be regarded as exceptions for an overall valid hypothesis in this thesis. Hence, generally spoken, sounds composed of wavelengths larger than the head diameter, which is in a first approximation equal to the inter-ear-distance, instead circle around the head before they impinge on the contralateral ear (Fig.1.5). The resulting cue is a well-defined delay dependent on (1) the medium the sound is transmitted in (2) the position of the sound source in the azimuth and (3) the head size. Head sizes of course vary amongst mammals. Larger species exhibit larger ITDs because the time sound waves need to travel from ear to ear increases with increasing inter-ear-distance (Masterton et al. 1967). Humans, for example, experience ITDs of up to 660µs (Feddersen et al. 1957), dogs up to 800µs (Goldberg and Brown 1968; 1969; Grothe and Neuweiler 2000), cats around 300µs (Yin and Chan 1990), whereas some bats, due to their small head size experience maximal ITDs of about 30µs (Pollak 1988).

As seen already for the processing of ILDs, the AVCN is also the first relay site in the ITD circuitry. Again, two cell populations contribute to the processing of binaural cues, namely globular bushy cells (GBCs) and SBCs (Brawer et al. 1974; Osen 1969). However unlike in the LSO, contra- as well as ipsilateral SBCs send direct glutamatergic excitatory projections to the MSO, mostly targeting the dendritic region of MSO neurons (Clark 1969; Stotler 1953) (Fig.1.5). By integrating these two excitatory inputs from each ear, the MSO functions as a coincidence detector for binaural input.

Figure 1.5: Interaural time differences (ITDs) are processed by neurons in the medial superior olive (MSO). Sounds with long wavelengths, deriving from the right or left side of the listener, circle the skull and cause a specific delay (Δ time) between the two ears. This small time difference between the arrivals of the sound at the two ears is further passed on through the eighth nerve and reaches the MSO via the AVCN, the MNTB and LNTB. Ipsilaterally, excitatory projections from the AVCN and inhibitory projections from the LNTB target the MSO. From the contralateral side, the MSO receives excitatory input directly from the AVCN as well as inhibitory input from the MNTB. Both MNTB and LNTB serve as a relay and turn the excitatory input from the AVCN into an inhibitory output to the MSO. (red arrows: excitation, blue arrows: inhibition)

This excitatory/excitatory detection mechanism could be sufficient to localize sound sources in the azimuthal plane by integrating delay lines as proposed in the Jeffress model (Jeffress 1948). As described above for the LSO, a labeled-line code of best ITD responses aligned in the physiological relevant range would code for the position of the sound source in the azimuth. For a long time, the model of delay lines was commonly accepted for all animal species, especially because studies in birds demonstrated that the theoretical concept of Jeffress fitted the anatomical properties of the avian auditory brainstem (Parks and Rubel 1975; Young and Rubel 1986; 1983). Furthermore, electrophysiological recordings from barn owls and chicken speak in favor of the Jeffress model even though slight modifications in the delay line model have been suggested (Carr and Konishi 1990; Overholt et al. 1992). Nevertheless, skepticism arose whether the Jeffress model is also applicable to the mammalian ITD detection system (Brand et al. 2002; Fitzpatrick et al. 2000; Grothe 2003; Grothe and Neuweiler 2000; McAlpine et al. 2001). Two major aspects contradict the idea that the mammalian MSO functions as a Jeffress-type coincidence encoding structure. First, the Jeffress model proposes different lengths of axons to compensate for differences in sound travel times outside the head. Neither the contra- nor the ipsilateral inputs to the MSO, as revealed by anatomical studies, followed the model postulated by Jeffress. Hence, no convincing evidence has been found to date for the existence of such delay lines in mammals (Beckius et al. 1999; Smith et al. 1993). Moreover, one has to take into consideration, that the Jeffress model does not incorporate inhibitory input. Although the nucleus laminaris (NL), the avian analog to the MSO, and the MSO itself receive both more than only two major inputs involved in sound localization, differences in the input pattern are present. In contrast to the NL, which receives one inhibitory gamma-aminobutyric-acid releasing (GABAergic) projection that has recently been shown to increase the precision of phase-locking (Funabiki et al. 1998), the MSO is targeted by two inhibitory glycinergic projections. These two inputs originate from the lateral and medial nucleus of the trapezoid

body (LNTB and MNTB, respectively) (Fig.1.5) projecting to the somatic region of the neurons in mature animals (Cant and Hyson 1992; Clark 1969; Kapfer et al. 2002; Kuwabara and Zook 1992; Wenthold et al. 1987; Werthat et al. 2008). MNTB and LNTB neurons are excited by GBCs and release the inhibitory neurotransmitters GABA (early in development) and glycine onto MSO neurons (Grothe and Sanes 1993; Helfert et al. 1989; Magnusson et al. 2005; Smith et al. 2000). Based on extremely fast synapses in the MNTB, the calyces of Held, and a defined distribution pattern of inputs, with inhibitory projections on the somata and excitatory projections on the dendrites (Kapfer et al. 2002), it has been suggested that the contralateral inhibitory input precedes the excitatory input to the MSO. Furthermore, due to the excitation-to-inhibition conversion in the LNTB without ultra-fast kinetics, the ipsilateral inhibition could lag the ipsilateral excitation (Brand 2003; Grothe 2003; Grothe and Park 1998; Grothe and Sanes 1994). A theoretical model predicts that inhibitory input shapes the sum of excitatory and inhibitory postsynaptic potentials (EPSPs and IPSPs, respectively) in such a way that the peak of the resulting net potential is slightly shifted (Brand et al. 2002; Pecka et al. 2008). At the ipsilateral side of the sound source, the summed postsynaptic potential would peak earlier due to the shift by glycinergic inhibition. On the contralateral side, however, the peak of the summed postsynaptic potential occurs with a small delay caused by glycinergic inhibition (Grothe 2003). Together, ipsi- and contralateral net potentials could now code for the position of the sound source in the azimuth based on the interaural delay between the peaks of the two net potentials. *In vivo* studies recently supported this model assumption by demonstrating that the maximal spike rate of MSO neurons was shifted towards ITD=0 without glycinergic inhibitory input (Brand et al. 2002; Pecka et al. 2008). These results clearly speak in favor of a substantial contribution from glycinergic inhibition to sound source encoding in the MSO. Sound localization in mammals is therefore seemingly achieved otherwise than only by differences in axonal length as proposed by Jeffress 70 years ago.

This brings us back to the divergent evolutionary pathways of tympanic ears. As described in chapter 1.1 hearing evolved differently in animal classes during the Triassic period. The mammalian MSO and the avian NL provide good evidence for the individual achievement of sound localization systems based on similar principles. Yet, from this evolutionary perspective ILDs represent the primary binaural cue for the localization of sound sources. Hence, it is not surprising that in humans, ILDs dominate over conflicting ITDs in the high frequency range (Grothe 2000; Wightman and Kistler 1992).

1.5 Early developmental changes in the superior olivary complex - preparing for the acoustic environment

Small rodents like mice, rats and gerbils cannot hear until approximately postnatal day 12 (P12). Before this hearing onset, the animals' ear canals are closed and the auditory system is not exposed to acoustic information. Nevertheless, the SOC performs several developmental changes to prepare itself for optimal sound localization. Here, activity independent factors as for instance, genetically determined factors, and activity-dependent, i.e., spontaneous activity, which is not sound evoked, have to be considered.

The SOC undergoes fundamental morphological alterations before hearing onset. Tracing experiments in rats demonstrated that target-specific innervations are formed at the level of the SOC already at embryonic stages (Kandler and Friauf 1993). The connections are established with remarkable precision and aberrant projections usually do not occur (Kandler and Friauf 1995). It therefore seems that a crude topography, most probably genetically determined by molecular markers including Eph receptors and their ligands, the ephrins (Cramer 2005; Huffman and Cramer 2007; Miko et al. 2007), emerges already early before hearing onset. However, the functional fine-structure of the topographic map is developed further after birth but still before hearing onset as it has been shown for the LSO-MNTB pathway (Kim and Kandler 2003; Noh et al. 2010). At that stage, spontaneous activity patterns, more precisely, the spontaneous glutamate co-release at inhibitory synapses is most likely responsible for the elimination and strengthening of synapses. An additional example for synapse refinement before acoustic experience is the calyx of Held, a giant presynaptic terminal in the MNTB (Held 1891; Morest 1968). It develops from a diffuse conglomerate of presynaptic endings (P0-P3) into a cup-shaped structure in neonatal rodents (P3-P7) almost fully covering the targeted MNTB neuron (Kandler and Friauf 1993; Kil et al. 1995). Spontaneous activity is likely to underlie this process as well as other structural refinement processes in the SOC.

In several brain structures including the SOC, the release of the neurotransmitters glycine and GABA depolarizes neurons at early perinatal stages (Chen et al. 1996; Cherubini et al. 1990; Kandler and Friauf 1995; Lohrke et al. 2005). Consequently, chloride currents mediated by glycine receptors (GlyRs) and $GABA_A$A receptors ($GABA_A$Rs) are usually excitatory in very young animals. Functional implications for the auditory brainstem have been proposed by Kandler and Friauf (1995) in such a way that early postnatal SOC neurons express voltage-sensitive Ca^{2+} channels which could be activated by glycine- and GABA-induced depolarization. Hence, the cytosolic Ca^{2+} concentration would increase in these neurons similar to what has been observed in embryonic spinal cord neurons (Reichling et al.

1994; Wang et al. 1994). During the very early development of neural structures in the auditory brainstem, the glycinergic pathway might therefore transiently behave like an excitatory pathway and use the same Ca^{2+}-dependent cellular mechanisms known to be involved in strengthening and reshaping excitatory connections (Malenka 1994). A chloride reversal potential (E_{Cl^-}) positive to the resting membrane potential is the underlying reason for the depolarizing action of inhibitory neurotransmitter. At least in the LSO it has been demonstrated that neurons become hyperpolarizing through the action of the outward-directed K-Cl cotransporter KCC2 (Balakrishnan et al. 2003). Although KCC2 is expressed in neonatal animals, the protein is not functionally embedded in the membrane rendering E_{Cl^-} more positive. KCC2 transporters then slowly become membrane bound and decrease the chloride reversal potential, a process that is completed before hearing onset and thus achieved devoid of evoked auditory activity.

Another striking difference between neonatal non-hearing and adult hearing rodents is the composition of inhibitory neurotransmitter in the auditory brainstem. For the neonatal SOC, GABA is the primary inhibitory neurotransmitter and a graded developmental switch towards glycine is performed a few days before hearing onset (Kotak et al. 1998; Nabekura et al. 2004; Smith et al. 2000). It is still not quite clear whether a presynaptic transition from GABA to glycine alone (Helfert et al. 1989) is responsible for the lack of GABAergic IPSPs shortly before hearing onset or whether the target receptors, $GABA_A$Rs, are constantly degenerating with ongoing development (Nabekura et al. 2004). Again, sound evoked activity is not likely to play a role for this transition of transmitter preference. The functional role of early GABAergic signaling is an ongoing discussion. A number of studies indicate that GABAergic transmission is an important signal during development. Results from *in vitro* experiments suggest that GABA can modulate synaptogenesis (Corner and Ramakers 1992; Redburn 1992), and $GABA_A$R expression (Hablitz et al. 1989). Furthermore, it has been suggested that GABA is released in neonates and activates a metabotropic pathway contributing to input deletion in the LSO (Kotak et al. 1998).

Most importantly, one has to mention that not all of these changes are completed precisely before hearing onset. These processes should be understood as ongoing changes of the SOC that occur mostly independent from evoked auditory input. Other processes, which are related more obviously to acoustic experience and directed auditory perception, will be described in the next chapter.

1.6 Activity-dependent adaptations in the superior olivary complex - optimizing sound localization

Although the auditory system provides a fitting model to study activity-dependent processes based on non-hearing and hearing conditions, attributing observed effects to one of the mentioned conditions is not always straightforward. Some adjustments are established early before hearing onset and are just more or less refined with the beginning of directional auditory input. One should not forget that neurons in the SOC experience spontaneous activity via GBCs and SBCs from the auditory nerve even in silence (Hermann et al. 2007; Kopp-Scheinpflug et al. 2008; Kreinest et al. 2009; Lu et al. 2007; Smith et al. 2000). Therefore, it might be appropriate to speak of an optimization in the SOC through the adaptation of existing structures by directional auditory input rather than to speak of a development of new structures per se at hearing onset.

So far, two approaches have been used to study the effects of sound evoked activity in the auditory brainstem. One possibility to gain insight in the role of activity for sound localization is to raise animals under conditions which omit the directivity of sound sources or even the perception of sound itself. This can be achieved either by rearing animals in an environment enriched with omnidirectional noise, or to some degree by deafening animals prior to hearing onset. For example, around hearing onset, a process named “fenestration” begins to decrease the surface of the calyx of Held (Kandler and Friauf 1993; Kil et al. 1995). With maturation, the appearance of the calyces turn into a more finger-like structure which has been suggested recently to allow better transmitter clearance and thus more precise signal transmission in the MNTB of adult rats (Taschenberger et al. 2002). This development, however, is partially dependent on auditory experience since pharmacological deafening of animals prior to hearing onset significantly delayed fenestration (Ford et al. 2009). Furthermore, as described earlier, inhibitory MSO inputs are widely scattered along the entire neuron before hearing onset but primarily target the somatic region in adult animals (see chapter 1.4). This confinement only occurs in species with good low frequency hearing underlining the importance of glycinergic inhibition for ITD detection. Interestingly, noise-reared animals lack this refinement of inhibitory inputs and maintain the dispersed distribution pattern of glycinergic projections even after maturation (Kapfer et al. 2002). Corroborating these data, the morphology of MNTB axons is crucially dependent on normal acoustic activity in the auditory system. The number of branch points and endsegments of the axonal arbor is strongly reduced in an environment containing ITD and ILD cues and inputs are selectively eliminated from the dendrites of MSO neurons (Werthat et al. 2008). Masking ITD and ILD cues by rearing gerbils in omnidirectional noise, though, halts the

development of MNTB axon morphology at a state comparable to animals before hearing onset. As structural conversions are happening in the MSO, synaptic properties change as well. The decay time of IPSCs and IPSPs decreases dramatically in MSO neurons with the onset of hearing (Chirila et al. 2007; Magnusson et al. 2005; Smith et al. 2000). These findings are in agreement with the somatic refinement of glycinergic inputs and the alterations in principal cell morphology regarding dendritic branch points, total cell length and cell membrane area after hearing onset (Kapfer et al. 2002; Rautenberg et al. 2009). Furthermore, the input resistance of MSO neurons in the gerbil decreases, possibly due to a higher expression and/or membrane bound occurrence of voltage-activated cation channels (Hassfurth et al. 2009; Scott et al. 2005) (see chapter 3.2.1 for comparison).
Anatomical data already ruled out that all changes in the SOC described so far originated from a simple signal transduction cascade based on spontaneous activity in the auditory nerve (Kapfer et al. 2002; Werthat et al. 2008). Nevertheless, in order to ascribe functional effects to observations made in noise-reared animals, it became necessary to conduct physiological studies under similar conditions. Yet Magnusson et al. (2005) as well as Seidel and Grothe (2005), reported results of altered acoustic conditions by rearing pups in constant uncorrelated noise, thus omitting directional sound cues. After this treatment, ITD coding was disturbed as shown by extracellular recordings from DNLL neurons suggesting that ITD tuning develops only with normal acoustic experience (Seidl and Grothe 2005). Evidence for the underlying process causing impaired ITD coding has been given in a patch-clamp study. Here, whole-cell recordings from the MSO showed that the frequency of miniature IPSCs as well as the peak conductance of evoked IPSCs in young adult gerbils significantly differed from normally raised animals and more or less resembled the current properties around hearing onset (Magnusson et al. 2005). Thus, a direct connection between directional sound evoked activity and SOC development has been demonstrated.

A different approach to prove activity-dependent adaptations in the auditory brainstem of rodents was undertaken by comparing the characteristics of congenitally deaf with wild type mice (Leao et al. 2006a). Congenitally deaf mice do not experience spontaneous auditory nerve activity prior to (or following) opening of the ear canals, thus making them an adequate model organism to study influences of spontaneous activity in the SOC. Previous physiological and anatomical studies in rodents indicated that a precise tonotopic organization, meaning the orderly representation of the sound frequency to which neurons are most sensitive, is present in the SOC even before central auditory pathways are activated by sound experience (Friauf 1992; Kandler and Friauf 1993; Sanes and Siverls 1991). Hence, the more interesting it was that in the MNTB of congenitally deaf mice this gradient does not exist shortly after hearing onset. At least in the MNTB, the absence of tonotopy is reflected by a lack of medio-lateral potassium channel gradients (Kv3.1 and

Kv1.1) as well as a lacking HCN channel gradient (Leao et al. 2006b). Unfortunately, long-term changes were not addressed in this study. It was suggested that the absence of spontaneous firing rates of AVCN neurons is responsible for the lack of a topographic potassium channel gradient. Interestingly, this gradient also weakened in the LSO of normal hearing rats with maturation (Barnes-Davies et al. 2004), thus it is debatable whether the Kv1.1 gradient is induced by spontaneous activity or whether the lack of acoustic experience just accelerates the decrease of the potassium channel gradient. However, in young adult congenitally deaf mice, an increase in the fenestration of the calyces of Held exists when compared to normal hearing mice. Both deaf and normal mice had evidence of spontaneous CN activity *in vivo*, even though in deaf mice, the auditory nerve had no spontaneous activity (Leao et al. 2006b). It is therefore possible that the spontaneous CN activity is responsible for the appropriate development of connections and fenestrated giant synapses in deaf mice (Youssoufian et al. 2008).

In summary it is difficult to determine the exact consequences acoustic experience would have on the development of current properties and cell morphology. Animal models, surgery techniques and rearing methods are always open to possible side effects and give rise to further controversy.

1.7 $GABA_B$ receptors and their relevance for auditory processes

Various ion channels and transmitter receptors are responsible for maintaining the proper function of neurons (Debanne et al. 2003; Perez-Otano and Ehlers 2005). The properties of SOC neurons are likewise controlled and regulated by distinct channels and receptors. Two major subdivisions of receptors can be classified in the mammalian brain: ionotropic and metabotropic receptors. Ionotropic receptors (or ligand-gated ion channels) possess a pore region and are characterized by their direct action on ion flow. Upon transmitter binding, their pore region is permeable for ions; hence an outward or inward current is built up, depending on the receptor, its ion permeability, the actual potential and the present ion concentration. Some examples for ionotropic receptors have been mentioned above as e.g. glycine receptors and $GABA_A$ receptors. These receptors usually generate hyperpolarizing currents in the SOC and function as chloride channels upon activation. Nevertheless, at neonatal stages the action of GABA and glycine is depolarizing with major implications for cell development (Kakazu et al. 1999; Kandler and Friauf 1995; Lohrke et al. 2005). Other examples for ionotropic receptors would be the excitatory AMPA and Kainate receptors as well as NMDA receptors which conduct mostly sodium, potassium and in some cases

calcium. Metabotropic receptors, in contrast, mediate indirect inhibitory or excitatory action. These receptors utilize neurotransmitters as ligands, which, when bound to the receptors, initiate cascades that can lead to channel-opening or other cellular effects. Metabotropic receptors mostly activate intracellular G-proteins and kinases which usually have manifold effects on cell properties. However, because the signaling is not direct as for ionotropic receptors, effects normally take longer to develop but also last longer. Recent studies described such a coupling to G-proteins for several classes of receptors, therefore classified as G-protein-coupled receptors (GPCRs). Attwood and Findlay (1994) have made great effort in defining the probably biggest class of GPCRs, the rhodopsin-like GPCRs, which comprises serotoninergic, dopaminergic and endocannabinoid neurotransmitter signaling (Attwood and Findlay 1994; Binzen et al. 2006; Guo and Ikeda 2004). Other well-investigated and important classes regarding signal regulation are metabotropic GPCRs including metabotropic glutamate receptors and $GABA_B$ receptors ($GABA_B$Rs) (Kaupmann et al. 1997; Nakanishi 1994).

First evidence that the MSO expresses $GABA_B$Rs was recently provided by histochemical studies in the Mongolian gerbil and the Rhesus Macaque (Heise et al. 2005; Hilbig et al. 2007). $GABA_B$Rs are relevant for auditory processing as physiological studies with focus on the AVCN, LSO and MNTB showed (Kotak et al. 2001; Lim et al. 2000; Magnusson et al. 2008; Sakaba and Neher 2003). Several functional implications have been suggested so far. The activation of $GABA_B$Rs was proposed, for instance, to help developing the temporal precision of LSO neurons by eliminating inappropriate inhibitory projections (Kotak and Sanes 2000). Furthermore, dendritically released GABA controls synaptic input by a $GABA_B$R based feedback mechanism. This in turn, allows LSO neurons to adapt and extend their range of coding in order to match the sensory environment and accurately represent auditory space (Magnusson et al. 2008). Additionally, the fidelity of spike trains could be increased in MNTB neurons after activation of $GABA_B$Rs since the downmodulation of calcium current is most important for all forms of synchronous release (Sakaba and Neher 2003). The putatively underlying principles of such control mechanisms based on the modulation of effective transmitter amount will be introduced in the following.

From a systematic view, $GABA_B$Rs are part of the seven-transmembrane domain receptor superfamily and are closely associated with G-proteins (Fig.1.6). Opposing to $GABA_A$Rs, $GABA_B$Rs do not open upon GABA binding but mediate indirect effects via a G-protein cascade. $GABA_B$Rs can be situated both, pre- and postsynaptically, however, the effects mediated by these receptors are differently established at the pre- and the postsynapse (Yamada et al. 1999).

Functional $GABA_BRs$ at the postsynaptic site activate G-protein coupled inwardly rectifying potassium channels (GIRK channels) which are permeable to K^+-ions, thus hyperpolarize the neuron upon activation (Jones et al. 1998; Luscher et al. 1997). The activation is enabled by a conformation change of the G-protein itself. The βγ-subunit of the heterotrimeric G-protein dissociates from the α-subunit and binds to GIRK channels thereby increasing the open-state of the channel. Due to the concentration gradient of K^+, an efflux of potassium is achieved, which is long lasting (seconds) compared to ionotropic signaling (milliseconds) (Isaacson 1998). Several forms of the α-subunit exist making it difficult to explain some effects straightforward. The αs-subunit e.g. activates the andenylate cyclase which synthesizes cyclic adenosine monophosphate (cAMP) from adenosine triphosphate (ATP). Depending on synaptic activity, cAMP levels increase and modulate the open-probability of HCN channels (DiFrancesco 1999). On the other hand, the αi-subunit inhibits the synthesis of cAMP from ATP, and thus can cause completely opposite effects upon activation. Hence, the knowledge of the present composition of G-protein subunits is of great importance for the comprehension of $GABA_BR$ mediated effects.

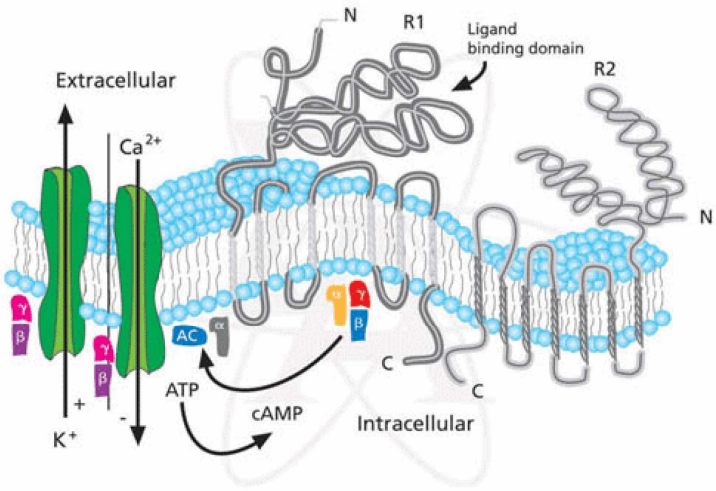

Figure 1.6: The $GABA_B$ receptor and two possible modes of action. Both subunits (R1 and R2) of the $GABA_BR$ need to be coupled for functionality. Upon activation by the neurotransmitter GABA, the $GABA_BR$ induces a conformation change in the bound heterotrimeric G-protein, which causes an exchange of GDP for GTP. In this high-energy state, the G-protein dissociates in its βγ-subunit and α-subunit, both further mediating distinct intrinsic processes. The βγ-subunit, for example, activates K^+ permeable GIRK channels and inhibits calcium channels whereas the α-subunit activates adenylate cyclase resulting in production of cAMP from ATP. Source: http://www.sigmaaldrich.com

Yet, $GABA_BRs$ are also expressed and functionally membrane bound at the presynapse. The most relevant mechanism here is the lowering of intracellular Ca^{2+} by inactivation of calcium channels (Isaacson 1998; Misgeld et al. 1995; Takahashi et al. 1998; Wojcik and Neff 1984). However, this feature is not solely restricted to the presynapse since studies also reported inhibition of calcium channels at the postsynaptic site (Harayama et al. 1998; Mann-Metzer and Yarom 2002). Calcium is at both locations essential for the proper function of the SNARE complex, a protein complex which brings intracellular vesicles in close distance to the cell's membrane, thus easing exocytosis. Due to the lowered Ca^{2+} concentration, the probability for a conformation change in the SNARE complex is decreased. Therefore neurotransmitter vesicles are less likely to fuse with the cell membrane. Conclusively, the

release probability of neurotransmitter is decreased resulting in a presynaptically mediated depression of synaptic strength. Since it was demonstrated that $GABA_BRs$ are expressed at inhibitory as well as at excitatory presynapses, the change in release probability can affect the inhibition as well as the excitation (Kabashima et al. 1997; Lei and McBain 2003; Lim et al. 2000).

1.8 HCN channels - structure and function

Unlike ligand-gated ion channels which open or close depending on binding of transmitter, voltage-gated ion channels open or close depending on a voltage gradient. In fact, these channels are activated by well-defined changes in the membrane potential at close proximity. The most important voltage-gated ion channels are probably potassium- and sodium-channels. Approximately 30% of the energy expended by cells is used to maintain the gradient of sodium and potassium ions across the cell membrane (Ackerman and Clapham 1997). Voltage-gated sodium-channels (Na_v channels) possess a selective filter in the pore region that is determined by the charge of the situated amino acids and allows only positive ions to pass. Furthermore, since the pore has a small diameter, the large K^+-ions cannot pass through this channel, making it only permeable for small Na^+ ions. Voltage-gated potassium-channels (K_v channels), though, possess an amino acid sequence (glycine-tyrosine-glycine) which is located in the pore region and represents a typical motif for the conductance of K^+-ions (Doyle et al. 1998). By actively gating K^+-ions through the pore via these charged amino acids, only this motif defines the ion-filter properties of K_v channels making it hundred-fold selective for the bigger K^+- over the smaller Na^+-ions.

Almost the same motif is present in the pore region of the hyperpolarization-activated and cyclic nucleotide-gated cation channel (HCN channel), another channel permeable for K^+ and Na^+ (Fig.1.7). As in K_v channels, its pore region is formed by 6 transmembrane helices (S1-6) with a positive charged segment S4 that functions as the voltage-sensor. However, this channel is the only known member among the superfamily of voltage-gated ion channels that is activated upon hyperpolarization (Ludwig et al. 1998; Santoro et al. 1998). Hence, the resulting cation current (I_h) is depolarizing and mainly Na^+-based since the selectivity filter in HCN channels is not as rigid, possibly due to the exchange of certain amino acids, compared to the filter in common K_v channels (Vaca et al. 2000). It therefore gates ions not as actively through HCN channels as through K_v channels and thus enables Na^+-ions to pass easily. This is reflected by the only four-fold preference of K^+-ions over Na^+-ions (Choe and Robinson 1998; Ludwig et al. 1999a).

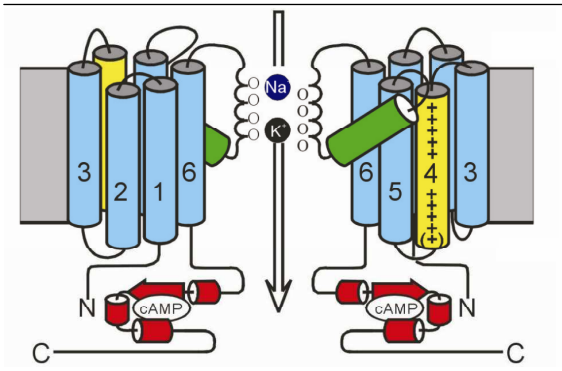

Figure 1.7: Model of an HCN channel. The pore region is positioned between segment 5 and 6 and enables the influx of Na^+ and K^+ ions. Segment 4 is the voltage sensor of the channel responsible for the proper activation during hyperpolarized states. The activation and deactivation of the HCN channel is regulated by modulation of the cAMP-binding site at the C-terminus. For clarity, only two of the four subunits are shown in this picture. Adapted from (Ludwig et al. 1999a)

Four members of the HCN family have been isolated so far (HCN1-4) and an assembly of four of these isoforms constitutes a functional tetrameric channel. However, the channel can be composed homomeric as well as heteromeric dependent on the cell's requirement. The major differences among the isoforms are the discrete activation kinetics. HCN1 channels activate fastest and at more depolarized voltages followed by HCN2 and HCN3. Homomeric HCN4 channels are by far the slowest activating HCN channels (Ludwig et al. 1999b; Stieber et al. 2005; Stieber et al. 2003; Wahl-Schott and Biel 2009). Furthermore, HCN channels are also ligand-gated, which additionally separates them from Na_v and K_v channels. The cyclic nucleotide-binding domain at the C terminus of the protein is responsible for modulating the activity of the channel and is connected to S6 by the so-called C-linker. Induced by the binding of cyclic nucleotides, mainly cAMP, the channel undergoes a conformation change at this linker domain. The C-terminus is pulled away from its original position in front of the pore opening to a more distant position, thereby facilitating the activation of the HCN channel (Wainger et al. 2001). HCN channels have profound assignments in the brain. Although it is almost not feasible to disclose the HCN subunit composition by electrophysiological means in native tissue, several basic properties underlying HCN channels have been revealed. They are thought to underlie the native pacemaker current termed I_h contributing to the control of the resting membrane potential and to the rhythmic activity of excitable cells (Bal and McCormick 1997; Luthi and McCormick 1998a; b; Robinson and Siegelbaum 2003).

The role of HCN channels in auditory processing is still an open field for research. HCN channels have been just recently demonstrated to be expressed at high levels in the auditory brainstem (Koch et al. 2004; Koch and Grothe 2003; Leao et al. 2006a; Notomi and Shigemoto 2004) which makes them an interesting target for electrophysiological studies (Bal and Oertel 2000; Golding et al. 1999). It has been already proven that in neurons of the auditory brainstem, the large I_h current lowers the membrane time constant and thus enables these neurons to process their sound evoked inputs on a very fast time scale (Golding et al. 1999; Koch and Grothe 2003; Leao et al. 2006a; Yamada et al. 2005). Short membrane time constants are typical features of the auditory circuitry and important for high-fidelity sound

localization. Hence, it is essential to understand the properties of I_h current in the auditory brainstem to gain further insight in the processing of auditory input per se.

1.9 Aims of this study

Basically, two major projects were conducted in this thesis which both addressed the question how the mammalian sound localization circuit develops and further adapts to altering activity levels during maturation.

In the first project (chapter 3), I investigated the highly expressed HCN channels in the SOC (see chapter 1.8). The depolarizing current I_h mediated by these channels has been shown to regulate the excitability of neurons and to enhance the temporally precise analysis of the binaural acoustic cues. Asking the question whether the properties of I_h current would change before and after hearing onset, I examined neurons of the LSO and the MNTB with electrophysiological means. Moreover, I tested the hypothesis that I_h currents are actively regulated by sensory input activity in performing bilateral and unilateral cochlear ablations before hearing onset, resulting in a chronic auditory deprivation.
Results of this project are also published in
Hassfurth B, Magnusson AK, Grothe B, Koch U. Sensory deprivation regulates the development of the hyperpolarization-activated current in auditory brainstem neuron. *Eur J Neurosci* 30(7):1227-38, 2009.

Throughout the development, $GABA_BRs$ are widely expressed in the mammalian brain. They contribute to long-term plastic changes in input strength in the immature auditory brainstem and are involved in the short-term regulation of the strength and dynamics of excitatory and inhibitory inputs in the LSO, thereby modulating sound analysis in mature animals (Magnusson et al. 2008). Thus, the primary goal of the second part of this thesis (chapter 4) was to determine if $GABA_BRs$ also play such a substantial role in the MSO. As the MSO performs several morphological and intrinsic adaptations during development I asked the following questions: To what extent are excitatory and inhibitory projections controlled by $GABA_BRs$? Do $GABA_BRs$ follow a developmental pattern in their regulation of the main inputs to the MSO? Additionally, I wanted to examine whether endogenous $GABA_BR$ activation in the MSO is altered during a critical period (P8-32) of auditory brainstem development. Using a combination of whole-cell patch-clamp recordings in acute brain slices and immunostainings, I characterized developmental changes in $GABA_BR$ mediated regulation of synaptic inputs to neurons in the MSO.
A manuscript of this project has been submitted to the *Journal of Neuroscience*.

In order to accomplish both of these *in vitro* studies, Mongolian gerbils (*Meriones unguiculatus*) were used as experimental animals. Compared with most other small rodents, gerbils are able to localize the emitted low frequency sounds of predators more efficiently and can communicate over longer distances in their natural habitat, tunnel systems as well as open steppe. The prerequisite for such outstanding localization of low frequency sound (<2kHz) as well as sound localization in the high frequency range (~2kHz-60kHz) is a well evolved MSO and LSO (see chapter 1.4 and 1.5). In contrast to e.g. mice, which lack a well-developed MSO, the gerbil SOC comprises both nuclei, thus rendering it an excellent model organism to investigate MSO and LSO related processes on an electrophysiological level. The fact, that these rodents possess auditory thresholds comparable to those measured for humans is interesting and probably most relevant for future research concerning auditory processes (Brown 1987; Heffner and Heffner 1988; Klumpp and Eady 1957; Ryan 1976). Additionally, since rodents undergo postnatal pre-hearing as well as hearing conditions, they have been the object of extensive electrophysiological studies and are well characterized regarding auditory development.

Carrying out this thesis, further insight in the physiological aspects of the mammalian superior olivary complex has been gained especially with respect to developmental adaptations of intrinsic cellular properties and the dynamic modulation of input strength.

2 MATERIAL AND METHODS

2.1 General methods

All experiments were performed in conformity with the rules set by the EC Council Directive (86/89/ECC) and German animal welfare legislation.

Acute transverse brain slices (140-190µm) of the auditory brainstem containing MSO, LSO, MNTB and LNTB were obtained from gerbils (*Meriones unguiculatus*) aged P8-P32. To minimize potentially damaging Ca^{2+}-influx into the neurons a low-sodium, high-sucrose slice solution containing 85 NaCl, 2.5 KCl, 1.3 NaH_2PO_4, 2.5 $NaHCO_3$, 75 sucrose, 25 glucose, 0.5 $CaCl_2$ and 4 $MgCl_2$ (all in mM) was used for the slicing procedure. Following decapitation under isofluorane anaesthesia, the brainstem was carefully removed and placed in the oxygenated ice-cold slice solution (95%O_2, 5%CO_2). The block of tissue was then glued with cynoacrylic glue onto a bath chamber that was filled with ice-cold slice solution. Slices were cut in the rostral direction from the level of the facial nerve, with a vibratome (VT1000S; Leica, Wetzlar, Germany), and subsequently incubated at 32°C in oxygenated (95%O_2, 5%CO_2) artificial cerebrospinal fluid (aCSF) containing (in mM): 125 NaCl, 2.5 KCl, 1.25 NaH_2PO_4, 26 $NaHCO_3$, 25 glucose, 2 $CaCl_2$ and 1 $MgCl_2$ (pH 7.4) for 5min, after which they were allowed to cool down to room temperature (22±2°C). Recordings were obtained within 4-5h after the preparation.

For recordings, slices were transferred to the recording chamber and superfused continuously with oxygenated aCSF at a rate of 1-2 ml/min. All recordings were made at 32±1°C. Slices were viewed through an upright microscope (Zeiss Axioscope; Oberkochen; Germany) using a 40× water-immersion objective (Achroplan, Zeiss) and infrared-differential interference optics equipped with an infrared-sensitive digital camera (KP-M2R, Hitachi Kokusai Electric, Tokyo, Japan). Whole-cell voltage- and current-clamp recordings were performed from the SOC with a Multiclamp 700A amplifier (Axon Instruments, Union City, CA, USA). Borosilicate glass microelectrodes (GC150F-10, Harvard Apparatus, Edenbridge, UK) were pulled on a DMZ Universal Puller (Zeitz Instruments, Munich, Germany), yielding a final tip resistance of 2-3.5MΩ. The series resistance ranged from 5-13MΩ and was compensated by 70-80% for voltage-clamp recordings. Furthermore, the series resistance was monitored throughout the duration of these experiments and was not allowed to vary by more than 20%. For current-clamp experiments, the bridge balance was applied.

2.2 HCN channel specific methods

2.2.1 Drugs and solutions

For all voltage- and current-clamp recordings glass electrodes were filled with an internal solution containing (in mM) 130 K-gluconate, 5 KCl, 10 HEPES, 1 EGTA, 2 Na_2-ATP, 2 Mg-ATP, 0.3 Na_2-GTP, 10 Na-phosphocreatine, adjusted to pH 7.3 with KOH. To isolate the I_h current during voltage clamp recordings, the following pharmacological agents were used: 1µM tetrodotoxin (TTX), (Tocris-Cookson, Bristol, UK), 2mM 4-aminopyridine (4-AP) and 200µM barium chloride dihydrate (BaCl) (both Sigma-Aldrich, Deisenhofen, Germany). I_h current was blocked with the specific HCN channel antagonist ZD7288 (20-50µM) (Tocris-Cookson, Bristol, UK). All drugs were dissolved in dH_2O stored at -20°C, diluted prior to the experiment and added to the perfusate during the experiment.

2.2.2 Data acquisition and analysis

Whole-cell voltage and current clamp signals were low pass filtered at 10kHz with a 4-pole Bessel filter and digitized at rate of 20-50kHz. pCLAMP (Version 10.2; Axon Instruments) was used for recordings and stimulus generation. Traces were digitally filtered at 2-5kHz. Data was analyzed with Clampfit (Version 10) or using custom-made routines in IGOR (Wavemetrics, Lake Oswego, OR).

LSO neurons were only included in the analysis if the compensated capacitance was larger than 20pF. These neurons display an onset spike in response to depolarizing currents and a depolarizing sag upon hyperpolarization and most likely correspond to the LSO principal neurons which show sensitivity to interaural level differences (ILDs) during sound stimulation (Adam et al. 1999; Magnusson et al. 2008). Since about 80% of the large neurons in the gerbil LSO show principal cell like bipolar morphology (Helfert and Schwartz 1987), we assume that the large majority of our data derives from LSO principle neurons.

All voltages were corrected for a liquid junction potential of -11.6mV. The input resistance (R_{in}) was calculated in the current-clamp mode by using Ohm's law from the peak or the steady state of the voltage deflection in response to a -200pA step current injection. Similarly, membrane time constants were measured from the voltage deflection induced by a -200pA current injection. During baseline voltage clamp recordings, the membrane potential was held at -62mV. To elicit the I_h current, voltage steps (1.5s) were applied from -52 to -127mV in steps of 5mV. Current amplitude was calculated as the current difference during

baseline voltage and 1.35s after the voltage step induction. Current density was calculated by dividing the current amplitude by the neuron's compensated capacitance as read from the MultiClamp Commander.

Activation time constants (τ) were obtained by fitting the current traces of the -127 to -72mV steps after the capacitive current artifact with the sum of two exponential functions,

$$f(t) = A_1 e^{-t/\tau_{fast}} + A_2 e^{-t/\tau_{slow}}$$

where τ_{fast} and τ_{slow} are the fast and slow time constants of the current activation and A1 and A2 the respective amplitudes. The effective time constant of I_h activation, the weighted τ, was calculated for each measurement according to (Balakrishnan *et al.*, 2009):

$\tau_{weighted} = (A_1*\tau_{fast}+A_2*\tau_{slow})/(A_1+A_2)$.

In order to obtain voltage-dependent steady-state activation curves, tail currents for each voltage step were measured about 10% below the maximal tail current amplitude for each test voltage, normalized to the maximal current (I_{max}) evoked by all test voltages and plotted as a function of the preceding test voltage. The resulting curves were fitted with the Boltzmann function:

$I = I_{max}/(1+\exp[(V-V_{half})/k)])+I_{off}$,

where I_{off} is the offset current, I_{max} is the maximal tail current, V is the test voltage, V_{half} is the half-activation voltage, and k is the slope of the Boltzmann function.

All numbers in the text refer to the values obtained by current measurements induced by a voltage step to -112mV. Results are presented as means ± S.E.M and statistical significance was determined with a paired or unpaired Student's two-tailed *t*-test.

2.2.3 Cochlear ablations

Bilateral and unilateral cochlear ablations (CA) were performed on gerbils at P10. Briefly, gerbils were anaesthetized with a mixture of Medetomidin (1µg/kg), Midazolam (0.1mg/kg) and Fentanyl (0.1mg/kg) (MMF). An incision in the skin was made behind the pinna, the muscles were gently removed and the bulla opened with forceps. After aspirating the middle ear mesenchyme, the round window was opened and the cochlea was removed either by using forceps or by aspiration with a fine cannula. Small pieces of gel foam were inserted

into the inner and middle ear cavities and the incision in the skin was closed using a cyanoacrylate adhesive.

The anaesthesia was antagonized with Atipamezol-Flumazenil-Naloxon (AFN), and 0.1ml of sterile 0.9% NaCl solution was injected under the skin to substitute fluid loss. The gerbils were returned to their mothers as quickly as possible. During the brainslice preparation, the temporal bone was checked under the microscope for a complete removal of the cochlea. Only animals in which the entire cochlea cavity was filled with gel foam were included in the study (about 80% of animals undergoing surgery). Bilaterally CA animals that were further processed for immunostaining (MAP2) showed the typically bilateral dendritic atrophy of neurons in the medial superior olive, which is indicative of a bilateral hearing loss.

2.3 $GABA_B$ receptor specific methods

2.3.1 Drugs and solutions

Whole-cell voltage-clamp recordings were carried out using a Cs-based internal solution comprising 70 $CsMeSO_4$, 70 CsCl, 10 HEPES, 10 EGTA, 2 Na_2-ATP, 2 Mg-ATP, 0.3 Na_2-GTP, 1 $CaCl_2$ (all in mM) and adjusted to pH 7.3 with CsOH. Voltage-gated sodium and potassium currents were blocked by adding QX-314 [1mM] and TEA-Cl [5mM] to the electrode solution before usage. For whole-cell current-clamp recordings we used an internal solution consisting of 130 K-gluconate, 5 KCl, 10 HEPES, 1 EGTA, 2 Na_2-ATP, 2 Mg-ATP, 0.3 Na_2-GTP, 10 Na-phosphocreatine, adjusted to pH 7.3 with KOH.

Additionally, the following pharmacological agents were used. 6,7-dinitroquinoxaline-2,3-dione (DNQX), DL-2-amino-5-phosphonopentanoic acid (DL-APV), SR95531, SCH50911, (R)-Baclofen (all Tocris-Cookson, Bristol, UK), strychnine, NO711 hydrochloride, 4-aminopyridine (4-AP) (all Sigma-Aldrich, Deisenhofen, Germany). All drugs were dissolved in dH_2O and stored at -20°C. Prior to the experiment, aliquots were thawed and added to the perfusate during the experiment.

2.3.2 Experimental procedure

MSO principal neurons were optically identified through the bipolar fusiform shape of their somata with dendrites extending medially and laterally. In addition, only neurons with capacities larger than 20pF, as read from the compensation of the MultiClamp amplifier,

were regarded as principal neurons and included in this study. Evoked synaptic responses were elicited with a glass microelectrode (tip opening 1-2µM) filled with NaCl [2M], which was positioned in the ipsilateral MNTB or the ipsilateral LNTB fiber tract 100 to 150µm away from the somatic region of the MSO. An analog isolated pulse generator (BSI 950, Dagan Corporation, Minneapolis, MN, USA) at a rate of 0.2Hz triggered a bipolar (+/–), paired stimulus pulse (from now on referred to as test pulse) with an inter-stimulus interval of 20ms. The threshold stimulus strength was typically 20-80V with pulse durations between 200 and 400*µ*s.

Inhibitory postsynaptic currents (IPSCs) were pharmacologically isolated by bath application of the AMPA receptor antagonist DNQX [10µM]. Excitatory postsynaptic currents (EPSCs) were evoked in the presence of the glycine receptor antagonist strychnine [1µM]. In all experiments, DL-APV [50µM] was applied to block NMDA receptors and SR95531 [10µM] to block $GABA_A$ receptors. To determine $GABA_BR$ mediated effects the corresponding agonist Baclofen [1µM] was applied to the perfusate. This Baclofen concentration is slightly above the IC_{50} values of the dose-response-curve for the excitatory ($[IC_{50}]$=0.62µM) and inhibitory ($[IC_{50}]$=0.2µM) inputs as measured in P14 old animals (Fig.4.2). Some of the train stimulation experiments were carried out under the presence of the synaptosomal GABA uptake blocker NO711 (preferred GAT-1 selectivity) to increase the residual GABA concentration during MNTB or LNTB stimulation. Dependent on the hypothesis, baseline conditions consisted in all experiments of 5 minutes with or without the 100Hz train preceding the test pulse. In some experiments, 4-AP [2mM] was used to raise spontaneous synaptic activity levels in the slice (Fig.4.9).

2.3.3 Data acquisition and analysis

The signals were filtered with a low-pass 4-pole Bessel filter at 10kHz, sampled at 20-50kHz and digitized using a Digidata 1322A interface (Axon Instruments). Traces were digitally filtered at 2-5kHz. Stimulus generation, data acquisition and offline analysis of data were performed using the pClamp Software (Version 10.2, Axon Instruments). The paired pulse ratio (PPR) was calculated as the mean amplitude of the synaptic response evoked by the second stimulus over that evoked by the first one. The coefficient of variation (CV) was calculated as the ratio between the standard deviation of synaptic current amplitude and the mean amplitude (Faber and Korn 1991). All data shown in percent reflect values normalized to baseline conditions. Figures, which display averaged evoked responses, consist of at least 13 traces. Stimulation artifacts have been deleted for clarity in figures that show averaged traces. Results are expressed as mean ± standard error of mean (S.E.M.). Significant

differences are marked with a single asterisk for values of $P<0.05$, with a double asterisk for $P<0.01$ and with a triple asterisk for $P<0.001$. *P*-values in this study were obtained by using Student's two-tailed paired or unpaired *t* test.

2.3.4 Immunohistochemistry

Animals of different age (P7, P18, P19, P30) were deeply anesthetized with isoflurane and then perfused with 0.9% Ringers solution (5min) followed by 4% paraformaldehyd (PFA) (30min). Brains were removed and postfixated in PFA over night at 4°C. The tissue was then sectioned at 40-60µm using a vibratome. Immunohistochemistry was applied to free floating sections. Following extensive rinsing in phosphate buffered saline (PBS), sections were exposed to a blocking solution (BS) containing 1% bovine serum albumin, 0.5% Triton X-100 and 0.1% Saponin in PBS (30min). Subsequently, a double immunofluorescence labeling was performed with the following primary antibody combinations: guinea pig anti-$GABA_BR1$ (1:2000; Chemicon International Inc., USA) / chicken anti-microtubule associated protein 2 (MAP2) (1:1000; Neuromics, USA) and guinea pig anti-glycine transporter 2 (GlyT2) (1:1000; Millipore, USA) / mouse anti-glutamate decarboxylase 65 (GAD65) (1:500; Chemicon International Inc., USA) in PBS, containing the same BS overnight at 4°C. The immunoreactivity was visualized by incubating the sections with secondary antibodies raised in donkey and conjugated to either Cy3 (1:300; Chemicon International Inc., USA), Alexa 488 (1:200; Molecular Probes, Germany) or Cy5 (1:200; Dianova, Germany) in BS for 3h at 37°C. Finally, the sections were rinsed, mounted, and cover-slipped with Vectashield medium (Vector Laboratories, Inc., USA). Confocal optical sections were acquired with a Leica TCS SP confocal laser-scanning microscope (Leica Microsystems, Germany) equipped with PL FLUOTAR 25x / 0.75 NA and HXC PL APO 63x / 1.32 NA oil immersion objectives. Fluorochromes were visualized using an argon laser with excitation wavelengths of 488nm (emission 510–540nm) for Alexa 488, a DPSS laser with a laser line of 561nm (emission 565–600nm) for Cy3, and a helium-neon laser with an excitation wavelength of 633nm (emission 640-760nm) for Cy5. Stacks of eight-bit greyscale images were obtained with axial distances of 300 or 1000nm between optical sections and pixel sizes of 310 to 781nm depending on the selected objective. After stack acquisition, Z chromatic shift between color channels was corrected. RGB stacks, montages of RGB optical sections, and average-intensity projections were created using ImageJ 1.37k plugins.

3 SENSORY DEPRIVATION REGULATES THE DEVELOPMENT OF THE HYPERPOLARIZATION-ACTIVATED CURRENT IN AUDITORY BRAINSTEM NEURONS

3.1. Introduction

Voltage-gated ion channels largely determine the excitability and the integrative properties of neurons. One important candidate are the HCN channels, which are widely expressed in the brain (Notomi and Shigemoto 2004), open upon hyperpolarization and produce a mixed cation depolarizing current (I_h). Four different HCN isoforms (HCN1-4) are expressed in the mammalian brain, which significantly differ in their physiological properties (Wahl-Schott and Biel 2009). HCN1 channels activate faster and at more depolarized voltages compared to HCN2-4 channels. Moreover, the modulation of the voltage dependence via cAMP is less pronounced in HCN1 compared to HCN2-4 channels. However, I_h channels can form heteromers with properties that are not the algebraic sum of the four different channel subunits (Chen et al. 2001). Functionally, I_h is thought to stabilize the membrane resting potential (Hu et al. 2002; Nolan et al. 2007) and to decrease membrane time constants to allow subthreshold integration of synaptic inputs with high temporal precision (Magee 1998; 1999). I_h also contributes to the generation of oscillatory or rhythmic behavior of single neurons or neural networks in the cortex, hippocampus and thalamus (Dickson et al. 2000; Fisahn et al. 2002; Nolan et al. 2004; Pape and McCormick 1989).

Neurons in the auditory brainstem display one of the largest I_h current amplitudes in the entire brain (Bal and Oertel 2000; Banks et al. 1993; Koch and Grothe 2003; Leao et al. 2006a). In these neurons, the large I_h current lowers the membrane time constant and thus enable these neurons to process their sound evoked inputs on a very fast time scale (Golding et al. 1999; Koch and Grothe 2003; Leao et al. 2006a; Yamada et al. 2005). Neurons in the superior olivary complex (SOC), the first site of binaural processing in the auditory brainstem, differentially express the various HCN subunits (Koch et al. 2004; Leao et al. 2006a; Notomi and Shigemoto 2004). Whereas HCN1 is mainly expressed in the lateral (LSO) and medial superior olive (MSO), the HCN2 and HCN4 isoforms are predominantly found in the MNTB. This distribution of HCN isoforms corresponds well to the I_h current properties measured in neurons of the LSO and MNTB of mice (Leao et al. 2006a). Thus, an important question is how I_h is regulated during development and what role neural activity levels play during this process. Here we show that at the onset of sound evoked activity I_h profoundly increases in LSO neurons but not in MNTB neurons. Moreover, a loss of sensory

activity considerably changes I_h amplitude and the voltage dependence of I_h activation in these neurons. These I_h changes are of opposite polarity in neurons of the LSO and the MNTB, which might reflect the differential HCN channel composition in the respective nuclei.

3.2 Results

3.2.1 The I_h current has a larger impact on the voltage response in the LSO than in the MNTB

The influence of I_h current activation on membrane properties of principal neurons in the LSO and the MNTB of gerbils was tested at postnatal day 17 (P17). After this developmental time point the cellular properties of superior olivary complex neurons change only little (Magnusson et al. 2005; Scott et al. 2005). The voltage response to step current injections of various amplitudes (duration: 1s) was recorded and compared between LSO and MNTB neurons. Both, LSO and MNTB neurons responded with a single spike to a depolarizing current injection and displayed a depolarizing sag (*arrow*) during hyperpolarizing current injections which is indicative of I_h activation (Fig.3.1A and B). However, input resistance to hyperpolarizing current injections (-200pA) was almost 10 times smaller in LSO compared to MNTB neurons for the peak (closed circle) (LSO: 29±10MΩ, n=9; MNTB: 206±22MΩ, n=4) as well as for the steady state (open circle) voltage (LSO: 14±4MΩ, n=9; MNTB; 132±9MΩ, n=4). In addition, membrane time constants were about five times shorter in LSO (2.0±0.7ms) compared to MNTB (7.9±1.2ms) neurons. In both types of neurons bath application of the selective HCN channel blocker ZD7288 [20µM] hyperpolarized the resting membrane potential and increased the input resistance as well as the membrane time constant for both LSO and MNTB neurons (Fig.3.1C). However, blocking I_h induced much larger changes in input resistance and membrane time constant in LSO compared to MNTB neurons. These results provide evidence that I_h differentially affects membrane properties of neurons in the gerbil LSO and MNTB, as previously shown for mouse auditory brainstem neurons (Leao et al. 2006a).

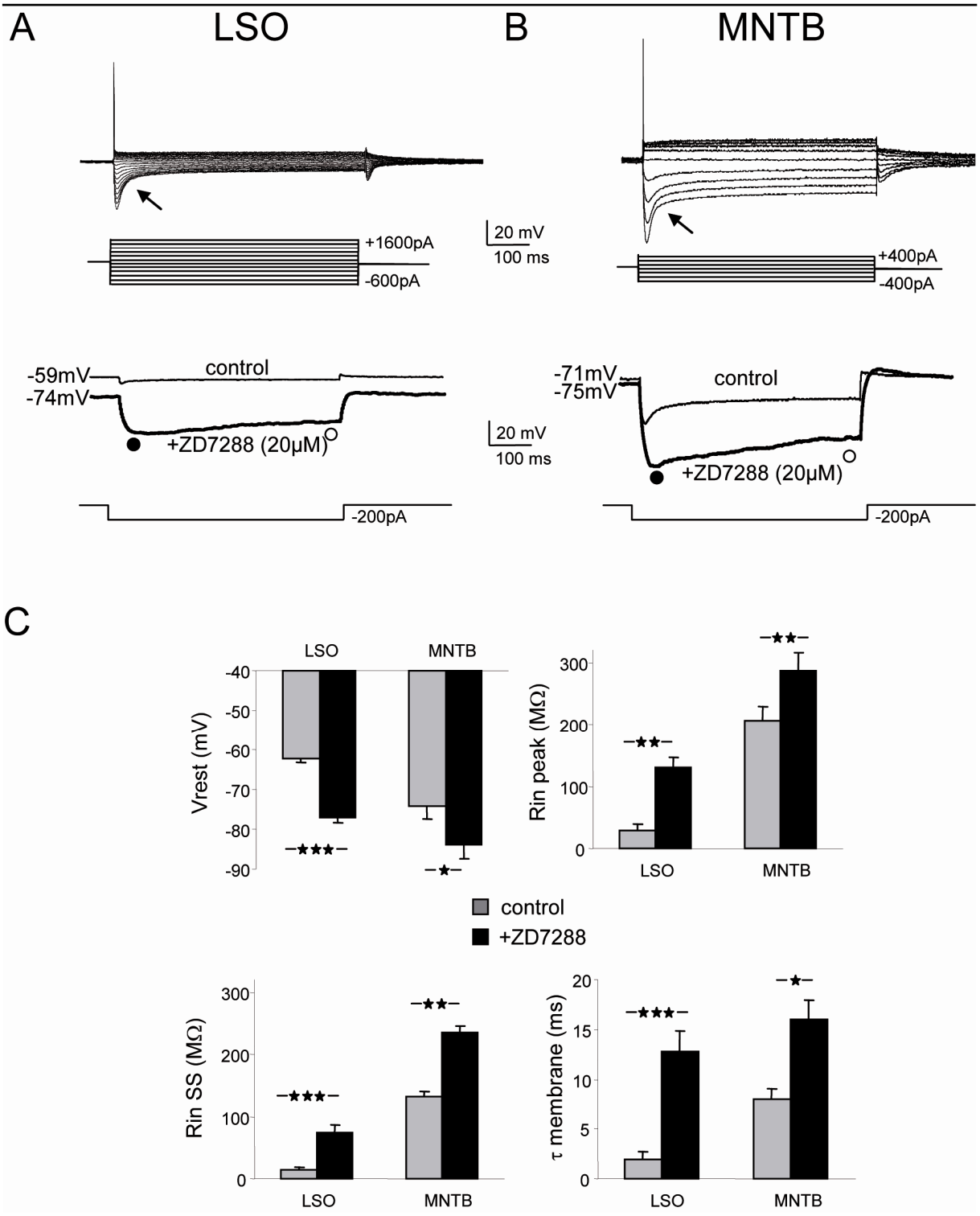

Figure 3.1: Pharmacological blockade of I_h changes the membrane properties of neurons in the LSO and MNTB in 17-day-old animals (P17). These changes are considerably larger in LSO compared to MNTB neurons. (A) *Upper panel:* Voltage response of an LSO neuron to depolarizing and hyperpolarizing current step injections (-600 to 1600pA). The arrow indicates the large depolarizing sag which is caused by the activation of the I_h current. *Lower panel:* voltage response of an LSO neuron to a hyperpolarizing current step injection (-200pA) under control conditions and during pharmacological blockade of I_h with ZD7288 [20µM]. (B) *Upper panel:* Voltage response of an MNTB neurons to a de- and hyperpolarizing current step injection (-400 to 400pA). The depolarizing sag induced by I_h activation (indicated by the arrow) was smaller compared to the LSO neurons indicating a smaller I_h current in MNTB compared to LSO neurons. *Lower panel:* voltage response of an MNTB neuron to a hyperpolarizing current step injection (-200pA) under control conditions and during pharmacological blockade of I_h with ZD7288 [20µM]. (C) Averages of the resting membrane potential (V_{rest}), the peak (R_{in} peak) (•), steady state input resistance (R_{in} SS) (o) and the membrane time constant (τ membrane) under control conditions and during pharmacological blockade of the I_h current with ZD7288 [20µm] in the LSO and the MNTB. The level of significance between the groups was determined by using Student's paired *t*-test. The n-values for each group are stated in the results section.

3.2.2 I_h current properties differ between the LSO and the MNTB

Differences in I_h current properties between LSO and MNTB neurons were measured by applying various holding potentials (-52mV to -127mV) from a holding potential of -62mV. I_h current was pharmacologically isolated by bath application of TTX [1µM], BaCl [200µM] and 4-AP [2mM]. In both LSO and MNTB neurons, a slowly activating, large inward current developed upon hyperpolarization of the membrane. This current was blocked by bath application of the specific I_h blocker ZD7288 [50µM] in both LSO and MNTB neurons (Fig.3.2A and B). The I_h current amplitude, measured when the evoked I_h current had reached steady state, was more than six times larger in LSO compared to MNTB neurons (at -112mV) (*LSO*: -3202±371pA, n=19, *MNTB*: -494±31pA, n=19; p≤0.001) (Fig.3.2C). I_h current density (at -112mV), which accounts for the neuron's size obtained by capacitance measurements, was still almost three times larger in LSO compared to MNTB neurons (*LSO*: -110±12pA/pF, n=19, *MNTB*: -41±3pA/pF, n=19; p≤0.001) (Fig.3.2D). Voltage dependence of I_h current activation was determined by a tail-current analysis (Fig.3.2E). Tail current amplitudes for various holding potentials were measured about 10% below the peak, normalized to the maximal current amplitude and fitted with a Boltzmann function. The half activation voltage was significantly more depolarized in the LSO compared to MNTB neurons (at -112mV) (*LSO*: -76±1.3 mV, n=19; *MNTB*: -84±2mV, n=19; p≤0.001) (Fig.3.2F). Moreover, I_h activation time constant ($\tau_{weighted}$: *see methods*) was significantly faster in LSO compared to MNTB neurons (at -112mV) (*LSO*: 82±6ms, n=18, *MNTB*: 268±16ms, n=18; p≤0.001) (Fig.3.2F). These finding corroborate previous data of I_h properties in the mouse auditory brainstem (Koch et al. 2004; Leao et al. 2006a; Notomi and Shigemoto 2004).

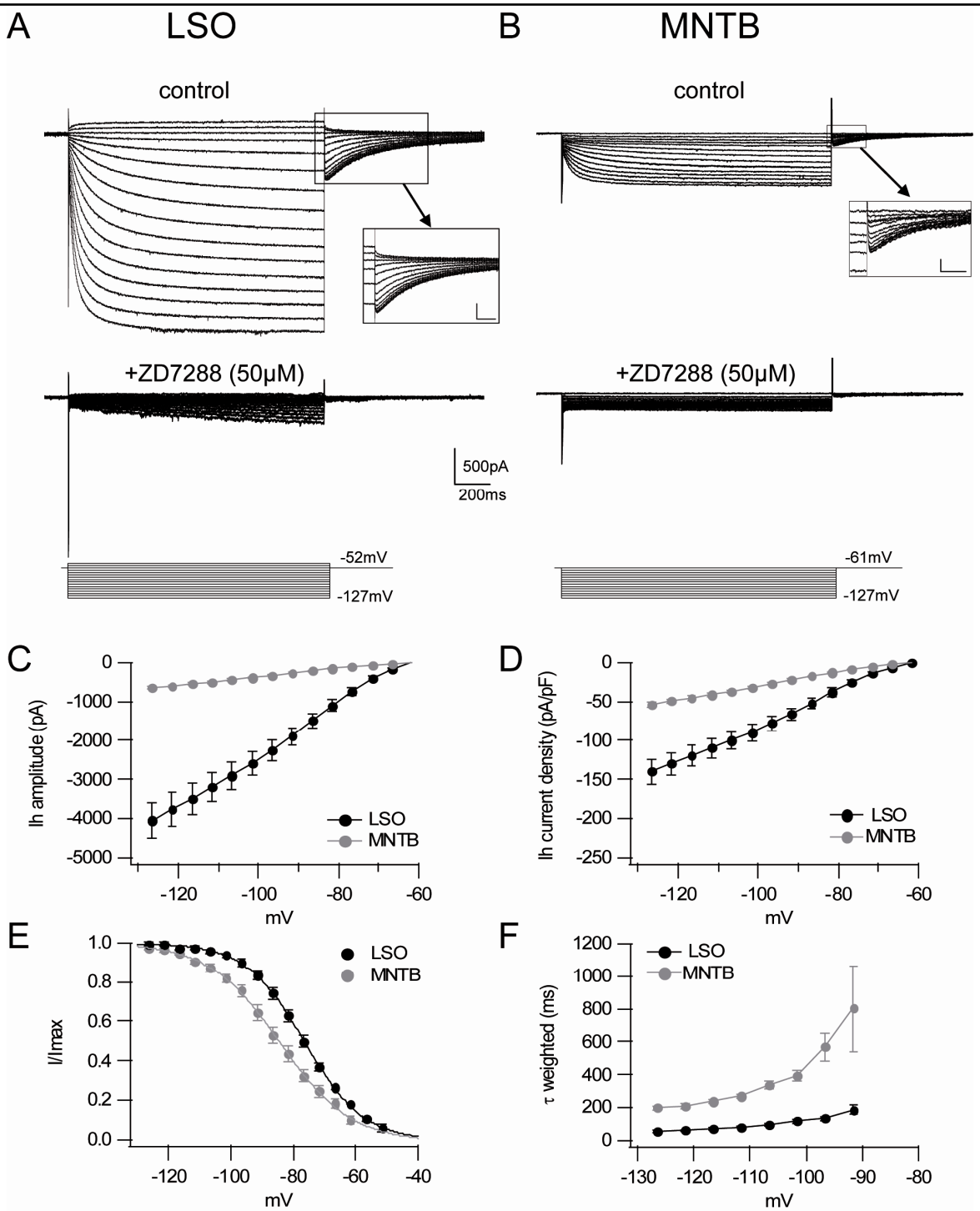

Figure 3.2: I_h current amplitude, activation time constants and voltage dependence differs between neurons in the LSO and MNTB. (A) Current traces recorded from an LSO at P17 neuron induced by de- and hyperpolarizing voltage steps (-52 to -127mV) from a holding potential of -62mV under control conditions and during pharmacological blockade of I_h with ZD7288 [50µM]. ZD7288 blocked more than 90% of the current in the beginning of the voltage step, however, a voltage-dependent slow unblocking effect of the channel was observed when measured at 32°C. The inset displays the enlarged tail current (scale bar: 200pA, 200ms). (B) Current traces recorded from an MNTB neuron induced by de- and hyperpolarizing voltage steps (-62 to -127mV) from a holding potential of -50mV under control conditions and during pharmacological blockade of I_h with ZD7288 [50µM]. The inset displays the enlarged tail current (scale bar: 50pA, 100ms). C) Averages of I_h amplitudes in LSO and MNTB neurons induced by hyperpolarizing voltage steps (-62 to -127mV) measured when the current had reached the steady state levels (approximately 1.35s after step voltage induction). I_h amplitude was more than six times larger in LSO compared to MNTB neurons. (D) Averages of I_h current density in LSO and MNTB neurons obtained by dividing the I_h amplitude by the compensated capacitance of each neuron. (E) Averages of the voltage dependence of I_h activation as obtained from tail current measurements in LSO and MNTB neurons. Values are fitted with a Boltzmann function to obtain half voltage activation. Values are displayed setting the maximum and the minimum of the Boltzmann function to 1 and 0 respectively (F) Averages of the weighted activation time constants of LSO and MNTB neurons obtained by fitting a double exponential function to the current traces and calculating the effective weighted activation time constant (*see methods*). Level of significance between the groups and the n-values for each group are stated in the results section.

3.2.3 I_h current but not current density differs along the tonotopic axis of the LSO but not the MNTB

Neurons in the MNTB and the LSO of gerbils are tonotopically organized with high frequencies represented in the medial part and low frequencies represented in the lateral part of the respective nuclei (Kopp-Scheinpflug et al. 2003; Sanes et al. 1989). Voltage-gated ion channels can account for differences in firing capability and subthreshold integration that has been shown to differ depending on the neuron's best frequency (Barnes-Davies et al. 2004; Brew and Forsythe 2005). We tested whether I_h properties of LSO and MNTB neurons differs depending on the neuron's position along the tonotopic axis of the nucleus. In the LSO, I_h current amplitude was significantly larger in the lateral (low frequency) compared to the medial (high frequency) part of the nucleus (LSO *medial*: -2452±493pA, n=9; *lateral*: -3878±470 pA, n=10; p≤0.05) (Fig.3.3A). However, neurons in the lateral part of the LSO had larger capacitance measurements compared to neurons in the medial part of the respective nuclei, which indicates that they were larger. This is in agreement with the differences in anatomically measured soma size across the tonotopic axis of the LSO (Koch and Sanes 1998). As a consequence, I_h current density did not differ along the tonotopic axis of the LSO (*LSO medial*: -113±25pA/pF, n=9; *LSO lateral*: -108±10pA/pF, n=10) (Fig.3.3B). Interestingly, neurons in the lateral part of the LSO, which are tuned to low sound frequency, had more depolarized voltage dependence than neurons in the medial, high frequency part of the nuclei (*LSO medial*: -80±1mV, n=9; *LSO lateral*: -72±2mV, n=10; p≤0.001) (Fig.3.3C). The differences in I_h current between medial and lateral LSO neurons are also reflected in the voltage response to hyperpolarizing step current injections (-200pA). Neurons in the lateral part of the LSO had on average a lower input resistance (*LSO medial*: 51±14MΩ, n=5; *LSO lateral*: 14±9MΩ, n=5; p≤0.05) (Fig.3.3D) and shorter membrane time constants (*LSO medial*: 1.1±0.4ms, n=5; *LSO lateral*: 3.2±1.3ms, n=5; p≤0.05) (Fig.3.3D) compared to neurons in the medial part of the LSO. Blocking I_h with ZD7288 [20µM] induced a larger change in resting potential, input resistance and membrane time constant in neurons located in the lateral compared to the medial part of the LSO (Fig.3.3D).

For MNTB neurons, no difference in I_h amplitude, I_h current density or the voltage dependence of I_h activation was observed between the medial and the lateral part of the nucleus (data not shown).

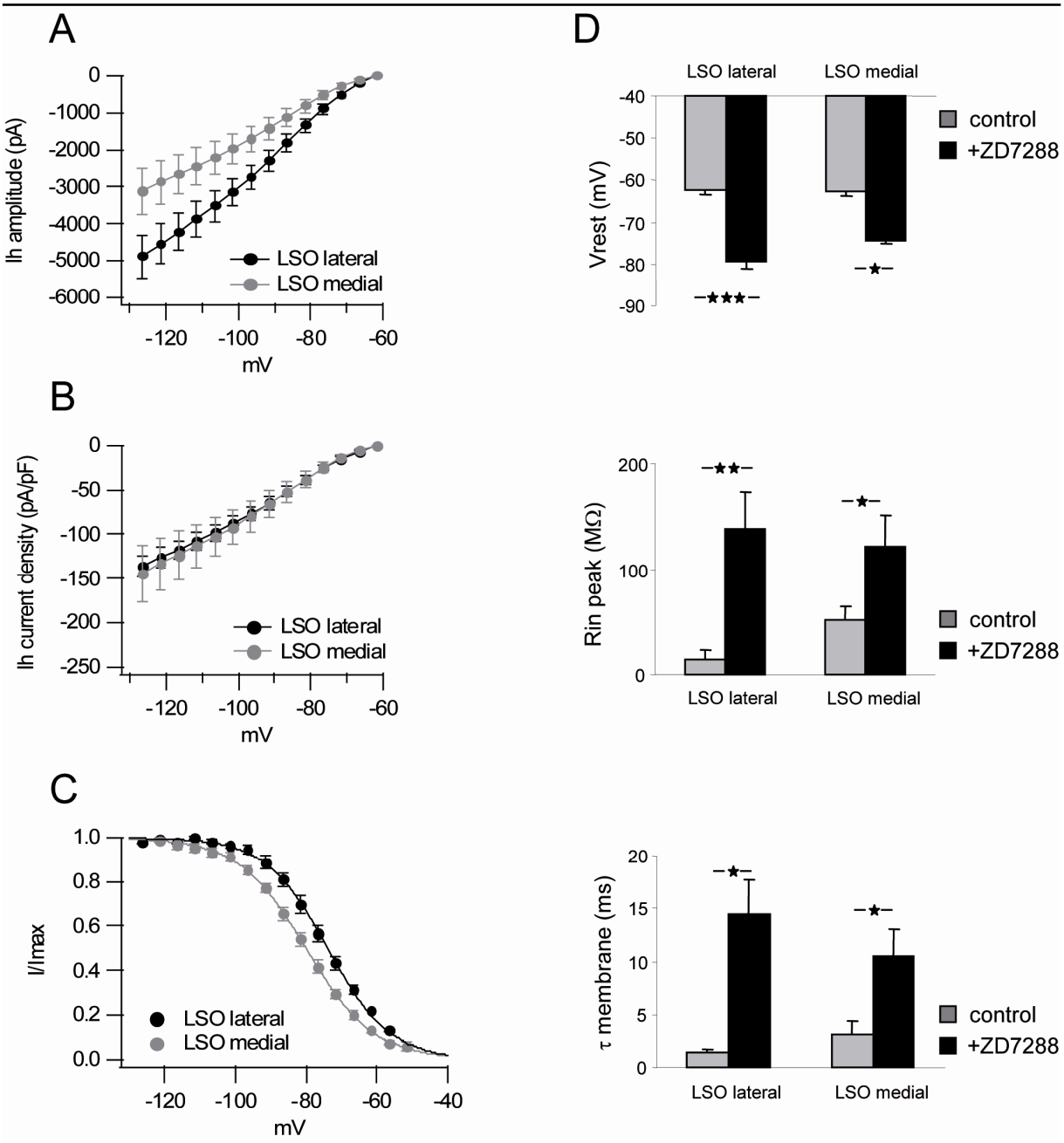

Figure 3.3: I_h amplitude but not current density differs across the tonotopic axis of the LSO. (A) Averages of I_h amplitude in the medial and the lateral part of the LSO. In the medial part of the LSO neurons are tuned to higher sound frequencies compared to the lateral part of each nucleus where low sound frequencies are represented. (B) Average I_h current densities in the medial and the lateral part of the LSO. (C) Averages of the normalized tail current amplitudes fitted with a Boltzmann equation in the medial and the lateral part of the LSO. (D) Changes in resting membrane potential (V_{rest}), input resistance (R_{in}) and membrane time constant (τ membrane) induced by pharmacological blockade of I_h with ZD7288 [20µM] during hyperpolarizing step current injection as in Fig.3.1. For A, B, C the level of significance between the groups is stated in the results section. For D the level of significance between the groups was determined by using Student's paired *t*-test. The n-values for each group are given in the result section.

3.2.4 I_h current increases after hearing onset in the LSO but not in the MNTB

Several studies support the idea that the various HCN subunits differ in their developmental time course (Surges et al. 2006; Vasilyev and Barish 2002). Analyzing the amplitude and the activation properties of I_h at several developmental stages before and after hearing onset revealed significant differences in I_h development between LSO and MNTB neurons. In the

LSO, I_h current density profoundly increased just after hearing onset (*P10*: -28±3pA/pF, n=14; *P14*: -119±11pA/pF, n=17; p≤0.001), whereas only a small change in I_h current density was detected in MNTB neurons (*P10*: -29±7pA/pF, n=10; *P14*: -36±2pA/pF, n=16; p≤0.05) (Fig.3.4A). No significant change in the neuron's measured capacity, an indicator for neuron cell size, was observed during this developmental period. In the LSO, changes in I_h current density were accompanied by a significant positive shift of the half activation voltage, meaning that more HCN channels were open at the neuron's resting membrane potential in P14 compared to P10 animals (Fig.3.4B) (*P10*: -87±1mV, n=14; *P14*: -78±1mV, n=17; p≤0.001). For both LSO and MNTB neurons, the activation time constants accelerated between P10 and P14 (*LSO P10*: 285±21ms, n=10; *LSO P14*: 96±9ms, n=17; p≤0.001; *MNTB P10*: 509±61ms, n=7; *MNTB P14*: 324±25ms, n=14; p≤0.001) (Fig.3.4C). After P14 no further significant changes in I_h properties were observed in the LSO and the MNTB. However, a small increase in I_h current density in LSO neurons between P17 and P22 (*LSO P17*: 110±12pA/pF, n=19; p≤0.001; *LSO P22*: 143±20pA/pF, n=7; p=0.17) cannot be excluded due to a reduced sample size in P22 animals, as revealed by power analysis.

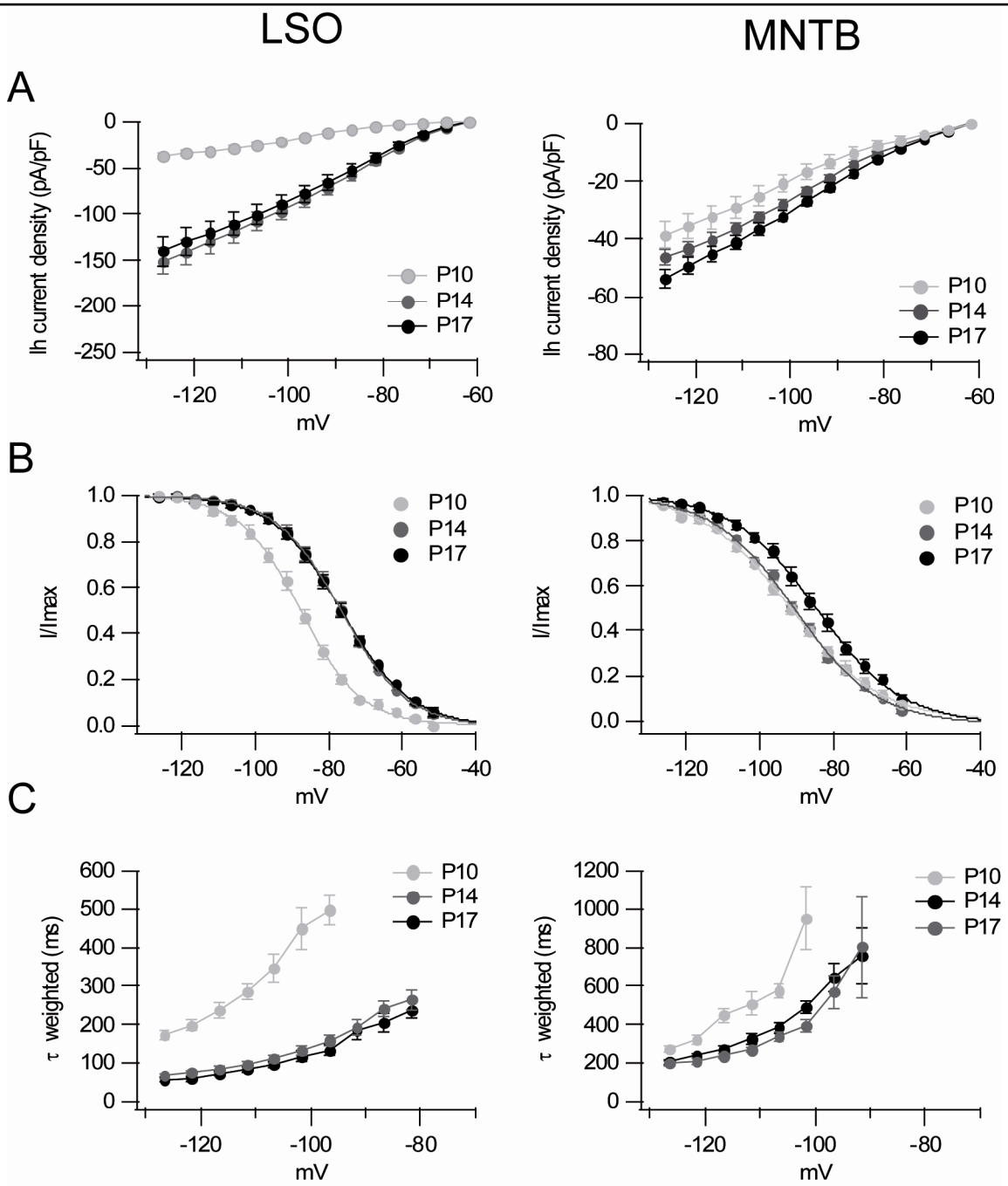

Figure 3.4: Developmental increase of I_h is considerably larger in the LSO compared to the MNTB. (A) Averages of I_h current density in LSO and MNTB neurons before hearing onset (P10), two days after hearing onset (P14) and at an age when neuronal properties are mature-like (P17). (B) Averages of normalized I_h tail current amplitudes of LSO and MNTB neurons at the same ages as in A. (C) Averages of the weighted activation time constant in LSO and MNTB neurons at different developmental stages. Level of significance between the groups and the n-values for each group are stated in the results section.

3.2.5 Bilateral cochlear ablations have opposite effects in the LSO and the MNTB

Several factors indicate that sensory activity might influence the expression density and the functional properties of I_h channels. For example, directly at hearing onset I_h currents are maximally upregulated in the LSO and the voltage dependence shifts towards more positive potentials. Moreover, a short- or long-term increase in neural activity can modulate I_h current

properties in the cortex (Shah et al. 2004) or the hippocampus (Campanac et al. 2008). We tested whether chronic auditory deprivation starting before hearing onset, which leads to a complete loss of sound evoked neuronal activity and presumably also to a substantial decrease in general auditory brainstem neuronal activity (Tucci et al. 1999), modulates I_h current properties in auditory brainstem neurons. Auditory deprivation was achieved by removing both cochleae (bilateral CA) at P10, two days before hearing onset. Four days after bilateral CA (at P14), I_h current density (*control*: -119±11pA/pF, n=16; *bilateral CA*: -116±10pA/pF, n=23; p=0.85), activation time constants (*control*: 97±9pA/pF, n=16; *bilateral CA*: 131±14pA/pF, n=23; p=0.07) and half-activation voltage (*control*: -77±1mV, n=16; *bilateral CA*: -77±1mV, n=23; p=0.95) did not differ significantly between LSO neurons of control and bilateral CA animals. However, only three days later, at P17, I_h current density in the LSO was significantly increased compared to control animals (*control*: -110±12pA/pF, n=19; *bilateral CA*: -174±15pA/pF, n=19; p≤0.01) (Fig.3.5A). This increase was paralleled by a small depolarization of I_h half activation voltage (*control*: -76±1mV, n=19; *bilateral CA*: -72±1mV, n=19; p≤0.05) (Fig.3.5B). Changes in current density and voltage dependence were, however, dependent on the tonotopic location of the neurons. Neurons in the high frequency limb of the LSO showed a larger increase in I_h current density (*control*: -113±25pA/pF, n=9; *bilateral CA*: -202±20pA/pF, n=10; p≤0.05) and a large depolarization of I_h half activation voltage (*control*: -80±1mV, n=9; *bilateral CA*: -70±1mV, n=10; p≤0.001) (Fig.3.5B *inset*) compared to neurons in the low frequency limb of the LSO, where the increase in I_h current density was much smaller (*control*: -108±10pA/pF, n=10; *bilateral CA*: -145±18pA/pF, n=9; p≤0.05) and the half activation voltage did not change (*control*: -72±2mV, n=10; *bilateral CA*: -75±1mV, n=9; n.s.). Capacitance changes induced by bilateral CA were only observed in the low frequency region of the LSO, where no neurons with capacitances above 35pF could be found anymore. Activation time constants changed neither in the high nor in the low frequency limb of the LSO (Fig.3.5C).

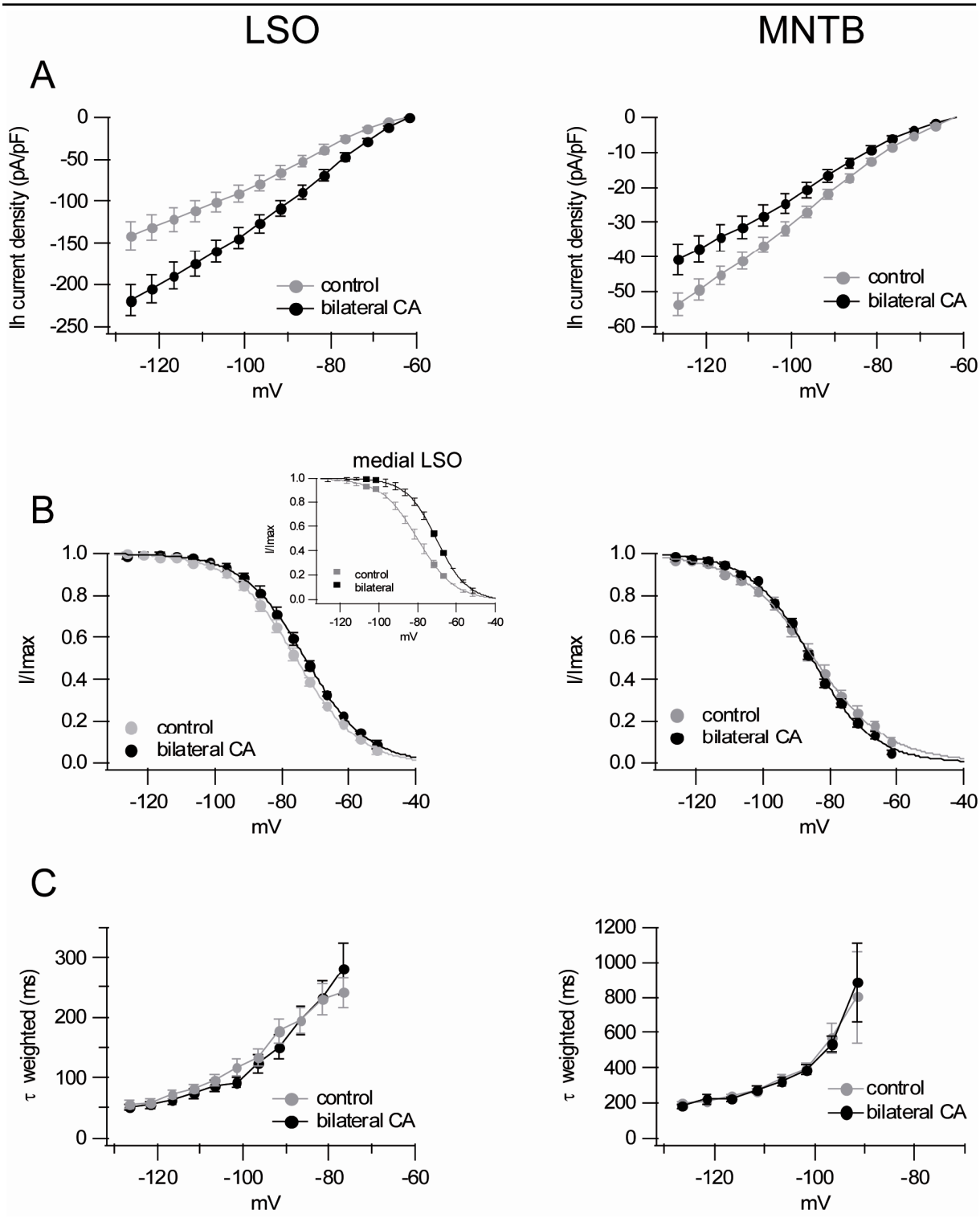

Figure 3.5: Bilateral cochlear ablations increase I_h in LSO neurons but decrease I_h in neurons of the MNTB. (A) Averages of I_h current density in LSO and MNTB neurons of control animals and of animals that were bilaterally cochlear ablated at P10. (B) Averages of normalized I_h tail current amplitudes of LSO and MNTB neurons of control and bilateral cochlear ablated (bilateral CA) animals. The inset in the right panel displays the averages of normalized tail current amplitudes of LSO neurons that were located in the medial (high frequency) limb of the LSO. (C) Averaged weighted I_h activation time constants of LSO and MNTB neurons in control and bilateral CA animals. Level of significance between the groups and the n-values for each group are stated in the results section.

In contrast to the LSO, at a comparable age (P17), the I_h current density in MNTB neurons was significantly reduced by bilateral cochlear ablation (*control*: -41±3pA/pF, n=19; *bilateral*

CA: -31±3pA/pF, n=15; p≤0.05) (Fig.3.5A). No significant changes in I_h activation time constant and I_h half activation voltage occurred in MNTB neurons (Fig.3.5B and C). Conversely to the LSO, the reduction in I_h current density in the MNTB was not dependent on the tonotopic arrangement of the neurons (*data not shown*). These results show that sensory deprivation differentially affects I_h currents in the LSO and the MNTB.

3.2.6 Bilateral cochlear ablation modulates the membrane properties of LSO neurons

A large increase in I_h current density and a positive shift of the voltage dependence should result in a decrease of membrane resistance and a change in the resting membrane potential of the sensory deprived neurons. This is especially true in the medial part of the LSO where changes in I_h current density are largest. To test this hypothesis, we compared the voltage responses to hyper- and depolarizing step current injections of control neurons and of neurons from bilateral CA animals exclusively from the high frequency, medial part of the LSO. As expected, injection of hyper- and depolarizing step currents resulted in smaller voltage changes in LSO neurons from bilateral CA compared to control animals (Fig.3.6A and B). On average LSO neurons from bilateral CA animals showed both a significantly lower input resistance at the peak (at -200pA: control: 45±5MΩ, n=7; bilateral CA: 29±4MΩ, n=6; p≤0.05) and the steady state voltage (at -200pA: control: 17±2MΩ, n=7; bilateral CA: 12±2MΩ, n=6; p≤0.05) (Fig.3.6C). Moreover, the resting membrane potential in bilateral CA animals was more depolarized compared to control animals (control: -64±1mV, n=7; bilateral CA: -59±1mV, n=6; p≤0.001) (Fig.3.6C).

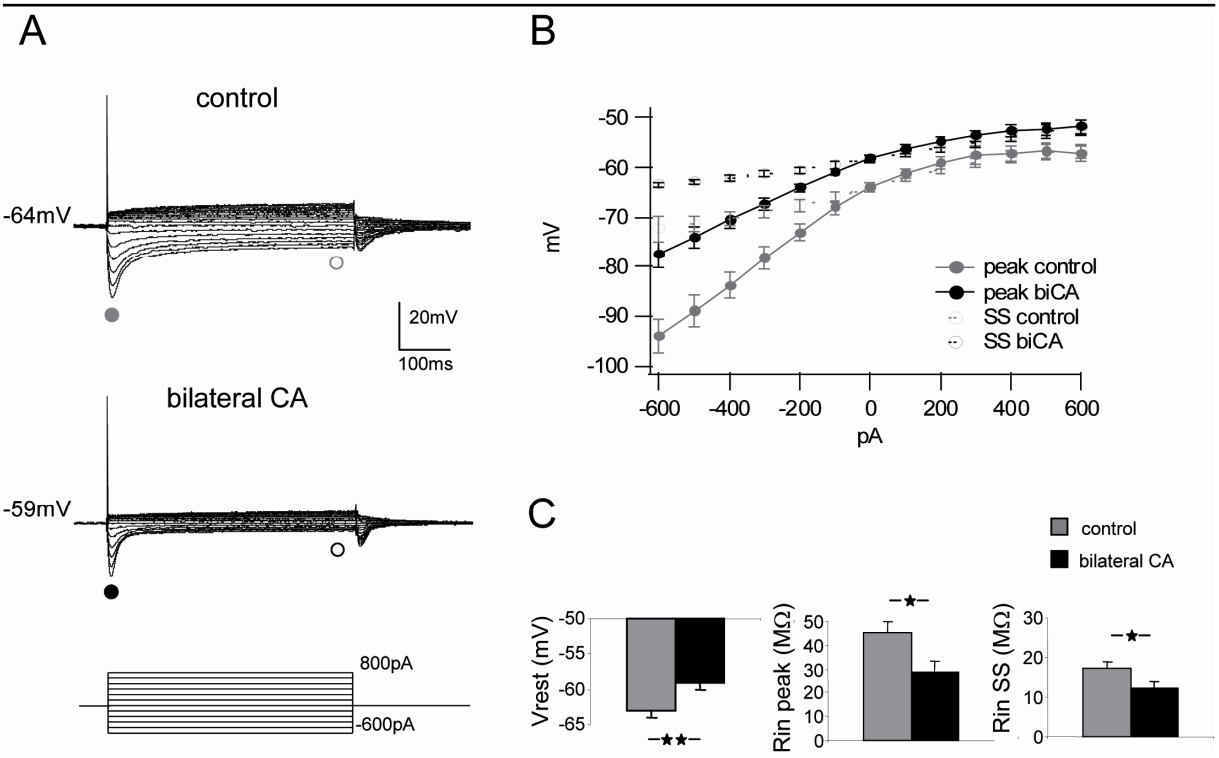

Figure 3.6: Bilateral cochlear ablations change the membrane properties of neurons in the high frequency region of the LSO. (A) Voltage responses to de- and hyperpolarizing current step injections (-600 to +800pA) of LSO neurons in control and bilateral CA animals. (B) Averaged voltage responses at the peak (•) and the steady state (◦) of LSO neurons in response to de- and hyperpolarizing current injections. (C) Averages of the resting membrane potential (V_{rest}), the peak (R_{in} peak) and the steady state (R_{in} SS) input resistance for -200pA step current injections in control and bilateral CA animals. The level of significance between the groups was determined by using the Student's unpaired *t*-test (* p≤0.05, ** p≤0.01, *** p≤0.001). The n-values for each group are stated in the results section.

3.2.7 Unilateral sensory deprivation changes I_h properties in the LSO

Neurons in the LSO receive an excitatory input from the ipsilateral cochlear nucleus and an inhibitory input from the ipsilateral MNTB, which is driven by sound activity from the contralateral ear. Here we tested whether a change in the balance of excitation and inhibition induced by unilateral deafening modulates I_h current properties in LSO neurons. Unilateral cochlear ablations resulted in a transient decrease in I_h current density at P14 on the ipsi- and the contralateral side (*control*: -119±11pA/pF, n=16; *ipsilateral CA*: -56±7pA/pF, n=12; *contralateral CA*: -32±7pA/pF, n=9; both p≤0.001) (Fig.3.7A). Moreover, the half activation voltage was shifted to more hyperpolarized potentials (*control*: -78±1mV, n=16; *ipsilateral CA*: -84±2mV, n=7; *contralateral CA*: -88±2mV, n=5; both p≤0.001). This could explain the previously observed increase in input resistance of LSO neurons a few days after unilateral cochlear ablation (Kotak and Sanes 1997). Only three days later, at P17, a small increase of I_h current density was observed ipsilateral to the ablated site, similar to the bilateral cochlea ablated animals (*control*: -110±12pA/pF, n=19; *ipsilateral CA*: -156±13pA/pF, n=16; p≤0.05) (Fig.3.7B). This increase was still present in 22-day-old animals (*control*: -144±20pA/pF, n=7; *ipsilateral CA*: -216±25pA/pF, n=6; p≤0.05) suggesting that a reduction of sound evoked

excitatory inputs slowly upregulates I_h. In contrast to bilateral cochlear ablations, there was no change in the voltage dependence. Ablation of the contralateral cochlea, which diminishes inhibitory neuronal activity, did not result in any significant changes of I_h current density after P14 (Fig.3.7B and D). This indicates that a reduction in inhibitory inputs alone is not sufficient to cause long-term changes in I_h properties. It is, however, also possible that other homeostatic mechanisms rebalance neuronal activity levels.

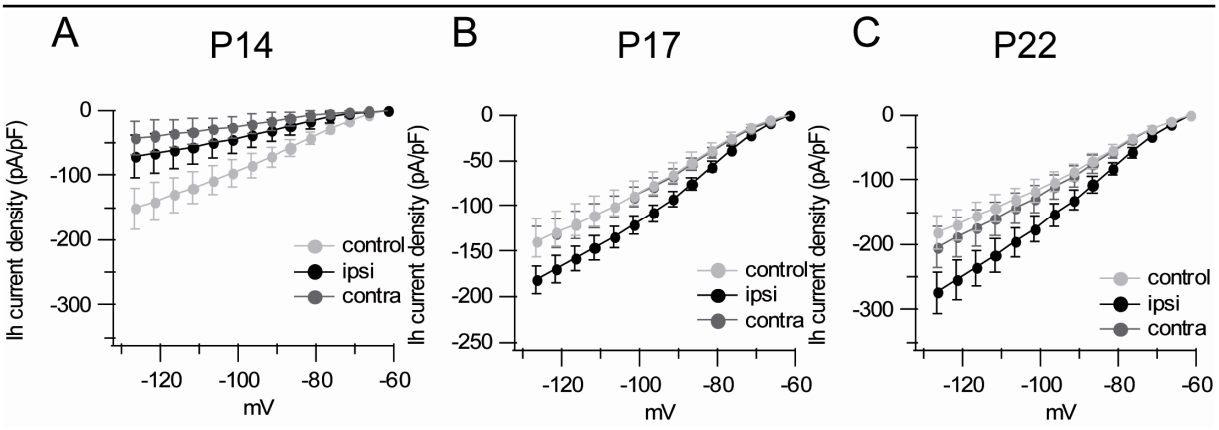

Figure 3.7: Unilateral cochlear ablation causes a transient bilateral decrease of I_h in LSO neuron around hearing onset. A few days later, at P17 and at P22, I_h is increased ipsilateral to the ablation, whereas no change occurs on the contralateral side. Averages of I_h current density of LSO neurons in P14 (A), P17 (B) and P22 (C) control animals and in age-matched unilateral cochlear ablated animals either ipsilateral or contralateral to the ablation. Level of significance between the groups and the n-values for each group are stated in the results section.

3.3 Discussion

The results of the present study demonstrate that the development of I_h current properties differs between LSO and MNTB neurons. Moreover, neuronal activity levels oppositely regulate I_h development in the two nuclei. In LSO neurons, the I_h current significantly increases within a few days after hearing onset, whereas during the same developmental period the increase of I_h in MNTB neurons is very small. Furthermore, at P17 LSO neurons have considerably larger I_h amplitudes, faster activation time constants and more depolarized voltage dependences compared to MNTB neurons, which corroborates previous data obtained in the mouse (Leao et al. 2006a). Changing neuronal activity levels by bilateral cochlear ablations before hearing onset causes an increase in I_h in LSO neurons, and also alters the integrative membrane properties of these cells. Conversely, MNTB neurons display a small decrease in I_h amplitude after sensory deprivation. We suggest that these differences in I_h development and regulation between the LSO and the MNTB could be a reflection of the different HCN subunits expressed in the respective nuclei (Koch et al. 2004; Leao et al. 2006a; Notomi and Shigemoto 2004).

3.3.1 Developmental changes in I_h properties differ between the LSO and the MNTB

Here we show that shortly after hearing onset, which occurs around P12, I_h amplitude of LSO neurons considerably increases, the activation time constant accelerate and the voltage activation shifts to more depolarized potentials. As a result the membrane properties of LSO neurons, such as input resistance and membrane time constant, profoundly change during the first days after hearing onset reaching similar levels in the low frequency region to neurons in the MSO (Magnusson et al. 2005; Scott et al. 2005). Since I_h strongly attenuates temporal summation of excitatory and inhibitory inputs (Koch and Grothe 2003; Magee 1999), LSO neurons in mature animals are likely to analyze their excitatory and inhibitory inputs with high temporal fidelity and little temporal integration.

Recent experiments show that developmental changes of I_h properties in hippocampal CA1 pyramidal neurons are similar to the present results (Surges et al. 2006). In these neurons changes in I_h properties are correlated to a relative increase in the HCN1 subunit expression, whereas the HCN2 and HCN4 subunit expression levels remain the same during postnatal development (Surges et al. 2006; Vasilyev and Barish 2002). A similar mechanism, namely a change in the HCN subunit composition from a mixed HCN1, HCN2, and HCN4 composition in immature animals to a predominant HCN1 composition in more mature animals, could also be the underlying cause for the acceleration of membrane time constants and the shift in the voltage dependence in LSO neurons. In contrast, developmental changes in I_h properties were much smaller in MNTB neurons, where I_h is mostly generated by HCN2 and HCN4 subunits that are expressed early during development and may display only small developmental changes in analogy with hippocampus (Surges et al. 2006; Vasilyev and Barish 2002).

3.3.2 Neuronal activity regulates I_h current amplitude

The profound up-regulation of I_h in LSO neurons directly after hearing onset strongly suggests that neuronal activity levels, which increase considerably with the onset of sound evoked activity (Kotak and Sanes 1995; Sanes and Rubel 1988), regulate I_h amplitude and properties. However, opposite to our expectations, sensory deprivation before hearing onset up-regulates I_h, shifts the voltage dependence of the current to a more positive potential and reduces the input resistance in principal neurons of the LSO. In a similar study in adult rats sensory deprivation depolarizes the resting membrane potential and decreases the membrane time constants and the input resistance in presumed bushy cells of the anteroventral cochlear nucleus (Francis and Manis 2000). Since bushy cells have large I_h

conductances (Cao et al. 2007), these changes might result from an up-regulation of I_h current in these neurons. In contrast, bushy cells in mutant deaf mice show no change in excitability or I_h amplitude, whereas in these mice I_h is up-regulated in MNTB neurons (Leao et al. 2005). These diverging effects depending on the auditory deprivation model point to the complexity of factors that regulate ion channel density and function in auditory brainstem neurons. An important question arising is how consistent the activity-dependent regulation of I_h is in other brain structures and whether it is dependent on the underlying HCN subunit. In cortical structures, a massive increase in neuronal activity during seizure activity causes a chronic decrease of I_h. For example, pharmacological induced seizures strongly reduce I_h current density and negatively shift the voltage dependence of the I_h current in pyramidal neurons of the hippocampal CA1 region and the enterorhinal cortex (Jung et al. 2007; Shah et al. 2004). This is also paralleled by a hyperpolarization of the resting membrane potential and an increase in input resistance of these neurons.

Moreover, previous studies have shown that activity-dependent changes in I_h are dependent on the subunits expressed in the respective neurons. Whereas HCN1 protein or mRNA levels consistently decrease after seizure activity (Jung et al. 2007; Richichi et al. 2008), HCN2 subunit levels can either increase or decrease dependent on the experimental situation (Brewster et al. 2002; Jung et al. 2007; Richichi et al. 2008). This could also explain why in contrast to the down-regulation of I_h in MNTB neurons by cochlear ablations, MNTB neurons in mutant deaf mice showed increased I_h amplitudes compared to normal hearing mice (Leao et al. 2005).

An alternative explanation for the differences in I_h regulation between cochlear ablated and mutant deaf mice could be different compensatory changes induced in the two deafness models. Anatomical labeling with activity markers has shown that total activity levels in auditory brainstem are substantially lower in unilateral and bilateral cochlear ablated animals or animals with genetic hearing loss (Durham et al. 1989; Tucci et al. 1999). Moreover, one study in the chicken indicate that the activity levels are virtually absent in the ipsilateral nucleus magnocellularis (analogue to cochlear nucleus) several hours after unilateral cochlear ablation (Born et al. 1991). However, to compensate for the decreased activity levels, bilateral cochlea ablated and congenitally deaf mice display a variety of synaptic adaptations such as increased release probability and receptor strength which are dependent on the specific synapse studied and the deafness model (Cao et al. 2008; Durham et al. 1989; Futai et al. 2001; Leao et al. 2004; Oleskevich and Walmsley 2002; Oleskevich et al. 2004; Tucci et al. 1999). In this respect, the observed increase in I_h in LSO neurons and the decrease in MNTB neurons cochlear ablations might be another mechanism by which the auditory brainstem nuclei recover some neural activity. Interestingly, the

olivocochlear efferent system has been shown to exert bilateral control of the auditory-nerve excitability (Darrow et al. 2006). A retrograde degeneration of the efferent terminals could therefore, following a unilateral cochlear ablation, affect the excitability of the remaining input driving the excitatory and inhibitory inputs to the LSO.

3.3.3 Mechanism of I_h modulation

A possible mechanism underlying the observed changes in I_h properties could be a change in transcription rate or turn-over rate of the HCN channels. Alternatively, these changes could also be due to alterations in basic second messenger activity such as cAMP which profoundly modulates HCN channel properties (Ludwig et al. 1998; Wainger et al. 2001). In fact, chronic changes in I_h amplitude induced by cortical seizures were in most cases paralleled by a change in HCN mRNA (Brewster et al. 2002; Richichi et al. 2008) or protein level (Jung et al. 2007; Shah et al. 2004). This indicates that neuronal activity can regulate I_h on the transcriptional level, a mechanism that depends on calcium influx (Richichi et al. 2008). Whether this is also the case following cochlear ablations remains to be determined in future experiments. What are the underlying mechanisms for the changes in voltage dependence and the activation time constant and how do these factors correlate to changes in I_h amplitude? The voltage dependence and the activation time constant of I_h are determined by the HCN subunit composition, but can also be transiently regulated by second messengers such as cAMP (Ludwig et al. 1998; Wainger et al. 2001). Therefore, changes in cAMP levels induced by the activation of G-protein coupled receptors could alter I_h properties (Frere and Luthi 2004; Ulens and Tytgat 2001). One possibility is that basal cAMP levels are modulated in LSO neurons of cochlear ablated animals there by shifting the voltage dependence of I_h in these cells. However, it is also possible that the responsiveness of the HCN channels to cAMP-levels is altered by cochlear ablations due to differences in the subunit composition or the heteromerization of the channels which both can be modulated by neuronal activity levels (Brewster et al. 2005; Zha et al. 2008).

3.3.4 Functional consequences of I_h modulation in the auditory brainstem

In this study we demonstrate an increase in I_h current amplitude in the LSO following auditory sensory deprivation. Since I_h modulates the excitability of neurons by two opposing effects, namely by a depolarization of the resting membrane potential which increases excitability, and by a decrease in input resistance rendering synaptic inputs less efficient, it is unclear

what net effect increased I_h currents have on the excitability of LSO neurons. Therefore, changes in the functional excitability can go either way depending on the relative contribution of the two effects (Fan et al. 2005; Jung et al. 2007). In the LSO, pharmacological up-regulation of I_h with forskolin, a cAMP activator generates an increase in spontaneous and sound-evoked discharge activity *in vivo* (Shaikh and Finlayson 2005), whereas pharmacological blockade of I_h decreases the excitability of these neurons (Shaikh and Finlayson 2003). The underlying mechanism could be related to the more positive voltage dependence of I_h in LSO neurons which causes a substantial depolarization of the resting membrane potential closer to spike threshold and thereby increases excitability in these neurons. It would be interesting to explore whether such a change in excitability, induced by an activity-dependent up-regulation of I_h, could relate to pathological conditions such as tinnitus and hyperacusis.

4 THE MAMMALIAN ITD DETECTION CIRCUIT IS DIFFERENTIALLY CONTROLLED BY $GABA_B$ RECEPTORS DURING DEVELOPMENT

4.1 Introduction

Neurons in the medial superior olive (MSO), a nucleus in the mammalian auditory brainstem, analyze sound direction based on interaural time differences (ITDs) (Brand et al. 2002; Goldberg and Brown 1968; Spitzer and Semple 1995; Yin and Chan 1990). This is achieved using a coincidence detection mechanism, which compares the relative arrival times of the two excitatory inputs deriving from the contralateral and the ipsilateral anteroventral cochlear nucleus (AVCN) (Cant and Casseday 1986; Skottun 1998). In addition, MSO neurons receive major inhibitory projections originating from the medial and the lateral nucleus of the trapezoid body (MNTB and LNTB) (Cant and Hyson 1992; Grothe and Sanes 1993; Kuwabara and Zook 1992) (Fig.4.1A). These inhibitory inputs adjust the output signal of MSO neurons such that large changes in the discharge rate are occurring within the physiological relevant range of ITDs an animal experiences (Brand et al. 2002; Pecka et al. 2008).

In adult animals, this inhibition is mediated by glycine (Helfert et al. 1989; Smith et al. 2000). Yet, in neonatal animals up to postnatal day 12 (P12), gamma-aminobutyric acid (GABA) also represents an important inhibitory transmitter, as MNTB fiber stimulation activates $GABA_A$ receptor mediated currents in neurons of the medial and lateral superior olive (Kotak et al. 1998; Kullmann et al. 2002; Nabekura et al. 2004; Smith et al. 2000). In most brain regions, GABA not only induces a chloride current via $GABA_A$ receptors, but also activates the metabotropic $GABA_B$ receptor ($GABA_BR$). On the postsynaptic site, $GABA_BR$ activation triggers a direct inhibitory action via the activation of potassium channels (Luscher et al. 1997; Nicoll 2004; Pitler and Alger 1994). Presynaptically situated $GABA_BRs$ modulate the release probability of inhibitory and excitatory neurotransmitters by depressing Ca^{2+}-currents (Isaacson 1998; Takahashi et al. 1998; Wojcik and Neff 1984). Additionally, $GABA_BRs$ can be indirectly involved in long-term plastic changes of synaptic efficacy (Chang et al. 2003; Kamikubo et al. 2007). In the mature auditory brainstem, $GABA_BRs$ primarily contribute to the dynamic regulation of transmitter release. We have previously shown that in the lateral superior olive (LSO), $GABA_BR$ activation by retrogradely released GABA regulates the balance of excitation and inhibition and thereby adjusts the sensitivity of these neurons to interaural intensity differences (Magnusson et al. 2008). Furthermore, presynaptic $GABA_BRs$ have been implicated in decreasing short-term synaptic depression and might thereby improve faithful synaptic transmission for the representation of sound structure (Brenowitz et

al. 1998; Mapelli et al. 2009). Preliminary immunostainings have revealed that in the auditory brainstem $GABA_B$Rs are not only present before hearing onset, when the MNTB releases both GABA and glycine, but also in adult animals, when the MNTB input has become glycinergic (Heise et al. 2005; Hilbig et al. 2007). The primary goal of this study was to determine whether the $GABA_B$R mediated regulation of the main excitatory and inhibitory inputs to the MSO changes during development. Moreover, we wanted to show to what extent endogenous $GABA_B$R activation in the MSO is altered during this developmental period.

4.2 Results

4.2.1 $GABA_B$ receptors modulate all four major inputs to MSO neurons

Neurons in the medial superior olive (MSO) show strong immunoreactivity against $GABA_B$ receptors ($GABA_B$Rs) (Fig.4.1B, *left panel*). At higher magnification, this staining appears punctuated with a distribution over the entire cell body and along the proximal dendrites (Fig.4.1B, *right panel*), which suggests a functional role of $GABA_B$Rs in MSO neurons. Using whole-cell voltage-clamp recordings from MSO neurons in acute brain slices, we investigated whether pharmacological activation of $GABA_B$Rs modulates the excitatory and inhibitory inputs to MSO neurons. These experiments, as well as the immunolabeling in Fig.4.1B were performed in 19-day-old animals, an age when the properties of the excitatory and inhibitory inputs to the MSO are considered to be adult-like (Magnusson et al. 2005; Scott et al. 2005; Sonntag et al. 2009). In adult animals, MSO neurons receive two excitatory glutamatergic inputs from the ipsi- and contralateral AVCN and two inhibitory glycinergic inputs from the ipsilateral MNTB and LNTB (Fig.4.1A). Inhibitory and excitatory postsynaptic currents (IPSCs and EPSCs) were evoked by either stimulation of the ipsi- or contralateral fiber tract to MSO neurons. Since the excitatory and inhibitory inputs from each side run in the same fiber bundle (Cant and Hyson 1992; Grothe and Sanes 1993; Kuwabara and Zook 1992; Smith et al. 1993), fiber stimulation usually resulted in a mixed excitatory/inhibitory response. For this reason EPSCs and IPSCs had to be isolated pharmacologically by antagonizing either the excitatory or the inhibitory inputs, respectively (*see methods*).

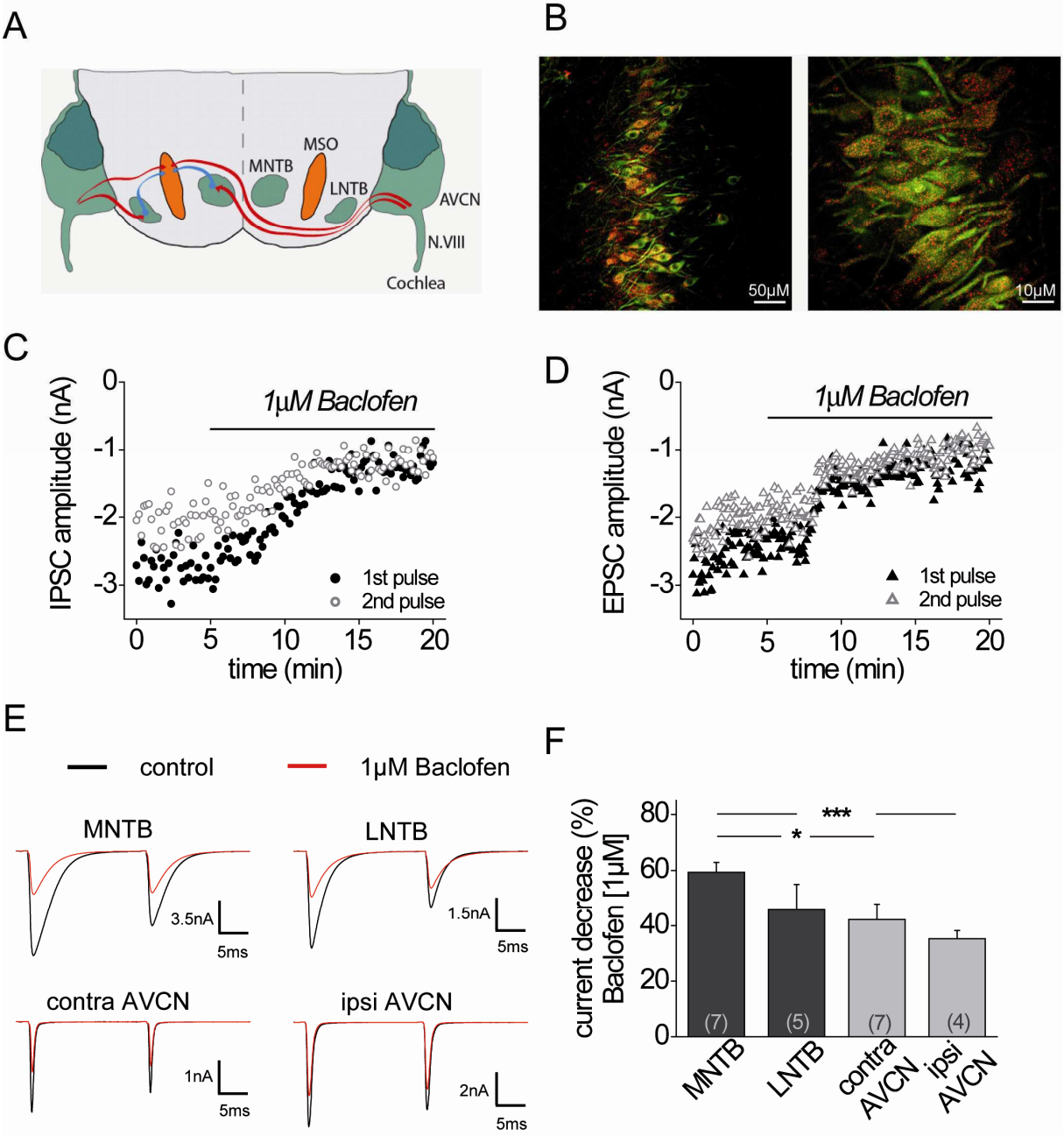

Figure 4.1: Pharmacological activation of GABA$_B$Rs depresses excitatory and inhibitory currents at all four major inputs to the MSO. (A) The MSO circuit with its respective inputs from the MNTB, LNTB ipsi- and contralateral AVCN (red afferents: excitatory, blue afferents: inhibitory). (B) Fluorescent GABA$_B$R staining of the MSO in P19 gerbils (red: GABA$_B$R1; green: MAP2). *left panel* GABA$_B$Rs were expressed along the entire dorso-ventral extent of the MSO (scale bar, 50µm). *right panel* Cytosolic as well as marginal GABA$_B$R1 staining was detectable (scale bar 10µm). (C) Example time course of IPSC amplitude depression during bath-application of Baclofen (MNTB fiber stimulation). (D) Example time course of EPSC amplitude depression during bath-application of Baclofen (contralateral AVCN fiber stimulation). (E) *top panels* IPSCs under control and Baclofen conditions. *bottom panels* EPSCs under control and Baclofen conditions (examples display averaged evoked responses). (F) Summary and statistics of the modulatory effect of Baclofen on current amplitude for all major inputs to the MSO. (asterisks represent *P*-values obtained by Student's two-tailed unpaired *t* test)

To find out whether GABA$_B$R activation regulates MSO inputs, GABA$_B$Rs were pharmacologically activated by bath-application of Baclofen [1µM], a concentration that lies within the dynamic part of the dose-response-curve for excitatory and inhibitory currents (Fig.4.2). As depicted in Figure 4.1C and D Baclofen rapidly decreased the amplitude of both evoked IPSCs and evoked EPSCs. In general, both excitatory and inhibitory inputs projecting

to the MSO profoundly decreased in amplitude upon activation of $GABA_B$Rs by Baclofen application (Fig.4.1E). (*MNTB*: control -6.9 ± 1.2nA, Baclofen -2.8 ± 0.5nA, n=7; *LNTB*: control -1.7 ± 0.5nA, Baclofen -0.8 ± 0.2nA, n=5; *contra AVCN*: control -3.1 ± 0.6nA, Baclofen -1.9 ± 0.6nA, n=7; *ipsi AVCN*: control -3.3 ± 1.0nA, Baclofen -2.1 ± 0.6nA, n=4). However, the relative decrease of current amplitude by Baclofen application was strongest for MNTB inputs whereas the excitatory inputs were significantly less affected (*MNTB*: 59.4 ± 3.5%, n=7; *contra AVCN*: 42.2 ± 5.8%, n=7; *LNTB*: 45.8 ± 9.2%, n=5; *ipsi AVCN*: 35.3 ± 2.9%, n=4; *MNTB-contra AVCN*: $P \leq 0.05$; *MNTB-ipsi AVCN*: $P \leq 0.001$) (Fig.4.1F). On the contrary, the time course (decay time) of both the inhibitory or excitatory currents was not changed by pharmacological activation of $GABA_B$Rs with Baclofen [1µM] (*data not shown*).

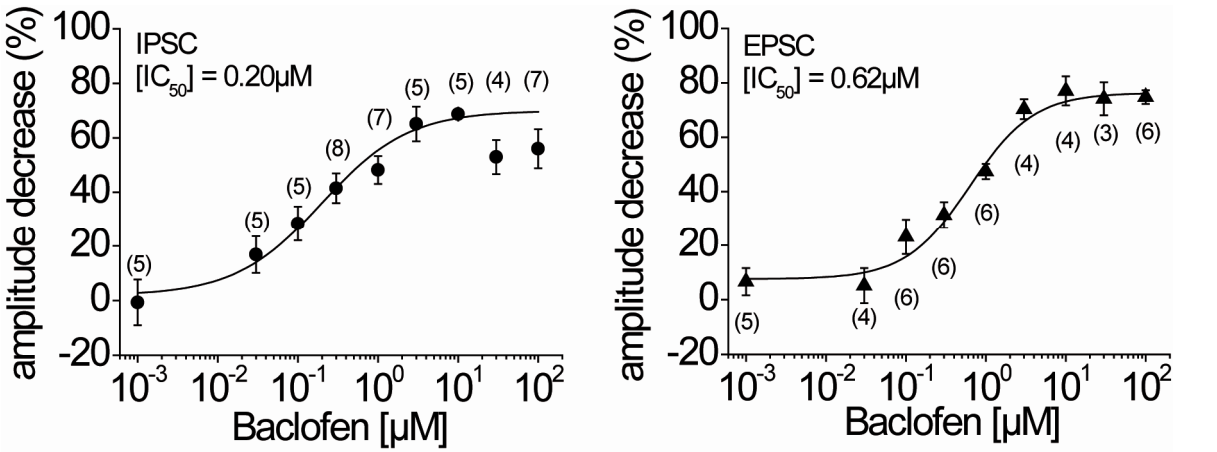

Figure 4.2: Baclofen modulates inhibitory and excitatory currents within a similar dynamic range in the MSO. *left panel* Dose-response-curve for the effect of Baclofen on IPSC amplitudes mediated by $GABA_B$R activation in P14 animals ($[IC_{50}]$=0.20µM). *right panel* Dose-response-curve for the effect of Baclofen on EPSC amplitudes mediated by $GABA_B$R activation in P14 animals ($[IC_{50}]$=0.62µM).

4.2.2 The relative effect of $GABA_B$R activation on inhibitory and excitatory currents changes during development

Before hearing onset, which occurs around P12, the MNTB projections to the lateral superior olive (LSO) and the MSO undergo several structural and functional changes. Most importantly, these inputs change from a mixed GABA/glycinergic to a pure glycinergic transmitter phenotype (Kotak et al. 1998; Kullmann et al. 2002; Nabekura et al. 2004; Smith et al. 2000). In addition, this input switches from being depolarizing to hyperpolarizing due to a significant decrease in the postsynaptic chloride concentration (Kakazu et al. 1999; Kandler and Friauf 1995; Lohrke et al. 2005). Our next goal was to determine whether $GABA_B$Rs might be involved in these functional changes. Therefore, we quantified $GABA_B$R induced input modulation in MSO neurons considerably before hearing onset (P9), shortly after hearing onset (P14), at a more mature stage (P19) and from mature animals (P32) by application of Baclofen [1µM]. In all age groups tested, Baclofen depressed the inhibitory

inputs evoked by MNTB fiber stimulation. Interestingly, this $GABA_BR$ mediated effect on the inhibitory inputs remained approximately constant during all developmental stages tested (Fig.4.3A). In contrast, $GABA_BR$ mediated depression of the excitatory, glutamatergic inputs decreased significantly after hearing onset (*P9 contra AVCN*: 78.1 ± 2.7%, n=5; *P14 contra AVCN*: 47.4 ± 2.8%, n=6; $P \leq 0.001$) (Fig.4.3B). This decrease of $GABA_BR$ mediated regulation of the excitatory inputs continued up to P32 when input properties are generally considered to be mature (*P19 contra AVCN*: 42.2 ± 5.7%, n=7; *P32 contra AVCN*: 19.6 ± 2.5%, n=4; $P \leq 0.05$) (Fig.4.2B). Similar developmental changes of $GABA_BR$ mediated modulation of inputs were observed for the projections from the LNTB and the ipsilateral AVCN (Tab.4.1). Taken together, these data suggest that before hearing onset $GABA_BRs$ more strongly regulate the excitation, whereas in the matured system their effect mainly remains in regulating the inhibitory input strength.

	contralateral stimulation		**ipsilateral stimulation**	
	inhibition	**excitation**	**inhibition**	**excitation**
P9	48.2 ± 4.5% n=7	78.1 ± 2.7% n=5	47.2 ± 4.2% n=4	71.8 ± 4.9% n=5
P14	48.2 ± 5.1% n=7	47.4 ± 2.8% n=6	–	–
P19	59.4 ± 3.5% n=7	42.2 ± 5.7% n=7	45.8 ± 9.2% n=5	35.3 ± 2.9% n=4
P32	46.5 ± 10.7% n=4	19.6 ± 2.5% n=4	–	–

Table 4.1: Values show the decrease in current amplitude by Baclofen [1µM] and are normalized to control conditions. Effect of Baclofen [1µM] on ISPC and EPSC amplitudes evoked by stimulation of the respective input fibers recorded from neurons in the MSO.

4.2.3 $GABA_BR$ immunostaining changes from a predominantly dendritic to a mostly somatic location during development

This developmental decrease of Baclofen effect on the excitatory MSO inputs was corroborated by immunostainings against the $GABA_BR1$ subunit in fixed tissue sections at different developmental stages (P7, P19, P30). In general, MSO neurons showed antibody reactivity for $GABA_BRs$ at all age groups tested (Fig.4.3C). Nevertheless, differences between the age groups became obvious by qualitatively comparing the distribution pattern of $GABA_BR$ staining with the general dendritic MAP2 staining. At P7, $GABA_BR$ staining was profound in the dendritic region medial and lateral to the MSO somata whereas the somatic

region was only slightly immunoreactive. In contrast, at P19 and even more pronounced later during development (at P30) $GABA_BR$ immunoreactivity was considerably stronger at the MSO somata, whereas an obvious decrease of dendritic staining was detectable compared to gerbils before hearing onset. Physiological and anatomical data together strongly indicate a developmental change of the presynaptic $GABA_BR$ distribution. During early developmental stages $GABA_BRs$ seem to be mainly located on the excitatory inputs, which mostly terminated on the dendrites (Clark 1969; Russell and Moore 1999; Stotler 1953). In more mature animals $GABA_BRs$ seem to be predominantly located on the presynaptic inputs at the soma, which are mostly glycinergic and thus inhibitory (Kapfer et al. 2002).

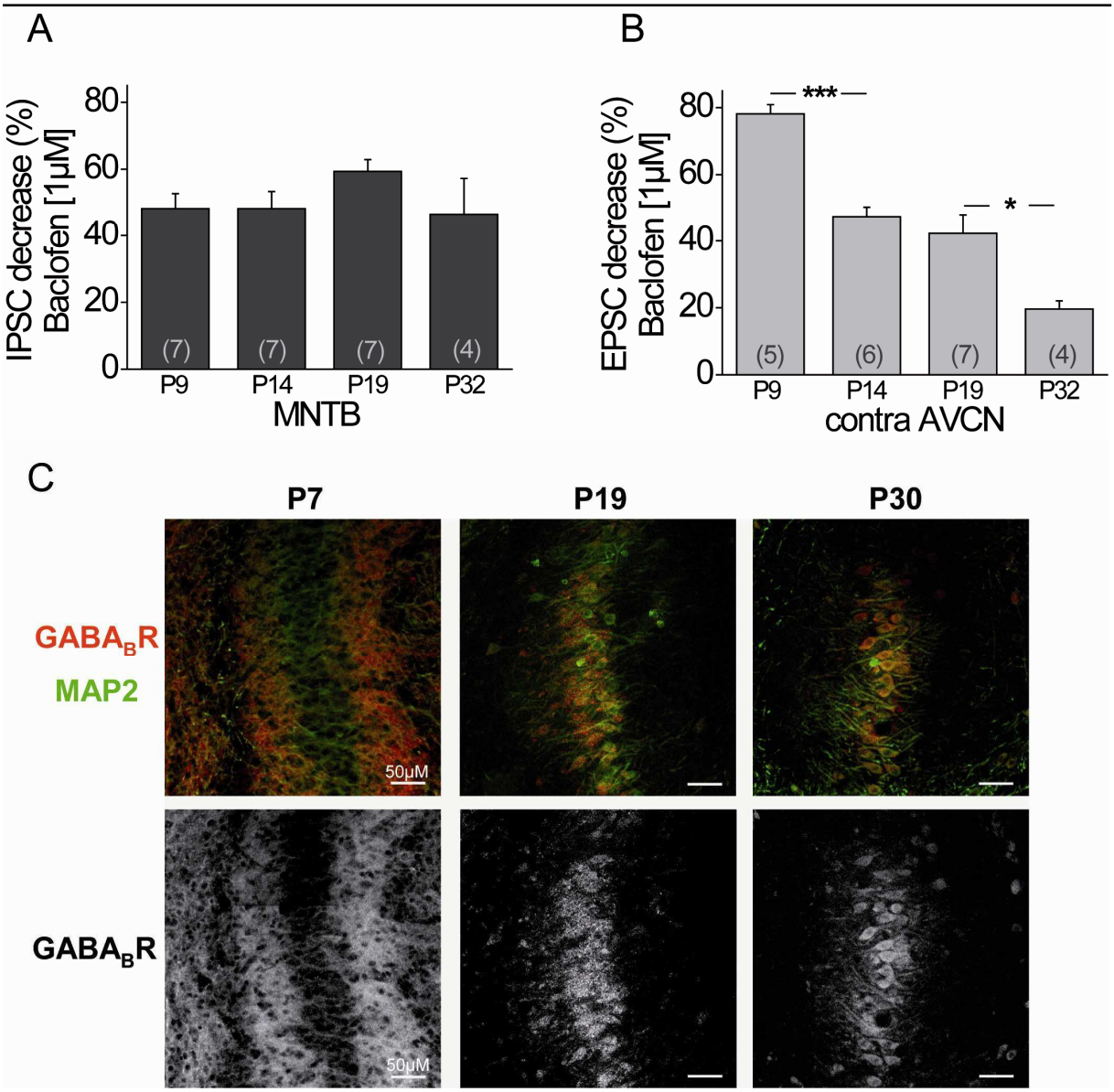

Figure 4.3: Physiological efficiency and anatomical distribution of $GABA_BRs$ changes during maturation for excitatory but not inhibitory inputs. (A) Average decrease of normalized IPSC amplitudes by Baclofen [1µM] for different age groups (MNTB fiber stimulation). (B) Average decrease of normalized EPSC amplitudes by Baclofen [1µM] for different age groups (contralateral AVCN fiber stimulation). (C) *top panels* Antibody labeling in the MSO against $GABA_BR1$ (*red*) and MAP2 (*green*) at different developmental stages *bottom panels* isolated immunofluorescence of $GABA_BR1$ (scale bars: 50µm). (asterisks represent *P*-values obtained by Student's two-tailed unpaired *t* test)

4.2.4 At all developmental stages $GABA_B$Rs control transmitter release probability on the excitatory and inhibitory inputs to MSO principal neurons

In most cases modulation of input strength by $GABA_B$R activation is achieved either by presynaptic changes in release probability or by postsynaptic activation of K^+-currents. Since in the previous experiments postsynaptic potassium channels were blocked pharmacologically (*see methods*), the above-described decrease in synaptic strength by Baclofen application is likely to be induced via activation of presynaptically situated $GABA_B$Rs. In order to test this hypothesis, we analyzed the paired pulse ratios (PPRs) of evoked IPSCs and EPSCs before and during pharmacological activation of $GABA_B$Rs. For both excitation and inhibition, Baclofen significantly increased the PPR before (P9) and after hearing onset (P19), most likely reflecting a reduction in transmitter release probability at the given presynaptic input (Fig.4.4A). We also analyzed the coefficient of variation (CV), an additional measurement to estimate changes in presynaptic release probability, for all major MSO inputs. Current amplitudes exhibited a stronger fluctuation in peak sizes after application of Baclofen (Fig.4.4B). To visualize this effect we show a Gaussian function fitted to the IPSC amplitude distribution evoked by MNTB stimulation. As for the PPR, Baclofen application increased the CV for excitatory and inhibitory inputs before and after hearing onset. Finally, the mean frequency of both, inhibitory and excitatory spontaneous events recorded in the absence of tetrodotoxin (TTX) declined significantly during Baclofen application for both pre-hearing and more mature animals (Fig.4.4C). Taken together, these data suggest that the observed reduction in input strength by $GABA_B$R activation is achieved by a reduction in transmitter release probability via presynaptic $GABA_B$Rs before hearing onset as well as later during development.

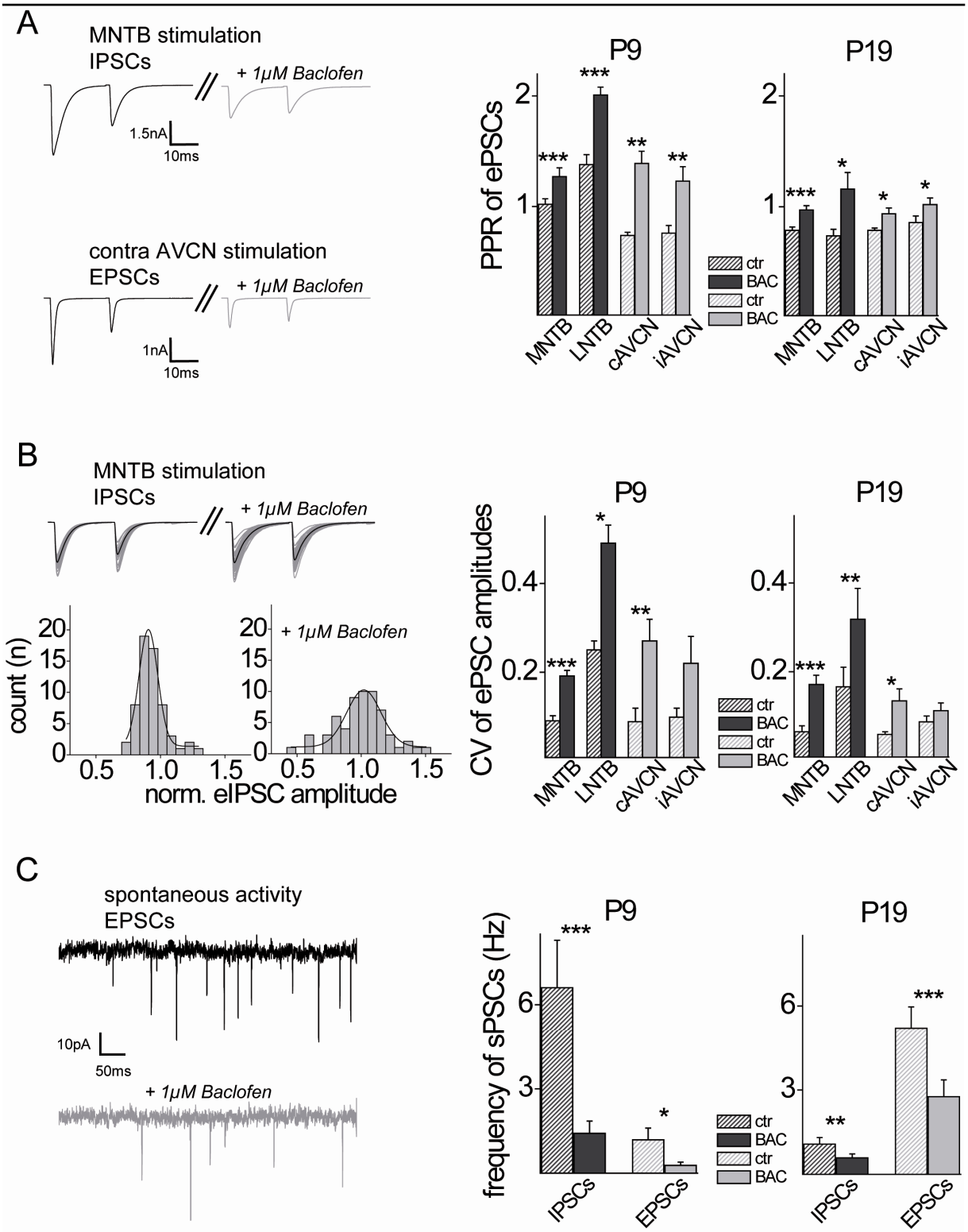

Figure 4.4: GABA$_B$Rs are located presynaptically at inhibitory and excitatory inputs to the MSO before and after hearing onset. (A) *left* PPR of IPSCs and EPSCs decreased during exposure to Baclofen (examples display averaged evoked responses of P19 neurons). *right* Summary and statistics of Baclofen [1µM] induced changes in PPR for all stimulation conditions in animals before (P9) and after (P19) hearing onset. (B) *left top* Single IPSCs (grey) illustrate the scatter around the mean (black) under control conditions and during Baclofen application in a P19 animal (IPSC amplitudes during Baclofen conditions were normalized to the mean of the first IPSCs under control conditions). *left bottom* Distribution of normalized IPSC amplitudes under control conditions and during Baclofen application. Gaussian fit for the variance of IPSC amplitudes around the mean became broader during Baclofen application. *right* Quantification of CVs of normalized evoked postsynaptic currents (ePSCs) for control conditions and with Baclofen for the two age groups. (C) *left* Example raw traces of spontaneous excitatory activity under control conditions (black) and during Baclofen exposure (grey). *right* Quantification of inhibitory and excitatory spontaneous activity changes induced by application of Baclofen [1µM]. (ctr: control; BAC: Baclofen) (asterisks represent *P*-values obtained by Student's two-tailed paired *t* test)

4.2.5 Before hearing onset MNTB fiber stimulation activates presynaptic $GABA_B$Rs

During early pre-hearing postnatal stages, LSO and MSO neurons receive a mixed GABAergic and glycinergic inhibition from inputs originating from the MNTB, whereas after hearing onset inhibitory transmission from the MNTB is predominantly glycinergic (Kotak et al. 1998; Smith et al. 2000). Hence, we next asked the question if in young animals (P8) GABA release from MNTB fibers activates $GABA_B$Rs and thereby modulates the glycinergic and/or glutamatergic inputs to MSO neurons. If, at this age, MNTB neurons indeed release GABA together with glycine from their terminals, this should activate $GABA_B$Rs located presynaptically on the same synapse and thereby decrease the release probability of the glycinergic transmission. This was tested by analyzing the amplitude of the glycinergic inhibitory currents in response to a test stimulus 200ms after a high frequency train stimulation of MNTB fibers (100Hz, 200ms). If $GABA_B$Rs were activated during this high frequency stimulation, the $GABA_B$R antagonist SCH50911 [10µM] should block the $GABA_B$R induced decrease in transmitter release probability of the glycinergic input. Surprisingly, pharmacological blockade of $GABA_B$Rs did not induce a significant change in the amplitude of the inhibitory current at this developmental stage (7.8 ± 5.6%, n=5) (Fig.4.5A and E). This suggested that high frequency firing of the MNTB inputs alone was not sufficient to elevate the GABA concentration high enough to activate $GABA_B$Rs effectively. However, performing the same experiment but applying the GABA uptake blocker NO711 [50µM] to increase the overall GABA concentration, resulted in a significant decrease in the IPSC amplitude (38.2 ± 5.3%, n=5; $P \leq 0.01$) (Fig.4.5B and E). This decrease in IPSC amplitude was completely abolished by the $GABA_B$R antagonist SCH50911 [10µM] (-1.8 ± 4.7%, n=4) (Fig.4.5C and E) and differed significantly from application of NO711 alone ($P \leq 0.01$).

Before hearing onset MNTB fibers also terminate on the dendrites of MSO neurons (Kapfer et al. 2002; Werthat et al. 2008) which also receive the majority of excitatory inputs from the ipsi- and contralateral AVCN (Clark 1969; Russell and Moore 1999; Stotler 1953). Therefore, GABA released from MNTB fibers should potentially also activate $GABA_B$Rs located on the excitatory presynaptic terminals, which at this developmental stage show high sensitivity to very low concentrations of Baclofen (see Fig.4.3B). Indeed, stimulating the fibers of the trapezoid body as in the previous experiment in combination with the application of the GABA uptake blocker NO711 resulted in a decrease of the excitatory currents similar to that observed for the inhibitory currents (25.7 ± 8.0%, n=4; $P \leq 0.05$) (Fig.4.5D and E). This indicates that before hearing onset GABA release most likely originating from MNTB terminals controls transmitter release via $GABA_B$R activation of both the excitatory and the inhibitory inputs of MSO neurons.

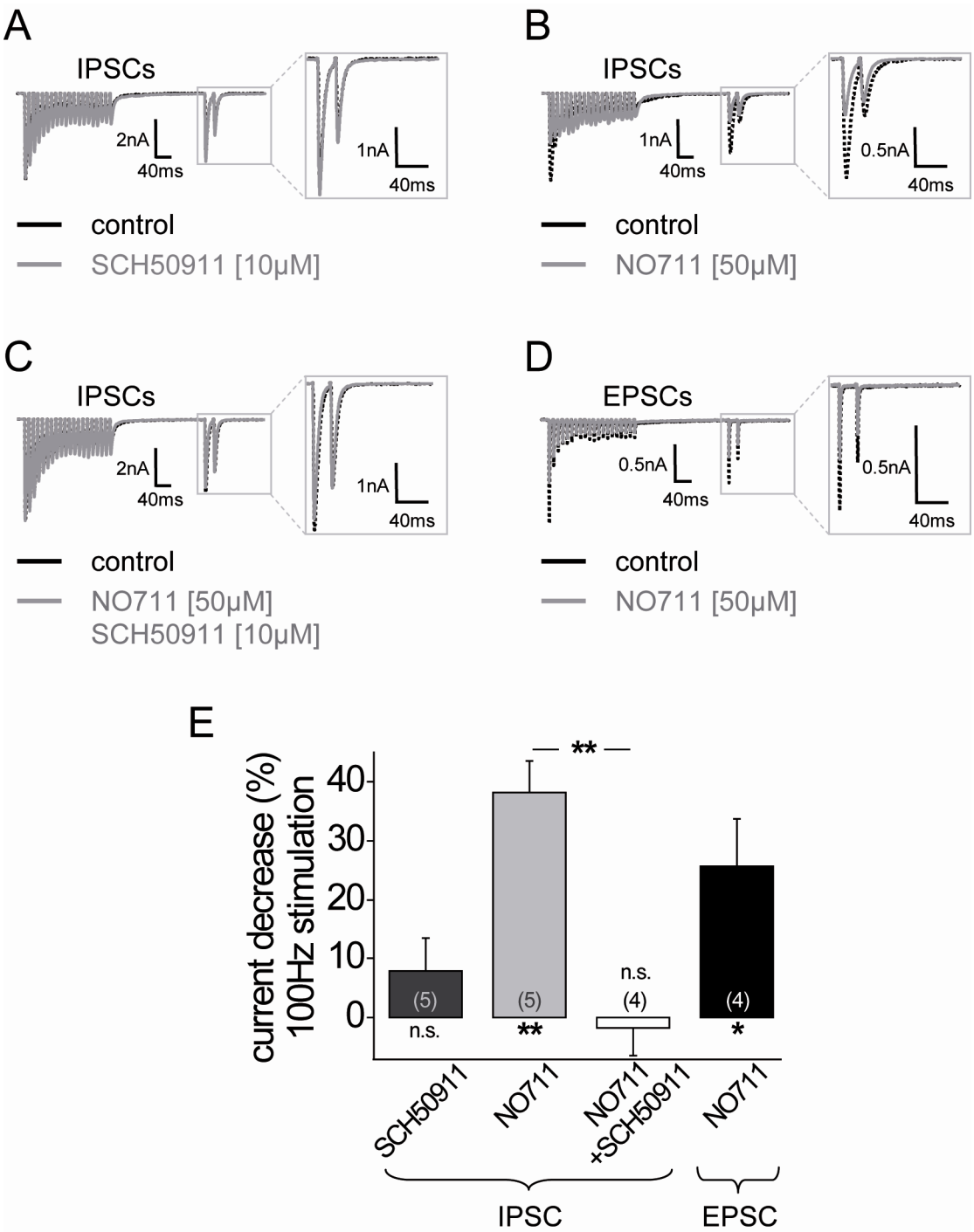

Figure 4.5: Before hearing onset (P8) high frequency MNTB fiber stimulation activates GABA$_B$Rs at the excitatory and inhibitory MSO inputs, but only under the prerequisite of a GABA uptake inhibitor. (A) Example traces of averaged IPSCs evoked by MNTB fiber stimulation (stimulation protocol: high frequency stimulation (100Hz, 200ms); 200ms gap; test pulse with ISI=20ms) under control conditions and during GABA$_B$R blockade with SCH50911. (B) Example traces of averaged IPSCs evoked by MNTB fiber stimulation (see A) under control conditions and during bath-application of the GABA uptake inhibitor NO711. NO711 application decreased the response to the test pulse after high frequency MNTB fiber stimulation. (C) Blocking GABA$_B$Rs abolished the NO711 induced amplitude change after high frequency MNTB fiber stimulation. (D) Example traces of averaged EPSCs evoked by AVCN fiber stimulation (stimulation protocol see A) under control conditions and during bath-application of the GABA uptake inhibitor NO711. NO711 application decreased also excitatory currents after high frequency fiber stimulation. (E) Quantification of the GABA$_B$R mediated decrease in IPSC and EPSC amplitudes induced by high frequency fiber stimulation during application of GABA$_B$R blocker and/or GABA uptake inhibitor (all at P8). (asterisks under columns represent *P*-values obtained by Student's two-tailed paired *t* test; asterisks between columns represent *P*-values obtained by Student's two-tailed unpaired *t* test)

Several studies show that even after hearing onset MNTB neurons release GABA from their synaptic terminals at their target sites (Kotak et al. 1998; Nabekura et al. 2004; Smith et al. 2000). Yet, these results are based on the activation of $GABA_A$ receptors induced by MNTB fiber stimulation. Focusing on $GABA_BR$, we asked whether at later developmental stages potential GABA release from MNTB terminals could activate $GABA_B$Rs on the presynaptic terminals of the MTNB inputs in animals just after hearing onset. However, at P14 high frequency stimulation of trapezoid body fibers in combination with NO711 application had only marginal effects on glycinergic IPSCs (4.1 ± 3.3%, n=5) (Fig.4.6C). This suggests that after hearing onset GABA release from MNTB neurons is not sufficient to activate $GABA_B$Rs even in the presence of GABA uptake blockers.

4.2.6 The LNTB-MSO projection has no GABAergic component after hearing onset

Previous anatomical studies provide evidence that the ipsilateral inhibitory input to the MSO, the LNTB, comprises GABAergic neurons also in adult animals (Helfert et al. 1989; Roberts and Ribak 1987; Spirou et al. 1998). Thus, we attempted to find out if the LNTB could serve as a GABA source for the activation of $GABA_B$Rs before hearing onset and also later during development. Accordingly, we stimulated the ipsilateral fiber tract projecting from the LNTB to the MSO. At P8, the application of NO711 depressed glycinergic current amplitudes to a similar degree as already observed for MNTB fiber stimulation (28.2 ± 3.2%, n=6; $P \leq 0.001$) (Fig.4.6A and C). At P14, however, high frequency stimulation of the LNTB fibers in combination with NO711 application did not activate presynaptic $GABA_B$Rs on the inhibitory inputs (NO711 5.2 ± 1.6%, n=5) (Fig.4.6B and C). This suggests that after hearing onset, despite the presence of GABA immunopositive LNTB cells, LNTB inputs to the MSO do not provide enough GABA to induce $GABA_BR$ mediated control of MSO inputs.

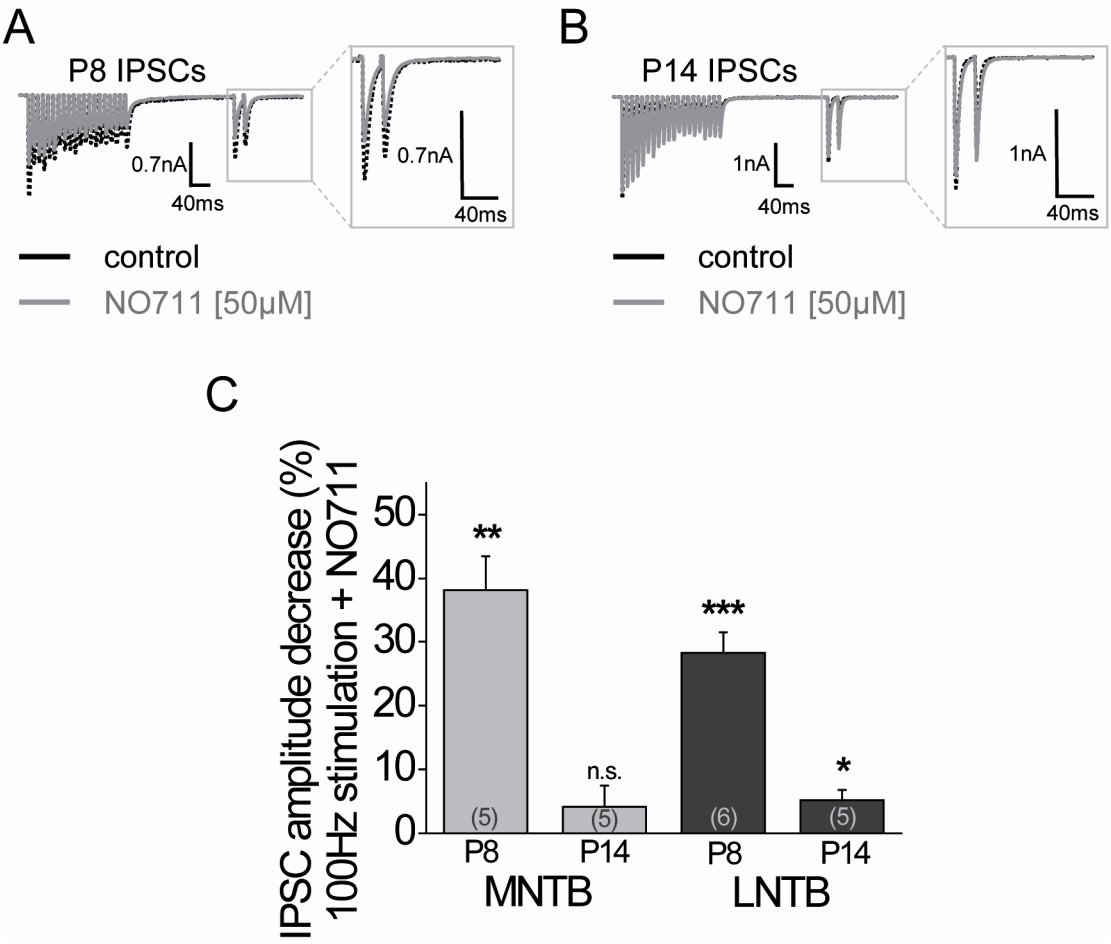

Figure 4.6: High frequency LNTB fiber stimulation only activates GABA$_B$Rs before but not after hearing onset. Similar to the MNTB, GABA$_B$Rs are only activated under the prerequisite of the GABA uptake inhibitor NO711. (A) Example traces of averaged IPSCs evoked by LNTB fiber stimulation (stimulation protocol same as in Fig.4.5A) under control conditions and together with the GABA uptake inhibitor NO711 in a pre-hearing animal (P8). (B) Example traces of averaged IPSCs evoked by LNTB fiber stimulation (stimulation protocol same as in Fig.4.5A) under control conditions and together with the GABA uptake inhibitor NO711 in animals after hearing onset (P14). (C) Statistical analysis of GABA$_B$R mediated changes in IPSC amplitude in response to the test pulse before and after hearing onset for MNTB and LNTB inputs to the MSO. (asterisks represent *P*-values obtained by Student's two-tailed paired *t* test)

4.2.7 Presynaptic GABA$_B$Rs are not activated by retrograde GABA release in the MSO

We have previously demonstrated that neurons in the LSO retrogradely release GABA upon spiking activity (Magnusson et al. 2008). This GABA activates presynaptic GABA$_B$Rs on the respective inputs thereby modulating transmitter release. Since neurons in the LSO and the MSO receive similar inputs, we tested whether this scenario might also hold for MSO principal cells. As in the LSO, this was tested by inducing high frequency spiking activity (100-300Hz, 500ms) in MSO principle cells by short current step injections well above spiking threshold (1.5-2.5nA) (Fig.4.7A). If spiking activity retrogradely released GABA and thereby activated presynaptic GABA$_B$Rs, the amplitude of the postsynaptic potentials induced by fiber stimulation should decrease and the PPR should increase. However, neither the amplitude nor the PPR of EPSPs or IPSPs were changed by the preceding high frequency spiking activity of the MSO neurons (Fig.4.7B and C). This indicates that, unlike in the LSO,

spiking activity of MSO neurons does not activate presynaptic GABA$_B$Rs by presumed retrograde release of GABA. This is also consistent with the lack of GABA- and GAD-immunoreactivity in neurons of the MSO (Roberts and Ribak 1987).

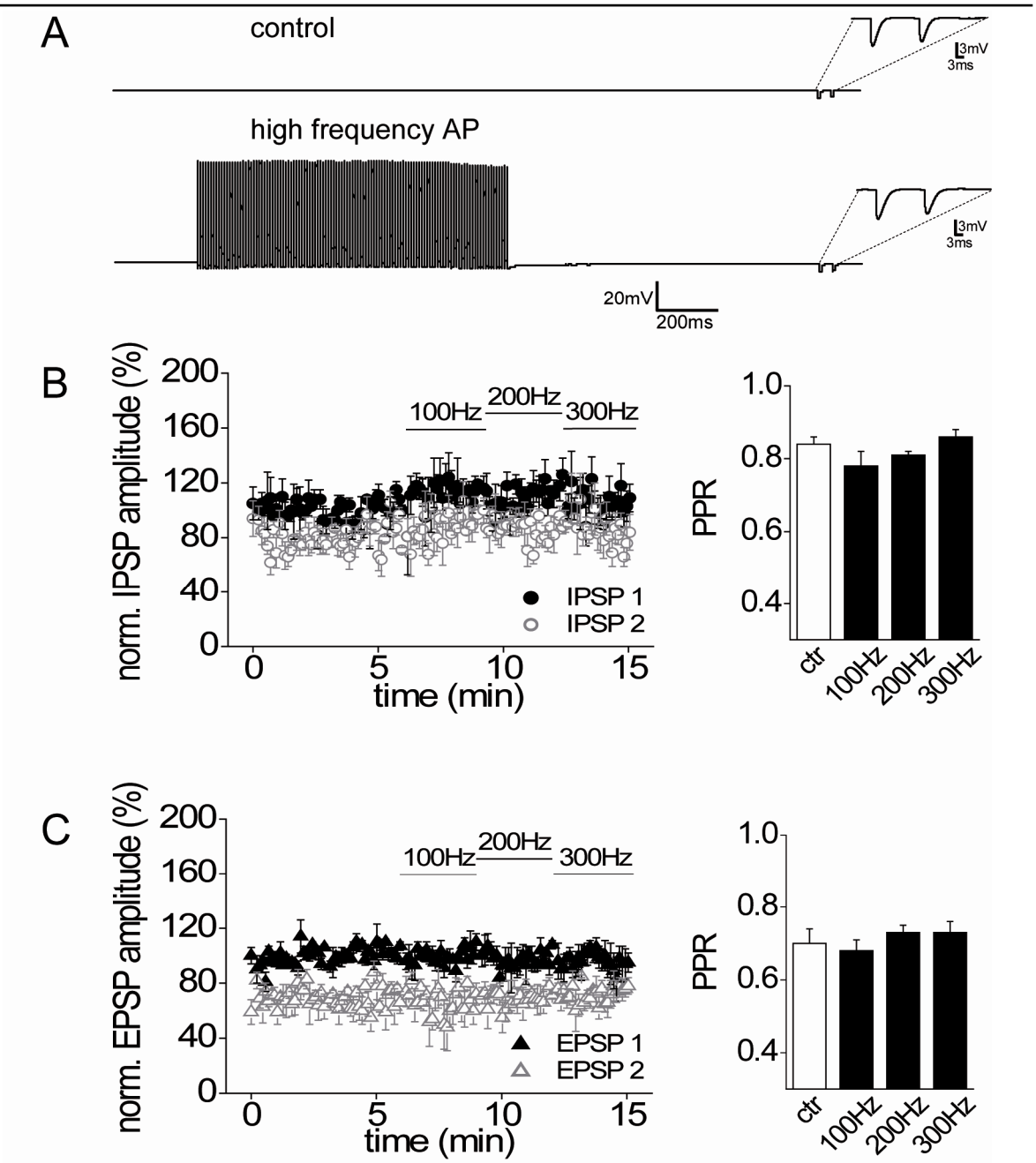

Figure 4.7: Presynaptic GABA$_B$Rs in the MSO are not activated via retrograde GABA release from MSO neurons. (A) Averaged traces (30 trials) of evoked IPSPs in response to MNTB fiber stimulation (ISI: 20ms) under control conditions (control) and with a preceding 300Hz action potential train (high frequency AP) induced by short current pulse injections (2nA). (B) *left panel* Normalized and averaged IPSP amplitudes (n=4) under control conditions (0-6min) and with preceding high frequency action potential firing of the MSO neuron at 100Hz, 200Hz, and 300Hz (6-15min). Averaged recordings show pharmacologically isolated IPSPs (action potentials were elicited by current injection). Preceding AP firing of MSO neurons did not induce significant amplitude modulations of IPSPs. *right panel* Quantification of PPR for each stimulation frequency revealed no significant changes induced by preceding AP firing of the neuron (C) *left panel* Normalized and averaged EPSPs (n=5) under control conditions (0-6min) and with preceding high frequency action potential firing of the MSO neuron at 100Hz, 200Hz, and 300Hz (6-15min). Averaged recordings show pharmacologically isolated EPSPs (action potentials were elicited by current injection). Preceding AP firing of MSO neurons did not induce significant amplitude modulations of EPSPs. *right panel* Quantification of PPR for each stimulation frequency revealed no significant changes induced by preceding AP firing of the neuron. (ctr: control)

4.2.8 Anatomical evidence for other GABAergic input to MSO neurons

In the previous experiments, we found that after hearing onset, despite clear evidence for pharmacological activation of presynaptic $GABA_BRs$ in adult animals, neither the MNTB nor the LNTB input seems to release enough GABA to activate these receptors. We also did not observe $GABA_BR$ activation by retrogradely released GABA from MSO principal neurons. To identify possible other sources of GABA on MSO neurons, we performed antibody stainings on paraformaldehyde fixed brainstem sections containing the MSO (P18) against the GABA synthesizing enzyme GAD65. To evaluate the distribution of GAD65 positive inputs, the dendrites of MSO neurons were visualized with a MAP2 antibody. Confocal microscopy at low magnification showed widely distributed GAD65 staining along the somata and dendrites of MSO neurons indicating the presence of GABAergic inputs at the soma and the dendrites. We also tested if possible GABAergic inputs colocalized with the presynaptic endings deriving from the MNTB or LNTB, by immunostaining against the glycine transporter 2 (GlyT2) (Fig.4.8A). In contrast to the GAD65 distribution, the GlyT2 staining was very focused and dense only on the somata. At higher magnification it became apparent that only little colocalization of GAD65 and GlyT2 positive synapses could be detected. Most of the GAD65 associated staining was not in close proximity to GlyT2 positive terminal endings. This indicates that MSO neurons at P18 receive GABAergic projections mainly from other sources than the glycinergic MNTB or LNTB neurons.

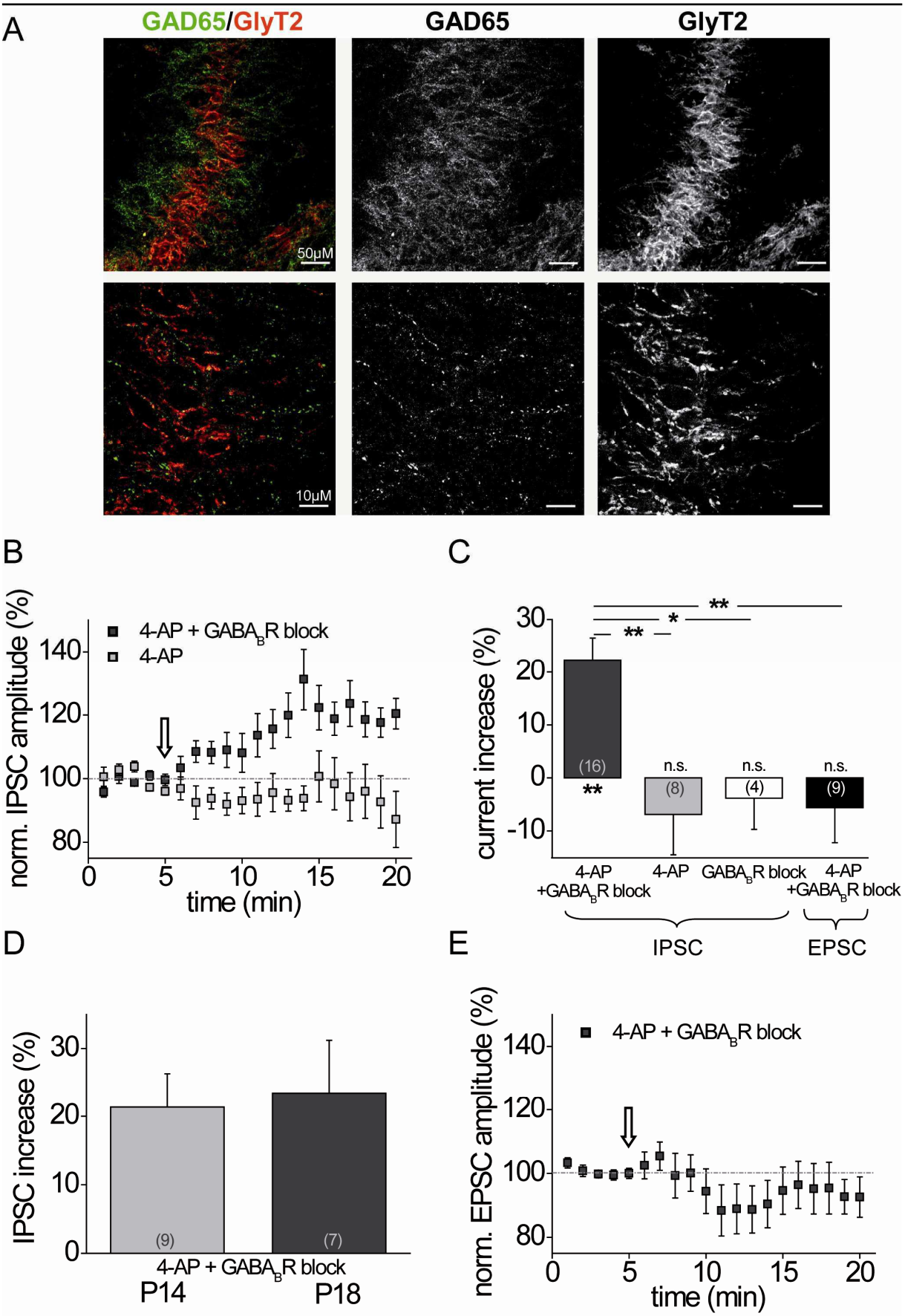

Figure 4.8: GABAergic inputs to the MSO after hearing onset are not colocalized with glycinergic inputs. Increasing spontaneous activity pharmacologically in slice preparations to *in vivo*-like levels activates GABA$_B$Rs with a significant effect on inhibitory inputs. (A) *top panels* low power (25x) magnification of antibody staining in P18 animals revealed a somatodendritic expression of GAD65 (green), whereas GlyT2 (red) was concentrated at the somatic region (scale bar, 50µm). *bottom panels* at high power magnification (63x) colocalization of GAD65 and GlyT2 was scarce (scale bar, 10µm). (B) Time course of averaged

IPSC amplitudes (n=16) evoked by MNTB fiber stimulation under *in vivo*-like spontaneous synaptic activity levels before and during $GABA_BR$ blocker application (arrow indicates the start of $GABA_BR$ blocker application). During the entire time course spontaneous activity levels had been raised by 4-AP [2mM] in the bath which had no effect on IPSC amplitudes (n=8). (C) Summary and statistics on the effect of in *vivo-like* spontaneous activity levels on $GABA_BR$ activation for IPSCs and EPSCs in P14-P18 animals. (D) IPSC amplitudes of P14 and P18 animals are equally affected by $GABA_BR$ activation. (E) Time course of averaged EPSC amplitudes (n=9) evoked by AVCN fiber stimulation under *in vivo*-like spontaneous activity levels before and during $GABA_BR$ blocker application (arrow indicates the start of $GABA_BR$ blocker application). During the entire time course spontaneous activity levels had been raised by 4-AP [2mM] in the bath. (asterisks under columns represent *P*-values obtained by Student's two-tailed paired *t* test; asterisks between columns represent *P*-values obtained by Student's two-tailed unpaired *t* test)

4.2.9 Raising spontaneous activity levels induces $GABA_BRs$ activation even later during development

We next asked the question whether these GABAergic terminals could serve as a possible source for GABA release that activates the $GABA_BRs$ located on the MSO inputs. To test this, spontaneous synaptic transmitter release was increased by applying 4-AP [2mM] to the perfusate. 4-AP is a non-selective blocker of low-threshold potassium channels (K_{LT}) and has been shown to depolarize neurons thereby lowering the action potential threshold and increasing the spontaneous firing rate in e.g. the hippocampus and mouse inner hair cells (Avoli et al. 1996; Marcotti et al. 2003). In the present experiment, 4-AP elevated the spontaneous frequency of IPSCs (Fig.4.9) in MSO neurons (55.8 ± 2.9Hz, n=23) to values that resemble *in vivo*-like spontaneous firing frequencies of MNTB neurons (Hermann et al. 2007).

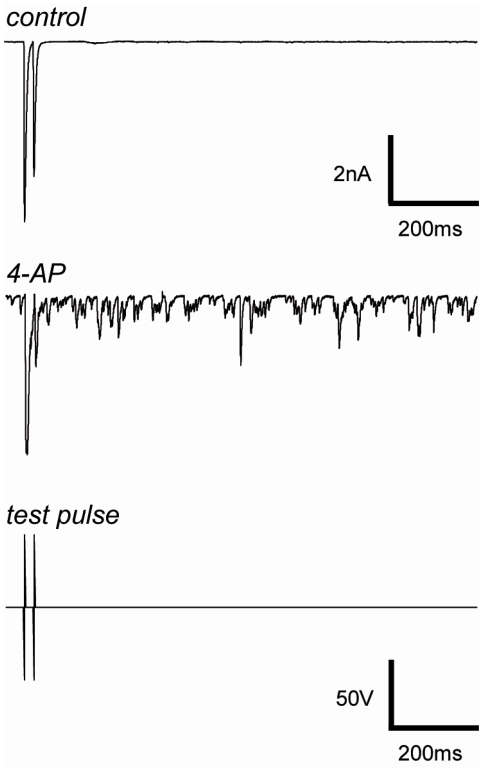

Figure 4.9: Single traces of evoked IPSCs in response to MNTB fiber stimulation (test pulse) under control conditions and with pharmacologically (4-AP [2mM]) increased spontaneous activity levels in P18 brainstem slices (EPSCs were pharmacologically blocked). *top panel* Under control conditions, hardly any spontaneous activity from MSO inputs was detectable. *middle panel* During 4-AP application, frequency and amplitude of spontaneous events dramatically increased. *bottom panel* Stimulation protocol with test pulse.

The influence of possible GABA release through elevated spontaneous release was now tested by application of the $GABA_BR$ inhibitors SCH50911 [10µM] or CGP55845 [2µM]. The results from these recordings were pooled since the data displayed no differences among drugs. MNTB fibers were stimulated to investigate $GABA_BRs$ induced changes of MNTB input currents. As depicted in Figure 4.8B IPSC amplitudes significantly increased when $GABA_BR$ activity was blocked compared to baseline conditions (4-AP alone). This implies that under baseline conditions, when spontaneous activity is raised by 4-AP, presynaptic $GABA_BRs$ were endogenously activated which resulted in a reduction of IPSC amplitudes. Application of the $GABA_BR$ antagonists then abolished this $GABA_BR$ mediated depression of the current, resulting in an increase of current amplitude (22.3 ± 4.2%, n=16; $P \leq 0.01$) (Fig.4.8C). Since neither 4-AP (-6.9 ± 7.6%, n=8) nor $GABA_BR$ inhibitors alone (-3.8 ± 5.9%, n=4) increased peak current amplitudes (Fig.4.8C), this effect could be ascribed directly to the activation of $GABA_BRs$. No difference was observed between P14 and P18 gerbils which indicates that this mechanism persists in more mature animals (*P14*: 21.3 ± 5.0%, n=9; *P18:* 23.5 ± 7.8%, n=7) (Fig.4.8D). Interestingly, excitatory input currents did not display an increase in amplitude during $GABA_BR$ blockade which suggests that the GABA released by spontaneous activity did not activate the $GABA_BRs$ on the excitatory inputs (Fig.4.8E) (*P14-18:* -5.6 ± 6.6%, n=9) (Fig.4.8C). This is in line with the observed downregulation of $GABA_BRs$ on the dendrites later during development. Taken together, these results show that even considerably beyond hearing onset, GABA is released onto MSO neurons, which selectively modulates the amplitude of the inhibitory inputs. The origin and thus the activation pattern of this GABAergic projection needs to be determined in future studies.

4.3 Discussion

The present data show that $GABA_BRs$ differentially modulate the excitatory and inhibitory inputs of MSO neurons at all developmental stages. Around hearing onset the $GABA_BR$ mediated depression of the excitatory inputs greatly decreases, whereas the $GABA_BR$ mediated depression of the inhibitory inputs remains constant throughout the same period. This developmental decay in $GABA_BR$ induced EPSC depression is paralleled by a progressive loss of $GABA_BR$ expression in the dendritic region after hearing onset. Furthermore, we provide evidence that the source of GABA for $GABA_BR$ activation changes during development. Only before hearing onset, MNTB and LNTB fiber stimulation activates presynaptic $GABA_BRs$ on the excitatory and inhibitory inputs to MSO neurons. After hearing onset, GAD65 positive endings that lack GlyT2 reactivity suggest GABA sources other than the MNTB or the LNTB.

4.3.1 Developmental changes of presynaptic $GABA_B$Rs distribution

We have found that $GABA_B$Rs regulate transmitter release at the major inhibitory and excitatory inputs to MSO neurons throughout all developmental stages. Yet, the relative effect of $GABA_B$Rs on excitation and inhibition changes during the first postnatal weeks. Regulation of transmitter release by presynaptic $GABA_B$Rs is a widespread mechanism in the brain, and has been described in several auditory regions, such as the auditory brainstem (Isaacson 1998; Lim et al. 2000; Magnusson et al. 2008; Takahashi et al. 1998; Tang et al. 2009; Yamauchi et al. 2000), midbrain (Sun et al. 2006), and the auditory cortex (Wehr and Zador 2005). Furthermore, $GABA_B$Rs have been implicated in both the regulation of circuit formation during development (Behar et al. 2000; Represa and Ben-Ari 2005), and in the acute modulation of network properties in the mature animal (Magnusson et al. 2008; Oswald et al. 2009; Pan et al. 2009; Scanziani 2000). Consistent with our data, anatomical and physiological studies in other brain structures suggest that presynaptic $GABA_B$Rs are present and functional on excitatory and inhibitory inputs early during development and in adult animals (Gaiarsa et al. 1995; Kirmse and Kirischuk 2006; Lopez-Bendito et al. 2002; Varela et al. 1997). However, there is little information on changes of $GABA_B$Rs function during development. Here, we show that $GABA_B$R mediated depression of the excitatory inputs declined significantly right after hearing onset with a further decline over several weeks. In contrast, we observed that $GABA_B$R mediated depression of inhibition remains constant during development similar to the CA3 region of the hippocampus (Caillard et al. 1998). An important question arising is how these $GABA_B$Rs are regulated. One possibility is that the decline in $GABA_B$R number is developmentally programmed. However, it is more likely that overall activity levels regulate the availability of $GABA_B$Rs. Indeed, excess excitation as well as augmented glutamate levels can down-regulate $GABA_B$R expression and increase internalization of receptor protein (Buhl et al. 1996; Haas et al. 1996; Vargas et al. 2008), which in both cases would result in an altered $GABA_B$R efficacy as observed for the excitatory MSO inputs.

4.3.2 MNTB and LNTB fiber stimulation activates $GABA_B$Rs in the MSO only before hearing onset

Our data indicate that before hearing onset high frequency firing of MNTB neuron activates $GABA_B$Rs on both the excitatory and inhibitory inputs to MSO neurons. Similarly, previous physiological data show that before hearing onset also postsynaptic $GABA_A$ receptors on MSO neurons are activated by MNTB fiber stimulation (Smith et al. 2000). This suggests that indeed GABA released from the MNTB fiber terminals activates the presynaptic $GABA_B$R.

The fact that at the MNTB-LSO projection GABA and glycine is even released from the same synaptic terminals or vesicles (Nabekura et al. 2004) indicates that $GABA_BR$ mediated regulation of glycine and GABA transmitter release is autosynaptic, and should therefore be similar for both transmitter types. Consequently, during prolonged firing of MNTB neurons GABA release should decrease and $GABA_BR$ activation of the inputs should decline in a self-regulating process.

As GABA is released from the inhibitory MNTB terminals and diffuses to the excitatory presynaptic sites, $GABA_BR$ mediated depression of excitation is most likely heterosynaptic. Heterosynaptic activation of $GABA_BRs$ has been shown to occur at many different sites in the brain (Guetg et al. 2009; Lei and McBain 2003; Mitchell and Silver 2000). In the MSO the relatively large distance between the release sites and the excitatory presynaptic endings should result in much lower concentrations of GABA at the excitatory compared to the inhibitory terminals (Kapfer et al. 2002). Why is the amplitude of $GABA_BR$ mediated depression then similar for inhibition and excitation? One possible explanation is a differential sensitivity of the receptors to GABA, which might be the underlying cause for the larger effect of baclofen on excitation than inhibition that we observed before hearing onset. In the hippocampus, heterosynaptic $GABA_BRs$ located on the excitatory inputs are indeed more efficient in down-regulating transmitter release compared to the $GABA_BRs$ on the inhibitory inputs due to a different subunit composition (Guetg et al. 2009).

One unexpected result of our measurements was that even several days before hearing onset MNTB fiber stimulation only activated presynaptic $GABA_BRs$ in the presence of the GABA uptake blocker NO711. It is possible that in P8 animals the concentration of released GABA is not sufficient to activate the presynaptic $GABA_BRs$ without N0711 (Smith et al. 2000). However, even at P5, when stimulation of the MNTB-MSO projection still elicits a substantial $GABA_A$ receptor response (Smith et al. 2000), presynaptic $GABA_BR$ activation in the absence of NO711 was negligible (*personal observation*). In general, physiological activation of $GABA_BRs$ usually requires strong stimulation intensities suggesting that the pooling of synaptically released GABA is required for their activation (Isaacson 1998; Scanziani 2000). This is consistent with ultrastructural data showing that most $GABA_BRs$ are located peri- or extrasynaptically (Fritschy et al. 2004; Lopez-Bendito et al. 2004; Lujan and Shigemoto 2006). Indeed, in many studies using acute brain slice preparations GABA uptake blockers were required to activate presynaptic $GABA_BRs$ (Lei and McBain 2003; Mitchell and Silver 2000; Mouginot et al. 1998). This also highlights the important role of GABA-uptake mechanisms for the regulation of GABA concentration.

4.3.3 Endogenous $GABA_BR$ activation in the MSO after hearing onset

All previous studies so far had focused on the developmental reduction in the activation of ionotropic $GABA_A$ receptors by MNTB fiber activity (Kotak et al. 1998; Smith et al. 2000). Our study indicates that also presynaptic $GABA_BRs$ cannot be activated by MNTB or LNTB fiber stimulation after hearing onset. Furthermore, unlike in the LSO, spiking activity of the MSO neurons does not retrogradely activate the $GABA_BRs$ on the presynaptic terminals. Under which physiological conditions are the $GABA_BRs$ in the MSO then activated? In agreement with previous anatomical studies (Adams and Mugnaini 1990; Helfert et al. 1989; Roberts and Ribak 1987), our antibody labeling against the GABA synthesizing enzyme GAD65 revealed a large number of GABAergic fibers contacting the soma and the proximal dendrites. We therefore propose that GABA released from these GAD65 positive terminals mediates this $GABA_BR$ induced depression of inhibitory inputs. But where do these GAD65 positive fibers originate, and under which physiological circumstances are they activated? Several possibilities have been discussed in the literature, including the ventral nucleus of the trapezoid body, the superior periolivary nucleus (SPN) and descending fibers from the inferior colliculus (Roberts and Ribak 1987). The experimental evidence for any of these projections is sparse (Kiss and Majorossy 1983; Schwartz and Wittebort 1976) and future experiments are required to determine the origin of the GABAergic terminals to MSO neurons in adult animals.

4.3.4 Possible functional significance of $GABA_BRs$ in the MSO before and after hearing onset

The observed shift in the effect of $GABA_BR$ mediated depression of excitation and inhibition suggests a change of $GABA_BR$ function before and after hearing onset. Before hearing onset, we found a profound depression of the excitatory inputs by $GABA_BR$ activation. The functional interpretation of the $GABA_BR$ mediated depression of inhibitory inputs before hearing onset is complex. In neonatal animals, the chloride reversal is positive to the resting membrane potential, which results in a depolarization of neurons during activation of the GABA/glycinergic inputs (Kakazu et al. 1999; Kandler and Friauf 1995; Lohrke et al. 2005). Hence, during this period all the main inputs to the MSO are excitatory. Accordingly, $GABA_BRs$ might be the main source of inhibition in the MSO by decreasing transmitter release from the excitatory and the depolarizing GABA/glycinergic inputs during periods of high frequency spontaneous spiking activity. This scenario has previously been suggested for the neonatal hippocampal network (Gaiarsa et al. 1995; McLean et al. 1996), and could represent an effective mechanism to prevent overexcitation of neurons in the neonatal brain

and protecting them from apoptosis. In this case, the $GABA_BR$ mediated inhibition of excitation should remain elevated in deafened animals where the chloride reversal potential stays depolarizing (Shibata et al. 2004).

Several lines of evidence indicate that the function of the presynaptic $GABA_BRs$ changes after hearing onset. First, at this developmental stage $GABA_BR$ activation mostly modulates the strength of the inhibitory inputs to the MSO, whereas in pre-hearing animals the main $GABA_BR$ effect is dampening excitation. Second, whereas in neonatal animals GABA is released during high frequency firing of MNTB and LNTB neurons, our data indicate that after hearing onset fibers other than the MNTB or LNTB release GABA. Whether these fibers are driven by sound or whether they are associated with an attention driven descending system is unclear at the moment, but in both cases activation of these fibers should result in a tonic downregulation of the inhibitory inputs to the MSO. We do know from previous experiments that the inhibitory inputs from the MNTB and LNTB to the MSO neurons modulate ITD processing by shifting the steepest slope of the ITD function to the physiological relevant range (Brand et al. 2002; Pecka et al. 2008). This implies that a $GABA_BR$ mediated downregulation of the inhibitory inputs would modify the shape of the ITD function, or more specifically, move the peak towards the midline and decrease spike frequency changes within the physiological relevant range. In this case, $GABA_BR$ activation would provide a mechanism to dynamically regulate ITD analysis in the MSO.

5 GENERAL DISCUSSION

The main emphasis of this thesis is put on developmental and activity-dependent processes in the mammalian superior olivary complex. Neuronal features contributing to sound localization were investigated in particular to contribute to a better understanding of auditory processes in the developing brain.

As outlined in the first part of this thesis I was able to demonstrate that the development of the slowly activating and depolarizing current I_h, is under control of activity-driven processes in the mammalian SOC. Several changes of neuronal properties in the auditory brainstem in response to altered activity levels after hearing onset have been discovered to date (Kapfer et al. 2002; Magnusson et al. 2005; Nabekura et al. 2004; Scott et al. 2005; Smith et al. 2000; Werthat et al. 2008). Hence, this study corroborates recent findings insofar as I find that acoustic experience is essential for the maintenance of appropriate ion channel levels, thus shifting excitability to the relevant working range in a neural brainstem circuit. Interestingly, two nuclei belonging to the same neural circuitry expose opposite I_h amplitude changes upon sensory deprivation. Therefore, in line with the observed differences in initial current characteristics these results strongly indicate either a change in the amount of functional HCN channels or a shift in the voltage dependence amongst the respective nuclei concurrently with a potentially different scheme of excitability regulation.

In a second study I could show how metabotropic receptors influence the balancing of excitatory and inhibitory inputs in the MSO during development. With ongoing maturation, the formerly dampening effect of presynaptic $GABA_BRs$ on excitatory currents is nearly abolished whereas it remains constant for inhibitory currents at all developmental stages. It seems that the age-dependent expression pattern of $GABA_BRs$, accompanied by a change of the main release site of GABA, is responsible for the graded effect on glutamatergic currents. Furthermore, I show for the first time that GABAergic projections exist even in the mature MSO, which modulate glycinergic currents via $GABA_BRs$. During *in vivo*-like spontaneous activity levels $GABA_BR$ activation affects glycinergic transmitter release. As a functional consequence, this process might adjust ITD analysis dynamically dependent on activity levels in the auditory brainstem (Brand et al. 2002; Pecka et al. 2008).

Aside from the auditory system, the entire brain has to perform several dynamic adaptations to maintain a neuronal environment that is able to cope with the ongoing processes of neural circuit refinement. Plasticity might be of anatomical, physiological or molecular nature, their common feature being the adaptation of the neural network to new environmental experience. However, these dynamic processes could theoretically endanger the stability of

networks. Hebbian forms of plasticity, for example, have a particularly strong destabilizing effect on network activity, because they tend to drive synaptic strengths towards their maximum or minimum values (Hebb 1949; Miller 1996; Turrigiano and Nelson 2004). These positive feedback mechanisms include long-term potentiation (LTP) and long-term depression (LTD) of synaptic inputs (Bliss and Collingridge 1993; Bliss and Lomo 1973; Goda and Stevens 1996; Hebb 1949). Without a negative feedback mechanism, ongoing plasticity would lead to network destabilization, a loss of information and at its worst to apoptosis (Yu and Goda 2009). The necessary counterpart to stabilize complex circuits is defined as homeostatic plasticity, comprising processes that dynamically adjust synaptic strengths and intrinsic properties in the correct direction to promote stability.

Results presented in this thesis show a dynamic regulation of intrinsic properties as well as an ongoing balancing of synaptic inputs in the developing auditory brainstem. In the following, I will discuss to what degree voltage-gated ion channels and metabotropic receptors contribute to adaptation or neural homeostasis as a whole and which tasks might fall to HCN channels and $GABA_BRs$ in particular to maintain the neuronal network for the processing of binaural information within an optimal operational range in the SOC.

5.1 Consequences of neuronal activity - adaptive and homeostatic mechanisms to regulate faithful auditory processing

Action potentials (APs) or “spikes” constitute the basis for activity-driven processes in the mammalian brain. Cell-to-cell communication, signal transduction, plastic changes and, first and foremost, cell viability are just some characteristics APs are responsible for. The studies of Katz, Hodgkin and Huxley (1952), conducted in the squid giant axon, demonstrated that the generation of sodium spikes is dependent on voltage-gated sodium and potassium channels. This result launched an entire field of research on voltage-gated ion channels (VGICs). Later, apart from studies on VGICs contributing to the generation of APs, channels largely responsible for the intrinsic properties of a neuron as e.g. the input resistance and the membrane time constant got into the focus of researchers. A prominent example for such a channel is the ligand- and voltage-gated HCN channel, which has been discovered and characterized in the mammalian heart and brain (Ludwig et al. 1998; Santoro et al. 1998). Both the channel protein and the underlying current I_h have previously been shown to be present in the auditory brainstem (Bal and Oertel 2000; Banks et al. 1993; Koch et al. 2004; Leao et al. 2006a). However, I could now show that altered sensory input to the auditory brainstem directly influences I_h in the SOC (Hassfurth et al. 2009). This result is supported by

studies, carried out in the SOC as well as in other regions of the brain, demonstrating that developing neural circuits are not hard-wired and undergo structural and functional changes including modified synaptic strength (Barth and Malenka 2001; Dailey and Smith 1996; Di Marco et al. 2009; Kotak and Sanes 2003). It is already known that spontaneous and evoked electrical activity plays a critical role in the maturation of central neuronal circuits. Complete or partial sensory deprivation influences activity levels producing alterations at all levels of the auditory system, and these effects are most profound during early development. Recent findings, in developing and young animals, make clear that synaptic and membrane properties, in fact, are altered following induced hearing loss (Francis and Manis 2000; Oleskevich and Walmsley 2002). A change in synaptic strength, for instance, was reported in the LSO, the AC and the IC before (Kotak et al. 2007; Kotak and Sanes 1996; Vale et al. 2004). Further, a change in sensory input has been shown to influence neuronal excitability in the auditory cortex (Kotak et al. 2005). Adaptations to altered sensory input regarding I_h in the SOC now strongly suggest that auditory experience changes excitability in brainstem neurons by regulating intrinsic properties and speaks for a contribution of VGICs to overall excitability in sensory systems.

5.1.1 Synaptic plasticity in the auditory system at different developmental stages

It is now apparent that we must distinguish increased or decreased efficacy of synaptic transmission (synaptic plasticity) from persistent changes in intrinsic neuronal excitability (intrinsic plasticity). While LTP and LTD of synaptic inputs is typically associated with a change in the efficacy of neurotransmission (Bliss and Collingridge 1993; Bliss and Lomo 1973; Goda and Stevens 1996; Hebb 1949), intrinsic plasticity is usually mediated by changes in the expression level or biophysical properties of ion channels in the cellular membrane (Zhang and Linden 2003). Classical NMDA receptor dependent synaptic plasticity, as it has been discovered for the first time in the mammalian hippocampus (Bashir et al. 1991; Malenka and Nicoll 1993; Mulkey and Malenka 1992), has not been revealed in the SOC to date and only one study provides weak evidence for NMDA receptor dependent LTP and LTD in the DCN, a brainstem structure with cerebellum-like characteristics (Fujino and Oertel 2003; Mugnaini et al. 1980). Recently, Tzounopoulos and colleagues (2004) found that synapses in the DCN can be modulated by precise timing-correlated stimulation patterns of pre- and postsynaptic neurons. This spike-timing dependent plasticity (STDP) is a phenomenon that is based on the rules of LTP and LTD, commonly referred to as the associativity and input specificity rules. Briefly, inputs targeting the same neuron can influence each other's synaptic strength if the sequence of excitatory or inhibitory

postsynaptic potentials falls in a critical time window, mostly in the order of tens of milliseconds (Bi and Poo 1998; Markram et al. 1997; Zhang et al. 1998). It is not unexpected that Tzounopoulos et al. observed activity-dependent modulation of synaptic strength since neurons of the DCN share many features with cerebellar neurons (Manis et al. 1994; Zhang and Oertel 1993). Synaptic connections in the cerebellum are known to adapt their properties to varying input patterns (Armano et al. 2000; Bosman et al. 2008; D'Angelo et al. 1999), which makes these brain regions suitable for ongoing memory storage and learning. The auditory brainstem, apart from the DCN, is in contrast thought to be more hard-wired than cortical and cerebellar structures.

Functional elimination of MNTB-LSO connections occurs primarily during the first postnatal week (Kim and Kandler 2003; but see Sanes and Siverls 1991). Thus, at least prior to hearing onset, a special form of LTD, which is Ca^{2+}-dependent and relies on postsynaptic $GABA_BRs$ can be found in the LSO of gerbils (Chang et al. 2003; Kotak et al. 2001; Kotak and Sanes 2000). Here, low-frequency stimulation of MNTB fibers induces a significant depression of inhibitory currents and it is possible that this reduction in synaptic efficacy causes some input refinement to the LSO before hearing onset. Additionally, Kullmann and Kandler (2008) reported recently that MNTB-elicited Na^+-spikes generate widespread, global Ca^{2+}-responses in the dendritic tree of neonatal LSO neurons. This Ca^{2+}-signal might be the trigger for early synaptic plasticity observed in the LSO. The mechanism, by which the Ca^{2+}-signal is conveyed, was not addressed in this study, but it seems possible that voltage-dependent Ca^{2+}-channels are involved. This is especially likely given the latest *in-vitro* recordings of MSO neurons performed in gerbils before hearing onset. These experiments revealed Ca^{2+}-spikes, which could be caused by spontaneous activity under natural conditions and are possibly mediated by L- and T-type voltage-gated calcium channels or even by NMDA receptors (Cherry and Golding 2010). In this respect, the Ca^{2+}-signal may constitute the basis for the generation of a basic projection pattern in the MSO.

Later in development, adaptive plasticity is embodied in the activity-dependent elimination of glycinergic MNTB-MSO projections (Kapfer et al. 2002; Werthat et al. 2008) and axonal pruning in the MNTB-LSO pathway of maturing rodents (Kim and Kandler 2003; Sanes et al. 1992; Sanes and Siverls 1991; Sanes and Takacs 1993). It has been suggested that, auditory experience during a critical period after hearing onset is responsible for the observed structural changes in the SOC. Yet, it is still not clear whether input refinement relies on Hebbian plasticity or if other intrinsic prerequisites, either at the pre- or the postsynaptic site, have to be fulfilled. The long time course (days) of this structural adaptation to sound localization requirements makes it almost impossible to be observed in slice preparations. It seems tempting to explain this input restriction by an input-specific decrease in glycinergic synaptic strength around hearing onset. This was proposed in a

theoretical model exploiting basic STDP rules. A critical time window for IPSPs or EPSPs paired with postsynaptic APs would consequently induce long-term potentiation or depression in MSO neurons (Leibold and van Hemmen 2005). However, STDP could not be induced experimentally in animals shortly after hearing onset (personal observation). Even though it is difficult to comment on negative results, one possible explanation for the absence of STDP in the MSO is the small fraction of NMDA receptor mediated current in these neurons (Kiri Couchman personal communication, Smith et al. 2000) compared to NMDA currents measured in hippocampal CA1 pyramidal neurons, which show prominent LTP and LTD of their inputs (Otmakhova et al. 2002). The probability for Ca^{2+} mediated synaptic plasticity decreases even further because the membrane time constant becomes shorter and APs of MSO neurons get extremely fast and small after hearing onset (Magnusson et al. 2005; Scott et al. 2005; Smith et al. 2000). This could mean that the small somatic depolarization and the rapidly attenuated backpropagating spikes (Scott et al. 2007) are not strong enough to evoke sufficient Ca^{2+}-influx in MSO neurons even during high-activity states. Thus, with ongoing development AP firing is less likely to influence internal Ca^{2+}-concentrations, which are essential for synaptic plasticity. In conclusion, latest findings regarding Ca^{2+}-signaling in the neonatal SOC (Cherry and Golding 2010; Kullmann and Kandler 2008) might partially account for developmental adaptations involving glycinergic currents during early maturation (Magnusson et al. 2005; Scott et al. 2005) but the molecular mechanism, which induces input refinement remains elusive.

The role of plasticity in the adult auditory system, however, is debatable. If we consider that ascending projections targeting higher nuclei remain within isofrequency bands (Kandler and Friauf 1993; Sanes and Siverls 1991) the question arises what kind of plasticity could be beneficial in the mature auditory system. Defined tonotopic maps are present at all developmental stages in the auditory brainstem (Kandler et al. 2009) and maintaining the well-established overall topographic organization seems reasonable in such a system. Nevertheless, some maps in higher auditory circuits can be adapted to altered sensory activity patterns in adult animals and Hebbian-like synaptic plasticity has been successfully induced in the auditory cortex (Chang and Merzenich 2003; Insanally et al. 2009; Kotak et al. 2007). However, the period at which adaptation to a given stimulus occurs is critically dependent on the complexity of the stimulus. The more complex the stimulus, the later adaptive changes take place. It has been shown for instance, that plasticity for FM direction selectivity in rats happens not before P32, an age at which strong cortical responses develop (Insanally et al. 2009). On the other hand, a fundamental intervention like monaural sensory deprivation or a simple pure tone stimulus altered topographic auditory maps in AI only if applied around hearing onset (de Villers-Sidani et al. 2007; Popescu and Polley 2010). However, parts of the auditory system are apparently still plastic at mature stages and seem

to adapt to complex environmental input. Topographic refinement of initially broad projections has been reported in subcortical areas of adult animals as well and was shown to be dependent on auditory activity (Leake et al. 2006; Leake et al. 2002). Despite a basic tonotopy arranged even before auditory experience (Friauf 1992; Kandler and Friauf 1993; Koundakjian et al. 2007; Sanes et al. 1989; Snyder and Leake 1997) this topographic refinement implicates adaptive plasticity even in the mature auditory brainstem. Although input refinement and increased sensitivity to narrow frequency bands probably improves auditory perception in adult animals, a mechanism to balance overall activity levels would be applicable in the mature auditory system. At this stage, nuclei-specific inputs have to be adjusted to more or less fixed firing frequencies and a fundamental tonotopy should be sustained (Boudreau and Tsuchitani 1968; Grothe and Neuweiler 2000; McAlpine et al. 2001; Tollin 2003). Thus, it appears likely that dynamic processes in the auditory brainstem are regulated by adapting levels of excitability, which counteract possible activity-induced changes (Zhang and Linden 2003). In this way, existing pathways could be stabilized rendering cell-cell communication more reliable. Processes monitoring excitation and maintaining the functional properties of neurons are by definition homeostatic and could achieve such a balance (Davis and Bezprozvanny 2001).

5.1.2 Excitability as an option to control overall activity levels in the auditory brainstem

Homeostatic plasticity of intrinsic excitability was reported for the first time in cultured lobster stomatogastric ganglion neurons (Turrigiano et al. 1995) and later for mammalian cultured visual cortical neurons obtained from postnatal rats. Long-term activity deprivation raised the intrinsic neuronal excitability of these neurons by driving the magnitude of Na^+ and K^+ currents in opposite directions (Desai et al. 1999). Several other studies then reported changed VGIC properties in neuronal tissue because of increased or decreased general activity levels (Aptowicz et al. 2004; Gibson et al. 2006; van Welie et al. 2006). We have now found that sensory deprivation early during development changes the amount of I_h in the SOC (Hassfurth et al. 2009). In accordance with the altered I_h amplitude, we also observed effects on resting membrane potential and input resistance. Both could individually affect neuronal excitability (Fan et al. 2005; Jung et al. 2007), but whether this reflects a compensatory mechanism to regulate the homeostasis of intrinsic excitability is not known to date.

Excitability in the auditory brainstem is regulated by the opposing interplay of two prominent currents: I_h and the low-threshold-activated potassium current I_{KLT} (Brew and Forsythe 1995; Manis and Marx 1991) mediated by K^+-channel of the K_V1-type (Barnes-Davies et al. 2004;

Grissmer et al. 1994; Scott et al. 2007). K_V1-channels produce an outward current, which is already activated at the membrane resting potentials thereby ensuring robust onset firing in response to prolonged current steps and phase-locked responses during repetitive stimulation. Thus, HCN channels might function as a counterweight to K_V1 channels in order to maintain stable excitability levels (Trussell 1999). Consequently, a functional implication for the described activity-dependent regulation of I_h would be that the K_V1 expression pattern is likewise affected by sensory activity. I have shown that with hearing onset, I_h increases substantially in the LSO and to a smaller degree in the MNTB. At the same time, RNA levels of the channel protein $K_V1.1$ increase in the entire rodent brain (Hallows and Tempel 1998) and channels become progressively membrane-bound reflecting mature localization (Brew et al. 2003). Moreover, K_V1 currents measured at the calyx of Held increase dramatically in the second postnatal week (Nakamura and Takahashi 2007) and were shown to increase even further in the MSO after hearing onset (Scott et al. 2005). It therefore seems possible that HCN and K_V1 channels balance their expression patterns in concert, strictly dependent on each other. Homeostatic plasticity of I_h channels has been described before. Results from electrophysiological studies in neocortical cultured neurons indicate that I_h is downregulated after activity blockade (Gibson et al. 2006), whereas upregulation of activity gradually increases the amplitude of I_h at the soma of hippocampal CA1 pyramidal neurons in slice preparations (van Welie et al. 2004). The regulatory mechanisms concerning I_h are complex, though. (2005) reported that lowering synaptic activity levels in hippocampal slices by inducing LTD decreases excitability concurrently with an increase in I_h current, which would be in contrast to findings by Gibson et al. and van Welie and colleagues. More recently, it has been hypothesized furthermore that balanced changes to the transient outward potassium current I_A and the inward current I_h could control neuronal gain while preserving intrinsic activity (Burdakov 2005), though experimental data is admittedly rare (MacLean et al. 2003).

In contrast, compensatory mechanisms, which would override homeostatic plasticity, have been suggested for a murine $K_V1.1$ knockout model (Brew et al. 2003). Here, MNTB neurons were highly hyperexcitable compared to wildtype animals without adaptive changes towards excitability. The observed hyperexcitability was explained by a shift in voltage dependency due to an exchange of K_V1 subunits and was seemingly not compensated by other VGICs as for example HCN channels. This assumption does not agree with the idea of balanced excitability achieved by homeostatic plasticity between VGICs of different families. A second study corroborates this work and confirms that disrupting native ion channel compositions is not necessarily compensated by adapting intrinsic homeostasis. Here, isomer-specific HCN1 knockout mice exhibited elevated excitability levels in cortical pyramidal cells, which are thought to influence neural network activity, especially with respect to epilepsy (Huang et al.

2009). This result would imply, that first, the loss of HCN subunits is not always compensated by VGICs alone (Chen et al. 2010), and second, HCN channels critically control neuronal excitability in an established network.

Although it remains difficult to ascribe the exact overall homeostatic mechanism underlying changes in I_h levels to sensory excitation or deprivation, it seems clear that altered activity regulates the properties of voltage-gated ion channels in the developing auditory brainstem.

5.2 Auditory circuits are balanced by metabotropic receptors

5.2.1 $GABA_BRs$ in developing neuronal circuits

The impact of $GABA_BR$ modulation on glutamatergic and glycinergic currents in the MSO differs during brainstem maturation (see chapter 4). Receptors initially expressed mainly in the dendritic region shift to exhibit a predominantly somatic expression pattern with ongoing development. It is known that inhibitory neurotransmitter, like GABA and glycine, initially depolarize neurons in the auditory brainstem due to a more positive E_{Cl^-} and thus convey excitatory action. Since presynaptic $GABA_BR$ activation strongly decreases transmitter release at both glutamatergic and glycinergic inputs before hearing onset, I conclude that $GABA_BRs$ might be the main source of inhibition in the MSO of neonatal animals by decreasing the overall released depolarizing neurotransmitter. Yet, $GABA_BRs$ have only recently become the focus of interest concerning the mammalian as well as the avian sound localization systems (Burger et al. 2005; Hilbig et al. 2007; Isaacson 1998; Ishikawa et al. 2005; Kotak et al. 2001; Lim et al. 2000; Lu et al. 2005; Magnusson et al. 2008; Tang et al. 2009) but the relevance of $GABA_BRs$ for the accurate development of neuronal circuits is known for long (Ben-Ari et al. 1994; Luhmann and Prince 1991; Wagner and Alger 1995). The development of a circuitry, however, requires longer periods of GPCR signaling. Second messenger cascades at the postsynaptic site are necessary to trigger effects, which could result in long-lasting phosphorylation and, finally, in novel protein expression. This just described mechanism has been proposed to underlie the elimination of MNTB projections to the LSO (Kotak et al. 2001; Kotak and Sanes 2000). Here, LTD at glycinergic synapses could be induced by stimulating the inhibitory inputs to the LSO at low frequencies and was proven to be dependent on postsynaptic $GABA_BRs$ (Chang et al. 2003). Interestingly, LTD could only be induced before hearing onset, a time when dramatic structural changes are happening within the SOC. This finding is supported by an earlier study showing that the $GABA_BR$ dependent LTD in the rat hippocampus is abolished in adult animals (Wagner and Alger 1995).

On a much shorter timescale, $GABA_BRs$ can control networks by regulating neurotransmitter release. This could be helpful to quickly adapt excitatory and/or inhibitory to altered experience. Additionally, a similar role as I suggest for the network activity in the neonatal SOC for $GABA_BRs$ has been proposed in the rat neonatal hippocampus (Gaiarsa et al. 1995; McLean et al. 1996). Here, the neuronal network in the CA3 region is controlled by the depressing action of $GABA_BRs$ achieved by high levels of spontaneous GABA release. Contrary to the situation in the neonatal hippocampus, $GABA_BRs$ in the mature hippocampus require highly synchronous release of GABAergic interneurons as seen for instance during epileptiform discharges (McLean et al. 1996). At this stage, the circuitry is mainly regulated by postsynaptic $GABA_ARs$. Another example for developmental changes in network regulation by $GABA_BRs$ was observed in cerebellar slices (Astori et al. 2009). Here, inputs from GABAergic interneurons to two cell types, Purkinje cells and other inhibitory interneurons, are differentially regulated during development by presynaptic $GABA_BRs$. While inhibitory currents in Purkinje cells are decreasingly affected by the $GABA_BR$ specific agonist Baclofen within two weeks, inhibitory currents and the frequency of mIPSCs in stellate cells are similarly reduced during drug application throughout development. The reason for the decrease in the effects of Baclofen is that synaptic terminals at Purkinje cells deriving from interneurons contain five-fold less $GABA_BRs$ at P28 compared to P14 with presumably no significant changes in Baclofen binding affinity or sensitivity. The results of this study illustrate that downregulation of presynaptic $GABA_BRs$ happens within days and thereby potentially increases neurotransmitter release.

It has been speculated whether changing $GABA_BR$ location patterns could originate from timely aligned expression of distinct subunits (GBR1a and GBR1b, respectively) since the predominant GBR1a subunits in the neonatal hippocampus might contribute to differential intracellular sorting and targeting by interaction with specific cytoplasmic proteins (Fritschy et al. 2004). Hence, tasks beyond G-protein activation might be devolved on $GABA_BRs$. Although I did not stain explicitly for GBR1a, its presence could explain the strong cytosolic $GABA_BR$ staining in more mature MSO neurons. Despite the presence of postsynaptic $GABA_BRs$ in prehearing animals affirmed by postsynaptic K^+-current activity with Baclofen application, hearing animals, in contrast, lacked postsynaptic $GABA_BR$ activity (own observations). GBR1a therefore might be important on a subcellular level in determining the final localization of $GABA_BRs$ in a mature neuron and could help transporting $GABA_BRs$ to the axonal terminal. Nevertheless, postsynaptic $GABA_BRs$ have been likewise found in the auditory brainstem (Chang et al. 2003) but implications for a role in network development are rare (Juiz et al. 1994; Lujan et al. 2004). It is quite possible that input refinement is achieved via postsynaptic $GABA_BRs$ in the LSO in particular because the amplitude of glycinergic currents is modulated by a G-protein dependent pathway, which can be achieved by

$GABA_BR$ activation (Yevenes et al. 2006; Yevenes et al. 2003). We were able to mimic these effects on GlyRs, formerly observed in spinal cord cell culture, in the acute brain slice by intracellular application of activated G-protein subunits. However, in the MSO it is unlikely though it cannot be excluded that the activation of G-proteins via postsynaptic $GABA_BRs$ influences GlyR characteristics. On a population level, Baclofen concentrations up to 100µM did not change the amplitude of glycinergic mIPSCs significantly, however, some MSO neurons showed a profound increase in mIPSC amplitudes, which could reflect postsynaptic $GABA_BR$ activation (own observation). Yet, G-proteins are not necessarily activated by $GABA_BRs$ alone.

5.2.2 A comparison of further GPCRs in the auditory brainstem

Also other metabotropic receptors have been thoroughly investigated and have been demonstrated to regulate developing or settled neuronal circuitries. Cannabinoid receptors (CB1Rs), serotonin (5-HT) receptors and metabotropic glutamate receptors (mGluRs) in particular, were scrutinized lately in the auditory system. Several studies dealt with the role of metabotropic receptors regarding network properties. Edwin Rubel was among the first scientists to investigate the function of metabotropic receptors in the auditory brainstem (Lachica et al. 1995; Lu et al. 2005; Lu and Rubel 2005; Zirpel et al. 1995). He focused on the avian auditory brainstem and found for instance that mGluRs are located postsynaptically in the nucleus magnocellularis (NM) likely contributing to Ca^{2+} homeostasis in NM neurons and thereby guaranteeing neuronal vitality. Moreover, presynaptically situated mGluRs in the nucleus laminaris (NL) (Lu et al. 2005) reduce transmitter release from neurons of the superior olivary nucleus (SON). In this mature neuronal network, metabotropic receptors (but $GABA_BRs$, too) have been shown to modulate exclusively single subsets of inputs. Hence, while the release of neurotransmitter is significantly dampened at GABAergic terminals, the efficacy of excitatory inputs remains unchanged. This study is of particular interest because I found a comparable effect on glycinergic and glutamatergic inputs in the MSO, the mammalian analogue to the NL. The authors postulated that such a circuit would possibly represent a feedback control, which could limit excessive GABA release and decrease the firing rate of GABA induced spikes (Tang et al. 2009). Metabotropic glutamate receptors are also found in the mammalian auditory brainstem (Barnes-Davies and Forsythe 1995; Elezgarai et al. 1999; Ene et al. 2003; Kushmerick et al. 2004; Sanes et al. 1998), the midbrain and the cerebrum (Bandrowski et al. 2002; Farazifard and Wu 2010; Petralia et al. 1996; Shigemoto et al. 1993). Alterations in the expression pattern of mGluRs before and after hearing onset have been reported for the MNTB and the LSO (Elezgarai et al. 1999;

Ene et al. 2007), but data on the existence of mGluRs in the MSO is missing. Nevertheless, with respect to the MNTB pathway, pre- as well as postsynaptic mGlurs diminish after hearing onset in the LSO (Ene et al. 2007; Nishimaki et al. 2007) emphasizing their putative importance for network modulation in prehearing animals.

Functional implications for CB1Rs and 5-HT receptors mostly cover mature networks (Hurley and Pollak 1999; 2005; Kushmerick et al. 2004; Penzo and Pena 2009; Thompson and Lauder 2005; Wang and Robertson 1997; Zhao et al. 2009). 5-HT receptors, too, have been associated with activity-driven developmental processes in the LSO. In neurons of animals younger than P9, serotonin increases the rate of spontaneous IPSCs. The presumptive mechanism for this change in inhibitory transmission is yet not ascribed to G-proteins on the postsynaptic site but rather to a direct excitatory action on MNTB neurons. One possibility might be that 5-HT modulates, thus, enhances a depolarizing current like I_h, which is prominent in MNTB neurons. An increase in spontaneous MNTB firing rate could thereby influence the structural and functional development of the SOC. In addition, it was suggested that presynaptic 5-HT receptors could modulate the balance of excitatory and inhibitory synaptic inputs to the LSO, thereby regulating ILD processing in mammals (Fitzgerald and Sanes 1999). More and more data is compiled during the last years clearly demonstrating the importance of regulatory mechanisms in the auditory brainstem. The abundance of metabotropic receptors in the brainstem emphasizes their significance for issues concerning structural refinement, gain and input balancing. Just recently, another example for the weighted balancing of excitatory and inhibitory inputs by GPCRs has been shown. Mature neurons of the DCN in rodents exhibited a disparity in input control upon activation of CB1Rs (Zhao et al. 2009). As CB1Rs are involved in long-term plasticity in the DCN (Tzounopoulos et al. 2007), the differential presynaptic modulation of excitatory and inhibitory inputs could exceed changes in transmitter release on a short timescale and build up to long-term effects implemented postsynaptically.

Since many G-protein dependent pathways interact, concurrent activation of several metabotropic receptors should influence each other. This has yet not received much attention. One interesting example of this receptor interaction has been investigated at the calyx of Held. Pharmacological activation of postsynaptic mGluRs activated presynaptic CB1Rs by retrograde endocannabinoid release from MNTB neurons. This in turn resulted in lowered glutamate transmission at the calyx of Held and decreased excitatory currents (Kushmerick et al. 2004). It is currently not disclosed which function such a mechanism would be ascribed to, but it remains attractive to further investigate a system that is modulated by a well-defined interaction of separate types of metabotropic receptors.

In conclusion, metabotropic receptors other than $GABA_BRs$ have been shown to modulate the synaptic drive in a developing system and to influence the proper formation of developing neural circuits.

5.2.3 The functional role of $GABA_BRs$ in an ITD detection circuit

If we contemplate on the functional relevance of $GABA_BR$ activation in the mature MSO one has to recall the distinct GABA release sites during development. We show that before hearing onset, inputs to the MSO are influenced by autosynaptic GABA release activating $GABA_BRs$ on MNTB terminals and heterosynaptic GABA release acting on AVCN terminals. Moreover, as we know that MNTB-MSO projections are almost exclusively glycinergic at hearing onset (Smith et al. 2000) the question arises which source contributes the necessary GABA concentrations to activate $GABA_BRs$ in mature MSO neurons. The results in this thesis exclude dendritic GABA release of the MSO itself as it has been shown for the LSO (Magnusson et al. 2008). Instead, we were able to stain for GABAergic terminals which were not co-localized with glycinergic MNTB/LNTB endings. Two possibilities now open up. First, GABA could be released by a set of fibers of yet unknown origin. Possible candidates for these sources are the SPN and the IC (Kiss and Majorossy 1983; Roberts and Ribak 1987; Schwartz and Wittebort 1976). The SPN receives bilateral, but predominantly contralateral input from neurons of the CN and ipsilateral input from the MNTB (Friauf and Ostwald 1988; Grothe et al. 1994). Despite differences in input pattern and firing characteristics between MSO and SPN neurons (Behrend et al. 2002; Dehmel et al. 2002) and assuming that SPN-MSO projections existed, the SPN could modulate transmitter release in the MSO by acting on heterosynaptic $GABA_BRs$ located at glycinergic and glutamatergic projections to MSO neurons. Therefore, the SPN might play a role in controlling the overall activity of the MSO in a feedforward-like manner. Such a mechanism could adapt the ITD function to altering levels of auditory input, similar as observed for the ILD function in the LSO. Although here GABA is released retrogradely, inhibitory and excitatory synapses are modulated with differential strength upon auditory input to fine-tune the binaural sensitivity (Magnusson et al. 2008). Fibers projecting back from the IC, in contrast, could refine the ratio of excitation and inhibition in the MSO via a feedback circuitry. In such a way, the output signal of MSO neurons could be dynamically adjusted by the IC to optimize the read-out of ITD signals in the midbrain.

However, if we consider that GABA releasing cells are not categorically primary neurons, putative candidates for GABA release might also be glial cells. Weak evidence is already existing, indicating that glial cells at least synthesize GABA in the hippocampus under certain

conditions (Jow et al. 2004). This finding would be consistent with the GAD65-positive staining obtained in the MSO although double-staining with glia markers would be necessary to confirm this assumption. One possibility is that glial cells release GABA by reversing the normal GABA-transporter dependent GABA-uptake mechanisms (Barakat and Bordey 2002; Wu et al. 2007). This process has been reported for Bergmann glial cells in the cerebellum and was achieved by depolarizing individual glial cells. Even though it is not known, how glial cells are depolarized under natural conditions, it might be possible, that the densely packed astrocytes in the MSO release tonic concentrations of GABA during periods of high activity. If so, due to the high probability for $GABA_BR$ activation even upon low concentrations of the agonist Baclofen, the free extracellular concentration of GABA in the auditory brainstem could have a profound effect on neurotransmission in the MSO (see chapter 4). If that was the case, GABA would act as a volume transmitter influencing $GABA_BRs$ globally rather than restricted to certain synapses (Fuxe et al. 2007; Steinert et al. 2008). In modulating all four major inputs to the MSO, the activation of $GABA_BRs$ would allow to dynamically adjust ITD coding on a longer timescale, possibly enabling azimuthal sound localization of high-fidelity even under varying environmental conditions.

5.3 Concluding remarks

The process of azimuthal sound localization demands a well-established neuronal network that is able to cope with exceptionally high firing frequencies at exceeding temporal accuracy. Faithful and stable neurotransmission is a key feature in the auditory brainstem.
In this thesis, however, I provide further evidence that the mature auditory brainstem is not fixed in its biophysical and synaptic properties but rather needs to be dynamically regulated to operate with an optimum efficiency. Pinpointing the exact interplay of intrinsic neuronal characteristics and extrinsic network factors contributing to auditory processing, remains a demanding challenge. Nevertheless, a better understanding of such dynamics in auditory processing could support future clinical projects regarding e.g. hyperacusis and tinnitus or the development of improved auditory brainstem implants.

6 BIBLIOGRAPHY

Ackerman MJ, and Clapham DE. Ion channels--basic science and clinical disease. *N Engl J Med* 336: 1575-1586, 1997.

Adam TJ, Schwarz DW, and Finlayson PG. Firing properties of chopper and delay neurons in the lateral superior olive of the rat. *Exp Brain Res* 124: 489-502, 1999.

Adams JC. Ascending projections to the inferior colliculus. *J Comp Neurol* 183: 519-538, 1979.

Adams JC, and Mugnaini E. Immunocytochemical evidence for inhibitory and disinhibitory circuits in the superior olive. *Hear Res* 49: 281-298, 1990.

Aitkin L, and Martin R. Neurons in the inferior colliculus of cats sensitive to sound-source elevation. *Hear Res* 50: 97-105, 1990.

Aitkin LM, and Martin RL. The representation of stimulus azimuth by high best-frequency azimuth-selective neurons in the central nucleus of the inferior colliculus of the cat. *J Neurophysiol* 57: 1185-1200, 1987.

Allin EF. Evolution of the mammalian middle ear. *J Morphol* 147: 403-437, 1975.

Aptowicz CO, Kunkler PE, and Kraig RP. Homeostatic plasticity in hippocampal slice cultures involves changes in voltage-gated Na+ channel expression. *Brain Res* 998: 155-163, 2004.

Armano S, Rossi P, Taglietti V, and D'Angelo E. Long-term potentiation of intrinsic excitability at the mossy fiber-granule cell synapse of rat cerebellum. *J Neurosci* 20: 5208-5216, 2000.

Astori S, Lujan R, and Kohr G. GABA release from cerebellar stellate cells is developmentally regulated by presynaptic GABA(B) receptors in a target-cell-specific manner. *Eur J Neurosci* 30: 551-559, 2009.

Attwood TK, and Findlay JB. Fingerprinting G-protein-coupled receptors. *Protein Eng* 7: 195-203, 1994.

Avoli M, Louvel J, Kurcewicz I, Pumain R, and Barbarosie M. Extracellular free potassium and calcium during synchronous activity induced by 4-aminopyridine in the juvenile rat hippocampus. *J Physiol* 493 (Pt 3): 707-717, 1996.

Bal R, and Oertel D. Hyperpolarization-activated, mixed-cation current (I(h)) in octopus cells of the mammalian cochlear nucleus. *J Neurophysiol* 84: 806-817, 2000.

Bal T, and McCormick DA. Synchronized oscillations in the inferior olive are controlled by the hyperpolarization-activated cation current I(h). *J Neurophysiol* 77: 3145-3156, 1997.

Balakrishnan V, Becker M, Lohrke S, Nothwang HG, Guresir E, and Friauf E. Expression and function of chloride transporters during development of inhibitory neurotransmission in the auditory brainstem. *J Neurosci* 23: 4134-4145, 2003.

Bandrowski AE, Moore SL, and Ashe JH. Activation of metabotropic glutamate receptors by repetitive stimulation in auditory cortex. *Synapse* 44: 146-157, 2002.

Banks MI, Pearce RA, and Smith PH. Hyperpolarization-activated cation current (Ih) in neurons of the medial nucleus of the trapezoid body: voltage-clamp analysis and enhancement by norepinephrine and cAMP suggest a modulatory mechanism in the auditory brain stem. *J Neurophysiol* 70: 1420-1432, 1993.

Barakat L, and Bordey A. GAT-1 and reversible GABA transport in Bergmann glia in slices. *J Neurophysiol* 88: 1407-1419, 2002.

Barnes-Davies M, Barker MC, Osmani F, and Forsythe ID. Kv1 currents mediate a gradient of principal neuron excitability across the tonotopic axis in the rat lateral superior olive. *Eur J Neurosci* 19: 325-333, 2004.

Barnes-Davies M, and Forsythe ID. Pre- and postsynaptic glutamate receptors at a giant excitatory synapse in rat auditory brainstem slices. *J Physiol* 488 (Pt 2): 387-406, 1995.

Barth AL, and Malenka RC. NMDAR EPSC kinetics do not regulate the critical period for LTP at thalamocortical synapses. *Nat Neurosci* 4: 235-236, 2001.

Bashir ZI, Alford S, Davies SN, Randall AD, and Collingridge GL. Long-term potentiation of NMDA receptor-mediated synaptic transmission in the hippocampus. *Nature* 349: 156-158, 1991.

Batra R. Responses of neurons in the ventral nucleus of the lateral lemniscus to sinusoidally amplitude modulated tones. *J Neurophysiol* 96: 2388-2398, 2006.

Beckius GE, Batra R, and Oliver DL. Axons from anteroventral cochlear nucleus that terminate in medial superior olive of cat: observations related to delay lines. *J Neurosci* 19: 3146-3161, 1999.

Behar TN, Schaffner AE, Scott CA, Greene CL, and Barker JL. GABA receptor antagonists modulate postmitotic cell migration in slice cultures of embryonic rat cortex. *Cereb Cortex* 10: 899-909, 2000.

Behrend O, Brand A, Kapfer C, and Grothe B. Auditory response properties in the superior paraolivary nucleus of the gerbil. *J Neurophysiol* 87: 2915-2928, 2002.

Ben-Ari Y, Tseeb V, Raggozzino D, Khazipov R, and Gaiarsa JL. gamma-Aminobutyric acid (GABA): a fast excitatory transmitter which may regulate the development of hippocampal neurones in early postnatal life. *Prog Brain Res* 102: 261-273, 1994.

Benson CG, and Cant NB. The ventral nucleus of the lateral lemniscus of the gerbil (Meriones unguiculatus): organization of connections with the cochlear nucleus and the inferior colliculus. *J Comp Neurol* 510: 673-690, 2008.

Bi GQ, and Poo MM. Synaptic modifications in cultured hippocampal neurons: dependence on spike timing, synaptic strength, and postsynaptic cell type. *J Neurosci* 18: 10464-10472, 1998.

Binzen U, Greffrath W, Hennessy S, Bausen M, Saaler-Reinhardt S, and Treede RD. Co-expression of the voltage-gated potassium channel Kv1.4 with transient receptor potential channels (TRPV1 and TRPV2) and the cannabinoid receptor CB1 in rat dorsal root ganglion neurons. *Neuroscience* 142: 527-539, 2006.

Bisiach E, Cornacchia L, Sterzi R, and Vallar G. Disorders of perceived auditory lateralization after lesions of the right hemisphere. *Brain* 107 (Pt 1): 37-52, 1984.

Blauert J. Spatial Hearing: The Psychophysics of Human Sound Localization. *MIT Press* 1996.

Bliss TV, and Collingridge GL. A synaptic model of memory: long-term potentiation in the hippocampus. *Nature* 361: 31-39, 1993.

Bliss TV, and Lomo T. Long-lasting potentiation of synaptic transmission in the dentate area of the anaesthetized rabbit following stimulation of the perforant path. *J Physiol* 232: 331-356, 1973.

Born DE, Durham D, and Rubel EW. Afferent influences on brainstem auditory nuclei of the chick: nucleus magnocellularis neuronal activity following cochlea removal. *Brain Res* 557: 37-47, 1991.

Bosman LW, Takechi H, Hartmann J, Eilers J, and Konnerth A. Homosynaptic long-term synaptic potentiation of the "winner" climbing fiber synapse in developing Purkinje cells. *J Neurosci* 28: 798-807, 2008.

Boudreau JC, and Tsuchitani C. Binaural interaction in the cat superior olive S segment. *J Neurophysiol* 31: 442-454, 1968.

Brand A. Precise temporal processing in the gerbil auditory brainstem. *PhD thesis* 2003.

Brand A, Behrend O, Marquardt T, McAlpine D, and Grothe B. Precise inhibition is essential for microsecond interaural time difference coding. *Nature* 417: 543-547, 2002.

Brawer JR, Morest DK, and Kane EC. The neuronal architecture of the cochlear nucleus of the cat. *J Comp Neurol* 155: 251-300, 1974.

Brenowitz S, David J, and Trussell L. Enhancement of synaptic efficacy by presynaptic GABA(B) receptors. *Neuron* 20: 135-141, 1998.

Brew HM, and Forsythe ID. Systematic variation of potassium current amplitudes across the tonotopic axis of the rat medial nucleus of the trapezoid body. *Hear Res* 206: 116-132, 2005.

Brew HM, and Forsythe ID. Two voltage-dependent K+ conductances with complementary functions in postsynaptic integration at a central auditory synapse. *J Neurosci* 15: 8011-8022, 1995.

Brew HM, Hallows JL, and Tempel BL. Hyperexcitability and reduced low threshold potassium currents in auditory neurons of mice lacking the channel subunit Kv1.1. *J Physiol* 548: 1-20, 2003.

Brewster A, Bender RA, Chen Y, Dube C, Eghbal-Ahmadi M, and Baram TZ. Developmental febrile seizures modulate hippocampal gene expression of hyperpolarization-activated channels in an isoform- and cell-specific manner. *J Neurosci* 22: 4591-4599, 2002.

Brewster AL, Bernard JA, Gall CM, and Baram TZ. Formation of heteromeric hyperpolarization-activated cyclic nucleotide-gated (HCN) channels in the hippocampus is regulated by developmental seizures. *Neurobiol Dis* 19: 200-207, 2005.

Brown AM. Acoustic distortion from rodent ears: a comparison of responses from rats, guinea pigs and gerbils. *Hear Res* 31: 25-37, 1987.

Brugge JF, Anderson DJ, and Aitkin LM. Responses of neurons in the dorsal nucleus of the lateral lemniscus of cat to binaural tonal stimulation. *J Neurophysiol* 33: 441-458, 1970.

Buhl EH, Otis TS, and Mody I. Zinc-induced collapse of augmented inhibition by GABA in a temporal lobe epilepsy model. *Science* 271: 369-373, 1996.

Burdakov D. Gain control by concerted changes in I(A) and I(H) conductances. *Neural Comput* 17: 991-995, 2005.

Burger RM, Pfeiffer JD, Westrum LE, Bernard A, and Rubel EW. Expression of GABA(B) receptor in the avian auditory brainstem: ontogeny, afferent deprivation, and ultrastructure. *J Comp Neurol* 489: 11-22, 2005.

Caillard O, McLean HA, Ben-Ari Y, and Gaiarsa JL. Ontogenesis of presynaptic GABAB receptor-mediated inhibition in the CA3 region of the rat hippocampus. *J Neurophysiol* 79: 1341-1348, 1998.

Caird D, and Klinke R. Processing of interaural time and intensity differences in the cat inferior colliculus. *Exp Brain Res* 68: 379-392, 1987.

Campanac E, Daoudal G, Ankri N, and Debanne D. Downregulation of dendritic I(h) in CA1 pyramidal neurons after LTP. *J Neurosci* 28: 8635-8643, 2008.

Cant NB, and Casseday JH. Projections from the anteroventral cochlear nucleus to the lateral and medial superior olivary nuclei. *J Comp Neurol* 247: 457-476, 1986.

Cant NB, and Hyson RL. Projections from the lateral nucleus of the trapezoid body to the medial superior olivary nucleus in the gerbil. *Hear Res* 58: 26-34, 1992.

Cao XJ, McGinley MJ, and Oertel D. Connections and synaptic function in the posteroventral cochlear nucleus of deaf jerker mice. *J Comp Neurol* 510: 297-308, 2008.

Cao XJ, Shatadal S, and Oertel D. Voltage-sensitive conductances of bushy cells of the Mammalian ventral cochlear nucleus. *J Neurophysiol* 97: 3961-3975, 2007.

Carr CE, and Konishi M. A circuit for detection of interaural time differences in the brain stem of the barn owl. *J Neurosci* 10: 3227-3246, 1990.

Caspary DM, Ling L, Turner JG, and Hughes LF. Inhibitory neurotransmission, plasticity and aging in the mammalian central auditory system. *J Exp Biol* 211: 1781-1791, 2008.

Casseday JH, Covey E, and Grothe B. Neural selectivity and tuning for sinusoidal frequency modulations in the inferior colliculus of the big brown bat, Eptesicus fuscus. *J Neurophysiol* 77: 1595-1605, 1997.

Chang EF, and Merzenich MM. Environmental noise retards auditory cortical development. *Science* 300: 498-502, 2003.

Chang EH, Kotak VC, and Sanes DH. Long-term depression of synaptic inhibition is expressed postsynaptically in the developing auditory system. *J Neurophysiol* 90: 1479-1488, 2003.

Chen G, Trombley PQ, and van den Pol AN. Excitatory actions of GABA in developing rat hypothalamic neurones. *J Physiol* 494 (Pt 2): 451-464, 1996.

Chen S, Wang J, and Siegelbaum SA. Properties of hyperpolarization-activated pacemaker current defined by coassembly of HCN1 and HCN2 subunits and basal modulation by cyclic nucleotide. *J Gen Physiol* 117: 491-504, 2001.

Chen X, Shu S, Schwartz LC, Sun C, Kapur J, and Bayliss DA. Homeostatic regulation of synaptic excitability: tonic GABA(A) receptor currents replace I(h) in cortical pyramidal neurons of HCN1 knock-out mice. *J Neurosci* 30: 2611-2622, 2010.

Cherry SD, and Golding N. Burst Firing of MSO Neurons *In Vitro* Prior to Hearing Onset *33rd ARO Meeting, Anaheim* 2010.

Cherubini E, Rovira C, Gaiarsa JL, Corradetti R, and Ben Ari Y. GABA mediated excitation in immature rat CA3 hippocampal neurons. *Int J Dev Neurosci* 8: 481-490, 1990.

Chirila FV, Rowland KC, Thompson JM, and Spirou GA. Development of gerbil medial superior olive: integration of temporally delayed excitation and inhibition at physiological temperature. *J Physiol* 584: 167-190, 2007.

Choe S, and Robinson R. An ingenious filter: the structural basis for ion channel selectivity. *Neuron* 20: 821-823, 1998.

Christensen-Dalsgaard J, and Carr CE. Evolution of a sensory novelty: tympanic ears and the associated neural processing. *Brain Res Bull* 75: 365-370, 2008.

Clack JA. The evolution of tetrapod ears and the fossil record. *Brain Behav Evol* 50: 198-212, 1997.

Clark GM. The ultrastructure of nerve endings in the medial superior olive of the cat. *Brain Res* 14: 293-305, 1969.

Corner MA, and Ramakers GJ. Spontaneous firing as an epigenetic factor in brain development--physiological consequences of chronic tetrodotoxin and picrotoxin exposure on cultured rat neocortex neurons. *Brain Res Dev Brain Res* 65: 57-64, 1992.

Covey E, and Casseday JH. The monaural nuclei of the lateral lemniscus in an echolocating bat: parallel pathways for analyzing temporal features of sound. *J Neurosci* 11: 3456-3470, 1991.

Cramer KS. Eph proteins and the assembly of auditory circuits. *Hear Res* 206: 42-51, 2005.

D'Angelo E, Rossi P, Armano S, and Taglietti V. Evidence for NMDA and mGlu receptor-dependent long-term potentiation of mossy fiber-granule cell transmission in rat cerebellum. *J Neurophysiol* 81: 277-287, 1999.

Dailey ME, and Smith SJ. The dynamics of dendritic structure in developing hippocampal slices. *J Neurosci* 16: 2983-2994, 1996.

Dallos P. The active cochlea. *J Neurosci* 12: 4575-4585, 1992.

Darrow KN, Maison SF, and Liberman MC. Cochlear efferent feedback balances interaural sensitivity. *Nat Neurosci* 9: 1474-1476, 2006.

Davis GW, and Bezprozvanny I. Maintaining the stability of neural function: a homeostatic hypothesis. *Annu Rev Physiol* 63: 847-869, 2001.

Davis KA. Evidence of a functionally segregated pathway from dorsal cochlear nucleus to inferior colliculus. *J Neurophysiol* 87: 1824-1835, 2002.

de Villers-Sidani E, Chang EF, Bao S, and Merzenich MM. Critical period window for spectral tuning defined in the primary auditory cortex (A1) in the rat. *J Neurosci* 27: 180-189, 2007.

Debanne D, Daoudal G, Sourdet V, and Russier M. Brain plasticity and ion channels. *J Physiol Paris* 97: 403-414, 2003.

Dehmel S, Kopp-Scheinpflug C, Dorrscheidt GJ, and Rubsamen R. Electrophysiological characterization of the superior paraolivary nucleus in the Mongolian gerbil. *Hear Res* 172: 18-36, 2002.

Delgutte B, Joris PX, Litovsky RY, and Yin TC. Receptive fields and binaural interactions for virtual-space stimuli in the cat inferior colliculus. *J Neurophysiol* 81: 2833-2851, 1999.

Denton EJ, and Gray JA. The rigidity of fish and patterns of lateral line stimulation. *Nature* 297: 679-681, 1982.

Desai NS, Rutherford LC, and Turrigiano GG. Plasticity in the intrinsic excitability of cortical pyramidal neurons. *Nat Neurosci* 2: 515-520, 1999.

Di Marco S, Nguyen VA, Bisti S, and Protti DA. Permanent functional reorganization of retinal circuits induced by early long-term visual deprivation. *J Neurosci* 29: 13691-13701, 2009.

Dickson CT, Magistretti J, Shalinsky MH, Fransen E, Hasselmo ME, and Alonso A. Properties and role of I(h) in the pacing of subthreshold oscillations in entorhinal cortex layer II neurons. *J Neurophysiol* 83: 2562-2579, 2000.

DiFrancesco D. Dual allosteric modulation of pacemaker (f) channels by cAMP and voltage in rabbit SA node. *J Physiol* 515 (Pt 2): 367-376, 1999.

Doyle DA, Morais Cabral J, Pfuetzner RA, Kuo A, Gulbis JM, Cohen SL, Chait BT, and MacKinnon R. The structure of the potassium channel: molecular basis of K+ conduction and selectivity. *Science* 280: 69-77, 1998.

Durham D, Rubel EW, and Steel KP. Cochlear ablation in deafness mutant mice: 2-deoxyglucose analysis suggests no spontaneous activity of cochlear origin. *Hear Res* 43: 39-46, 1989.

Elezgarai I, Benitez R, Mateos JM, Lazaro E, Osorio A, Azkue JJ, Bilbao A, Lingenhoehl K, Van Der Putten H, Hampson DR, Kuhn R, Knopfel T, and Grandes P. Developmental expression of the group III metabotropic glutamate receptor mGluR4a in the medial nucleus of the trapezoid body of the rat. *J Comp Neurol* 411: 431-440, 1999.

Ene FA, Kalmbach A, and Kandler K. Metabotropic glutamate receptors in the lateral superior olive activate TRP-like channels: age- and experience-dependent regulation. *J Neurophysiol* 97: 3365-3375, 2007.

Ene FA, Kullmann PH, Gillespie DC, and Kandler K. Glutamatergic calcium responses in the developing lateral superior olive: receptor types and their specific activation by synaptic activity patterns. *J Neurophysiol* 90: 2581-2591, 2003.

Faber DS, and Korn H. Applicability of the coefficient of variation method for analyzing synaptic plasticity. *Biophys J* 60: 1288-1294, 1991.

Fan Y, Fricker D, Brager DH, Chen X, Lu HC, Chitwood RA, and Johnston D. Activity-dependent decrease of excitability in rat hippocampal neurons through increases in I(h). *Nat Neurosci* 8: 1542-1551, 2005.

Farazifard R, and Wu SH. Metabotropic glutamate receptors modulate glutamatergic and GABAergic synaptic transmission in the central nucleus of the inferior colliculus. *Brain Res* 1325: 28-40, 2010.

Feddersen WE, Sandel TT, Teas DC, and Jeffress LA. Localization of high frequency tones. *J Acoust Soc Am* 29: 988–991, 1957.

Fettiplace R, and Hackney CM. The sensory and motor roles of auditory hair cells. *Nat Rev Neurosci* 7: 19-29, 2006.

Fisahn A, Yamada M, Duttaroy A, Gan JW, Deng CX, McBain CJ, and Wess J. Muscarinic induction of hippocampal gamma oscillations requires coupling of the M1 receptor to two mixed cation currents. *Neuron* 33: 615-624, 2002.

Fitzgerald KK, and Sanes DH. Serotonergic modulation of synapses in the developing gerbil lateral superior olive. *J Neurophysiol* 81: 2743-2752, 1999.

Fitzpatrick DC, Kuwada S, and Batra R. Neural sensitivity to interaural time differences: beyond the Jeffress model. *J Neurosci* 20: 1605-1615, 2000.

Ford MC, Grothe B, and Klug A. Fenestration of the calyx of Held occurs sequentially along the tonotopic axis, is influenced by afferent activity, and facilitates glutamate clearance. *J Comp Neurol* 514: 92-106, 2009.

Francis HW, and Manis PB. Effects of deafferentation on the electrophysiology of ventral cochlear nucleus neurons. *Hear Res* 149: 91-105, 2000.

Frere SG, and Luthi A. Pacemaker channels in mouse thalamocortical neurones are regulated by distinct pathways of cAMP synthesis. *J Physiol* 554: 111-125, 2004.

Friauf E. Tonotopic Order in the Adult and Developing Auditory System of the Rat as Shown by c-fos Immunocytochemistry. *Eur J Neurosci* 4: 798-812, 1992.

Friauf E, and Ostwald J. Divergent projections of physiologically characterized rat ventral cochlear nucleus neurons as shown by intra-axonal injection of horseradish peroxidase. *Exp Brain Res* 73: 263-284, 1988.

Fritschy JM, Sidler C, Parpan F, Gassmann M, Kaupmann K, Bettler B, and Benke D. Independent maturation of the GABA(B) receptor subunits GABA(B1) and GABA(B2) during postnatal development in rodent brain. *J Comp Neurol* 477: 235-252, 2004.

Fujino K, and Oertel D. Bidirectional synaptic plasticity in the cerebellum-like mammalian dorsal cochlear nucleus. *Proc Natl Acad Sci U S A* 100: 265-270, 2003.

Funabiki K, Koyano K, and Ohmori H. The role of GABAergic inputs for coincidence detection in the neurones of nucleus laminaris of the chick. *J Physiol* 508 (Pt 3): 851-869, 1998.

Futai K, Okada M, Matsuyama K, and Takahashi T. High-fidelity transmission acquired via a developmental decrease in NMDA receptor expression at an auditory synapse. *J Neurosci* 21: 3342-3349, 2001.

Fuxe K, Dahlstrom A, Hoistad M, Marcellino D, Jansson A, Rivera A, Diaz-Cabiale Z, Jacobsen K, Tinner-Staines B, Hagman B, Leo G, Staines W, Guidolin D, Kehr J, Genedani S, Belluardo N, and Agnati LF. From the Golgi-Cajal mapping to the transmitter-based characterization of the neuronal networks leading to two modes of brain communication: wiring and volume transmission. *Brain Res Rev* 55: 17-54, 2007.

Gaiarsa JL, Tseeb V, and Ben-Ari Y. Postnatal development of pre- and postsynaptic GABAB-mediated inhibitions in the CA3 hippocampal region of the rat. *J Neurophysiol* 73: 246-255, 1995.

Galambos R, and Davis H. The response of single auditory-nerve fibres to acoustic stimulation. *J Neurophysiol* 6: 39-57, 1943.

Gao E, and Suga N. Experience-dependent corticofugal adjustment of midbrain frequency map in bat auditory system. *Proc Natl Acad Sci U S A* 95: 12663-12670, 1998.

Gao E, and Suga N. Experience-dependent plasticity in the auditory cortex and the inferior colliculus of bats: role of the corticofugal system. *Proc Natl Acad Sci U S A* 97: 8081-8086, 2000.

Gibson JR, Bartley AF, and Huber KM. Role for the subthreshold currents ILeak and IH in the homeostatic control of excitability in neocortical somatostatin-positive inhibitory neurons. *J Neurophysiol* 96: 420-432, 2006.

Glendenning KK, Brunso-Bechtold JK, Thompson GC, and Masterton RB. Ascending auditory afferents to the nuclei of the lateral lemniscus. *J Comp Neurol* 197: 673-703, 1981.

Goda Y, and Stevens CF. Long-term depression properties in a simple system. *Neuron* 16: 103-111, 1996.

Goldberg JM, and Brown PB. Functional organization of the dog superior olivary complex: an anatomical and electrophysiological study. *J Neurophysiol* 31: 639-656, 1968.

Goldberg JM, and Brown PB. Response of binaural neurons of dog superior olivary complex to dichotic tonal stimuli: some physiological mechanisms of sound localization. *J Neurophysiol* 32: 613-636, 1969.

Goldberg JM, and Brownell WE. Discharge characteristics of neurons in anteroventral and dorsal cochlear nuclei of cat. *Brain Res* 64: 35-54, 1973.

Golding NL, Ferragamo MJ, and Oertel D. Role of intrinsic conductances underlying responses to transients in octopus cells of the cochlear nucleus. *J Neurosci* 19: 2897-2905, 1999.

Griffin SJ, Bernstein LR, Ingham NJ, and McAlpine D. Neural sensitivity to interaural envelope delays in the inferior colliculus of the guinea pig. *J Neurophysiol* 93: 3463-3478, 2005.

Grissmer S, Nguyen AN, Aiyar J, Hanson DC, Mather RJ, Gutman GA, Karmilowicz MJ, Auperin DD, and Chandy KG. Pharmacological characterization of five cloned voltage-gated K+ channels, types Kv1.1, 1.2, 1.3, 1.5, and 3.1, stably expressed in mammalian cell lines. *Mol Pharmacol* 45: 1227-1234, 1994.

Grothe B. The evolution of temporal processing in the medial superior olive, an auditory brainstem structure. *Prog Neurobiol* 61: 581-610, 2000.

Grothe B. Interaction of excitation and inhibition in processing of pure tone and amplitude-modulated stimuli in the medial superior olive of the mustached bat. *J Neurophysiol* 71: 706-721, 1994.

Grothe B. New roles for synaptic inhibition in sound localization. *Nat Rev Neurosci* 4: 540-550, 2003.

Grothe B, and Neuweiler G. The function of the medial superior olive in small mammals: temporal receptive fields in auditory analysis. *J Comp Physiol A* 186: 413-423, 2000.

Grothe B, and Park TJ. Sensitivity to interaural time differences in the medial superior olive of a small mammal, the Mexican free-tailed bat. *J Neurosci* 18: 6608-6622, 1998.

Grothe B, and Sanes DH. Bilateral inhibition by glycinergic afferents in the medial superior olive. *J Neurophysiol* 69: 1192-1196, 1993.

Grothe B, and Sanes DH. Synaptic inhibition influences the temporal coding properties of medial superior olivary neurons: an in vitro study. *J Neurosci* 14: 1701-1709, 1994.

Grothe B, Schweizer H, Pollak GD, Schuller G, and Rosemann C. Anatomy and projection patterns of the superior olivary complex in the Mexican free-tailed bat, Tadarida brasiliensis mexicana. *J Comp Neurol* 343: 630-646, 1994.

Guetg N, Seddik R, Vigot R, Turecek R, Gassmann M, Vogt KE, Brauner-Osborne H, Shigemoto R, Kretz O, Frotscher M, Kulik A, and Bettler B. The GABAB1a Isoform Mediates Heterosynaptic Depression at Hippocampal Mossy Fiber Synapses. *J Neurosci* 29: 1414-1423, 2009.

Guo J, and Ikeda SR. Endocannabinoids modulate N-type calcium channels and G-protein-coupled inwardly rectifying potassium channels via CB1 cannabinoid receptors heterologously expressed in mammalian neurons. *Mol Pharmacol* 65: 665-674, 2004.

Haas KZ, Sperber EF, Moshe SL, and Stanton PK. Kainic acid-induced seizures enhance dentate gyrus inhibition by downregulation of GABA(B) receptors. *J Neurosci* 16: 4250-4260, 1996.

Hablitz JJ, Tehrani MH, and Barnes EM, Jr. Chronic exposure of developing cortical neurons to GABA down-regulates GABA/benzodiazepine receptors and GABA-gated chloride currents. *Brain Res* 501: 332-338, 1989.

Hallows JL, and Tempel BL. Expression of Kv1.1, a Shaker-like potassium channel, is temporally regulated in embryonic neurons and glia. *J Neurosci* 18: 5682-5691, 1998.

Harayama N, Shibuya I, Tanaka K, Kabashima N, Ueta Y, and Yamashita H. Inhibition of N- and P/Q-type calcium channels by postsynaptic GABAB receptor activation in rat supraoptic neurones. *J Physiol* 509 (Pt 2): 371-383, 1998.

Harrison JM, and Irving R. Nucleus of the Trapezoid Body: Dual Afferent Innervation. *Science* 143: 473-474, 1964.

Hassfurth B, Magnusson AK, Grothe B, and Koch U. Sensory deprivation regulates the development of the hyperpolarization-activated current in auditory brainstem neurons. *Eur J Neurosci* 2009.

Hebb DO. The organization of behavior. *Wiley* 1949.

Heffner RS, and Heffner HE. Sound localization and use of binaural cues by the gerbil (Meriones unguiculatus). *Behav Neurosci* 102: 422-428, 1988.

Heise I, Magnusson AK, Grothe B, and Koch U. Development of GABAB receptor distribution in the gerbil medial superior olive. *Abstract at the Society for Neuroscience Meeting 2005* 2005.

Held H. Die centralen Bahnen des Nervus acusticus bei der Katze. *Archiv für Anatomie und Physiologie-Anatomische Abteilung* 271-291, 1891.

Helfert RH, Bonneau JM, Wenthold RJ, and Altschuler RA. GABA and glycine immunoreactivity in the guinea pig superior olivary complex. *Brain Res* 501: 269-286, 1989.

Helfert RH, and Schwartz IR. Morphological features of five neuronal classes in the gerbil lateral superior olive. *Am J Anat* 179: 55-69, 1987.

Hermann J, Pecka M, von Gersdorff H, Grothe B, and Klug A. Synaptic transmission at the calyx of Held under in vivo like activity levels. *J Neurophysiol* 98: 807-820, 2007.

Hilbig H, Nowack S, Boeckler K, Bidmon HJ, and Zilles K. Characterization of neuronal subsets surrounded by perineuronal nets in the rhesus auditory brainstem. *J Anat* 210: 507-517, 2007.

Hodgkin AL, and Huxley AF. Currents carried by sodium and potassium ions through the membrane of the giant axon of Loligo. *J Physiol* 116: 449-472, 1952.

Hodgkin AL, Huxley AF, and Katz B. Measurement of current-voltage relations in the membrane of the giant axon of Loligo. *J Physiol* 116: 424-448, 1952.

Hu H, Vervaeke K, and Storm JF. Two forms of electrical resonance at theta frequencies, generated by M-current, h-current and persistent Na+ current in rat hippocampal pyramidal cells. *J Physiol* 545: 783-805, 2002.

Huang CL, and Winer JA. Auditory thalamocortical projections in the cat: laminar and areal patterns of input. *J Comp Neurol* 427: 302-331, 2000.

Huang Z, Walker MC, and Shah MM. Loss of dendritic HCN1 subunits enhances cortical excitability and epileptogenesis. *J Neurosci* 29: 10979-10988, 2009.

Huffman KJ, and Cramer KS. EphA4 misexpression alters tonotopic projections in the auditory brainstem. *Dev Neurobiol* 67: 1655-1668, 2007.

Huffman RF, Argeles PC, and Covey E. Processing of sinusoidally amplitude modulated signals in the nuclei of the lateral lemniscus of the big brown bat, Eptesicus fuscus. *Hear Res* 126: 181-200, 1998a.

Huffman RF, Argeles PC, and Covey E. Processing of sinusoidally frequency modulated signals in the nuclei of the lateral lemniscus of the big brown bat, Eptesicus fuscus. *Hear Res* 126: 161-180, 1998b.

Hurley LM, and Pollak GD. Serotonin differentially modulates responses to tones and frequency-modulated sweeps in the inferior colliculus. *J Neurosci* 19: 8071-8082, 1999.

Hurley LM, and Pollak GD. Serotonin shifts first-spike latencies of inferior colliculus neurons. *J Neurosci* 25: 7876-7886, 2005.

Insanally MN, Kover H, Kim H, and Bao S. Feature-dependent sensitive periods in the development of complex sound representation. *J Neurosci* 29: 5456-5462, 2009.

Isaacson JS. GABAB receptor-mediated modulation of presynaptic currents and excitatory transmission at a fast central synapse. *J Neurophysiol* 80: 1571-1576, 1998.

Ishikawa T, Kaneko M, Shin HS, and Takahashi T. Presynaptic N-type and P/Q-type Ca2+ channels mediating synaptic transmission at the calyx of Held of mice. *J Physiol* 568: 199-209, 2005.

Ito M, van Adel B, and Kelly JB. Sound localization after transection of the commissure of Probst in the albino rat. *J Neurophysiol* 76: 3493-3502, 1996.

Jeffress LA. A place theory of sound localization. *J Comp Physiol Psychol* 41: 35-39, 1948.

Jenkins WM, and Merzenich MM. Role of cat primary auditory cortex for sound-localization behavior. *J Neurophysiol* 52: 819-847, 1984.

Jones KA, Borowsky B, Tamm JA, Craig DA, Durkin MM, Dai M, Yao WJ, Johnson M, Gunwaldsen C, Huang LY, Tang C, Shen Q, Salon JA, Morse K, Laz T, Smith KE, Nagarathnam D, Noble SA, Branchek TA, and Gerald C. GABA(B) receptors function as a heteromeric assembly of the subunits GABA(B)R1 and GABA(B)R2. *Nature* 396: 674-679, 1998.

Joris PX, Schreiner CE, and Rees A. Neural processing of amplitude-modulated sounds. *Physiol Rev* 84: 541-577, 2004.

Joris PX, and Yin TC. Envelope coding in the lateral superior olive. I. Sensitivity to interaural time differences. *J Neurophysiol* 73: 1043-1062, 1995.

Jow F, Chiu D, Lim HK, Novak T, and Lin S. Production of GABA by cultured hippocampal glial cells. *Neurochem Int* 45: 273-283, 2004.

Juiz JM, Albin RL, Helfert RH, and Altschuler RA. Distribution of GABAA and GABAB binding sites in the cochlear nucleus of the guinea pig. *Brain Res* 639: 193-201, 1994.

Jung S, Jones TD, Lugo JN, Jr., Sheerin AH, Miller JW, D'Ambrosio R, Anderson AE, and Poolos NP. Progressive dendritic HCN channelopathy during epileptogenesis in the rat pilocarpine model of epilepsy. *J Neurosci* 27: 13012-13021, 2007.

Kabashima N, Shibuya I, Ibrahim N, Ueta Y, and Yamashita H. Inhibition of spontaneous EPSCs and IPSCs by presynaptic GABAB receptors on rat supraoptic magnocellular neurons. *J Physiol* 504 (Pt 1): 113-126, 1997.

Kakazu Y, Akaike N, Komiyama S, and Nabekura J. Regulation of intracellular chloride by cotransporters in developing lateral superior olive neurons. *J Neurosci* 19: 2843-2851, 1999.

Kamikubo Y, Tabata T, Kakizawa S, Kawakami D, Watanabe M, Ogura A, Iino M, and Kano M. Postsynaptic GABAB receptor signalling enhances LTD in mouse cerebellar Purkinje cells. *J Physiol* 585: 549-563, 2007.

Kandler K, Clause A, and Noh J. Tonotopic reorganization of developing auditory brainstem circuits. *Nat Neurosci* 12: 711-717, 2009.

Kandler K, and Friauf E. Development of glycinergic and glutamatergic synaptic transmission in the auditory brainstem of perinatal rats. *J Neurosci* 15: 6890-6904, 1995.

Kandler K, and Friauf E. Pre- and postnatal development of efferent connections of the cochlear nucleus in the rat. *J Comp Neurol* 328: 161-184, 1993.

Kapfer C, Seidl AH, Schweizer H, and Grothe B. Experience-dependent refinement of inhibitory inputs to auditory coincidence-detector neurons. *Nat Neurosci* 5: 247-253, 2002.

Kaupmann K, Huggel K, Heid J, Flor PJ, Bischoff S, Mickel SJ, McMaster G, Angst C, Bittiger H, Froestl W, and Bettler B. Expression cloning of GABA(B) receptors uncovers similarity to metabotropic glutamate receptors. *Nature* 386: 239-246, 1997.

Kelly JB, Buckthought AD, and Kidd SA. Monaural and binaural response properties of single neurons in the rat's dorsal nucleus of the lateral lemniscus. *Hear Res* 122: 25-40, 1998.

Kelly MC, and Chen P. Development of form and function in the mammalian cochlea. *Curr Opin Neurobiol* 19: 395-401, 2009.

Kiang NYS, Watanabe T, Thomas EC, and Clark LF. Discharge patterns of single fibers in the cat's auditory nerve. *Cambridge, Mass: MIT Press* 1965.

Kil J, Kageyama GH, Semple MN, and Kitzes LM. Development of ventral cochlear nucleus projections to the superior olivary complex in gerbil. *J Comp Neurol* 353: 317-340, 1995.

Kim G, and Kandler K. Elimination and strengthening of glycinergic/GABAergic connections during tonotopic map formation. *Nat Neurosci* 6: 282-290, 2003.

Kirmse K, and Kirischuk S. Ambient GABA constrains the strength of GABAergic synapses at Cajal-Retzius cells in the developing visual cortex. *J Neurosci* 26: 4216-4227, 2006.

Kiss A, and Majorossy K. Neuron morphology and synaptic architecture in the medial superior olivary nucleus. Light- and electron microscope studies in the cat. *Exp Brain Res* 52: 315-327, 1983.

Klumpp RG, and Eady HR. Some measurements of interaural time difference thresholds. *J Acoust Soc Am* 28: 859–860, 1957.

Koch U, Braun M, Kapfer C, and Grothe B. Distribution of HCN1 and HCN2 in rat auditory brainstem nuclei. *Eur J Neurosci* 20: 79-91, 2004.

Koch U, and Grothe B. GABAergic and glycinergic inhibition sharpens tuning for frequency modulations in the inferior colliculus of the big brown bat. *J Neurophysiol* 80: 71-82, 1998.

Koch U, and Grothe B. Hyperpolarization-activated current (Ih) in the inferior colliculus: distribution and contribution to temporal processing. *J Neurophysiol* 90: 3679-3687, 2003.

Koch U, and Sanes DH. Afferent regulation of glycine receptor distribution in the gerbil LSO. *Microsc Res Tech* 41: 263-269, 1998.

Kopp-Scheinpflug C, Dehmel S, Tolnai S, Dietz B, Milenkovic I, and Rubsamen R. Glycine-mediated changes of onset reliability at a mammalian central synapse. *Neuroscience* 157: 432-445, 2008.

Kopp-Scheinpflug C, Lippe WR, Dorrscheidt GJ, and Rubsamen R. The medial nucleus of the trapezoid body in the gerbil is more than a relay: comparison of pre- and postsynaptic activity. *J Assoc Res Otolaryngol* 4: 1-23, 2003.

Koppl C. Phase locking to high frequencies in the auditory nerve and cochlear nucleus magnocellularis of the barn owl, Tyto alba. *J Neurosci* 17: 3312-3321, 1997.

Kotak VC, Breithaupt AD, and Sanes DH. Developmental hearing loss eliminates long-term potentiation in the auditory cortex. *Proc Natl Acad Sci U S A* 104: 3550-3555, 2007.

Kotak VC, DiMattina C, and Sanes DH. GABA(B) and Trk receptor signaling mediates long-lasting inhibitory synaptic depression. *J Neurophysiol* 86: 536-540, 2001.

Kotak VC, Fujisawa S, Lee FA, Karthikeyan O, Aoki C, and Sanes DH. Hearing loss raises excitability in the auditory cortex. *J Neurosci* 25: 3908-3918, 2005.

Kotak VC, Korada S, Schwartz IR, and Sanes DH. A developmental shift from GABAergic to glycinergic transmission in the central auditory system. *J Neurosci* 18: 4646-4655, 1998.

Kotak VC, and Sanes DH. Deafferentation weakens excitatory synapses in the developing central auditory system. *Eur J Neurosci* 9: 2340-2347, 1997.

Kotak VC, and Sanes DH. Developmental influence of glycinergic transmission: regulation of NMDA receptor-mediated EPSPs. *J Neurosci* 16: 1836-1843, 1996.

Kotak VC, and Sanes DH. Gain adjustment of inhibitory synapses in the auditory system. *Biol Cybern* 89: 363-370, 2003.

Kotak VC, and Sanes DH. Long-lasting inhibitory synaptic depression is age- and calcium-dependent. *J Neurosci* 20: 5820-5826, 2000.

Kotak VC, and Sanes DH. Synaptically evoked prolonged depolarizations in the developing auditory system. *J Neurophysiol* 74: 1611-1620, 1995.

Koundakjian EJ, Appler JL, and Goodrich LV. Auditory neurons make stereotyped wiring decisions before maturation of their targets. *J Neurosci* 27: 14078-14088, 2007.

Kreinest M, Muller B, Winkelhoff J, Friauf E, and Lohrke S. Miniature EPSCs in the lateral superior olive before hearing onset: regional and cell-type-specific differences and heterogeneous neuromodulatory effects of ATP. *Brain Res* 1295: 21-36, 2009.

Kullmann PH, Ene FA, and Kandler K. Glycinergic and GABAergic calcium responses in the developing lateral superior olive. *Eur J Neurosci* 15: 1093-1104, 2002.

Kullmann PH, and Kandler K. Dendritic Ca2+ responses in neonatal lateral superior olive neurons elicited by glycinergic/GABAergic synapses and action potentials. *Neuroscience* 154: 338-345, 2008.

Kushmerick C, Price GD, Taschenberger H, Puente N, Renden R, Wadiche JI, Duvoisin RM, Grandes P, and von Gersdorff H. Retroinhibition of presynaptic Ca2+ currents by endocannabinoids released via postsynaptic mGluR activation at a calyx synapse. *J Neurosci* 24: 5955-5965, 2004.

Kuwabara N, and Zook JM. Projections to the medial superior olive from the medial and lateral nuclei of the trapezoid body in rodents and bats. *J Comp Neurol* 324: 522-538, 1992.

Kuwada S, Fitzpatrick DC, Batra R, and Ostapoff EM. Sensitivity to interaural time differences in the dorsal nucleus of the lateral lemniscus of the unanesthetized rabbit: comparison with other structures. *J Neurophysiol* 95: 1309-1322, 2005.

Kuwada S, and Yin TC. Binaural interaction in low-frequency neurons in inferior colliculus of the cat. I. Effects of long interaural delays, intensity, and repetition rate on interaural delay function. *J Neurophysiol* 50: 981-999, 1983.

Lachica EA, Rubsamen R, Zirpel L, and Rubel EW. Glutamatergic inhibition of voltage-operated calcium channels in the avian cochlear nucleus. *J Neurosci* 15: 1724-1734, 1995.

Langner G, Albert M, and Briede T. Temporal and spatial coding of periodicity information in the inferior colliculus of awake chinchilla (Chinchilla laniger). *Hear Res* 168: 110-130, 2002.

Langner G, and Schreiner CE. Periodicity coding in the inferior colliculus of the cat. I. Neuronal mechanisms. *J Neurophysiol* 60: 1799-1822, 1988.

Leake PA, Hradek GT, Chair L, and Snyder RL. Neonatal deafness results in degraded topographic specificity of auditory nerve projections to the cochlear nucleus in cats. *J Comp Neurol* 497: 13-31, 2006.

Leake PA, Snyder RL, and Hradek GT. Postnatal refinement of auditory nerve projections to the cochlear nucleus in cats. *J Comp Neurol* 448: 6-27, 2002.

Leao KE, Leao RN, Sun H, Fyffe RE, and Walmsley B. Hyperpolarization-activated currents are differentially expressed in mice brainstem auditory nuclei. *J Physiol* 576: 849-864, 2006a.

Leao RN, Oleskevich S, Sun H, Bautista M, Fyffe RE, and Walmsley B. Differences in glycinergic mIPSCs in the auditory brain stem of normal and congenitally deaf neonatal mice. *J Neurophysiol* 91: 1006-1012, 2004.

Leao RN, Sun H, Svahn K, Berntson A, Youssoufian M, Paolini AG, Fyffe RE, and Walmsley B. Topographic organization in the auditory brainstem of juvenile mice is disrupted in congenital deafness. *J Physiol* 571: 563-578, 2006b.

Leao RN, Svahn K, Berntson A, and Walmsley B. Hyperpolarization-activated (I) currents in auditory brainstem neurons of normal and congenitally deaf mice. *Eur J Neurosci* 22: 147-157, 2005.

LeDoux JE, Sakaguchi A, Iwata J, and Reis DJ. Interruption of projections from the medial geniculate body to an archi-neostriatal field disrupts the classical conditioning of emotional responses to acoustic stimuli. *Neuroscience* 17: 615-627, 1986.

Lei S, and McBain CJ. GABA B receptor modulation of excitatory and inhibitory synaptic transmission onto rat CA3 hippocampal interneurons. *J Physiol* 546: 439-453, 2003.

Leibold C, and van Hemmen JL. Spiking neurons learning phase delays: how mammals may develop auditory time-difference sensitivity. *Phys Rev Lett* 94: 168102, 2005.

Lim R, Alvarez FJ, and Walmsley B. GABA mediates presynaptic inhibition at glycinergic synapses in a rat auditory brainstem nucleus. *J Physiol* 525 Pt 2: 447-459, 2000.

Lohrke S, Srinivasan G, Oberhofer M, Doncheva E, and Friauf E. Shift from depolarizing to hyperpolarizing glycine action occurs at different perinatal ages in superior olivary complex nuclei. *Eur J Neurosci* 22: 2708-2722, 2005.

Lopez-Bendito G, Shigemoto R, Kulik A, Paulsen O, Fairen A, and Lujan R. Expression and distribution of metabotropic GABA receptor subtypes GABABR1 and GABABR2 during rat neocortical development. *Eur J Neurosci* 15: 1766-1778, 2002.

Lopez-Bendito G, Shigemoto R, Kulik A, Vida I, Fairen A, and Lujan R. Distribution of metabotropic GABA receptor subunits GABAB1a/b and GABAB2 in the rat hippocampus during prenatal and postnatal development. *Hippocampus* 14: 836-848, 2004.

Lu Y, Burger RM, and Rubel EW. GABA(B) receptor activation modulates GABA(A) receptor-mediated inhibition in chicken nucleus magnocellularis neurons. *J Neurophysiol* 93: 1429-1438, 2005.

Lu Y, Harris JA, and Rubel EW. Development of spontaneous miniature EPSCs in mouse AVCN neurons during a critical period of afferent-dependent neuron survival. *J Neurophysiol* 97: 635-646, 2007.

Lu Y, and Rubel EW. Activation of metabotropic glutamate receptors inhibits high-voltage-gated calcium channel currents of chicken nucleus magnocellularis neurons. *J Neurophysiol* 93: 1418-1428, 2005.

Ludwig A, Zong X, Hofmann F, and Biel M. Structure and function of cardiac pacemaker channels. *Cell Physiol Biochem* 9: 179-186, 1999a.

Ludwig A, Zong X, Jeglitsch M, Hofmann F, and Biel M. A family of hyperpolarization-activated mammalian cation channels. *Nature* 393: 587-591, 1998.

Ludwig A, Zong X, Stieber J, Hullin R, Hofmann F, and Biel M. Two pacemaker channels from human heart with profoundly different activation kinetics. *EMBO J* 18: 2323-2329, 1999b.

Luhmann HJ, and Prince DA. Postnatal maturation of the GABAergic system in rat neocortex. *J Neurophysiol* 65: 247-263, 1991.

Lujan R, and Shigemoto R. Localization of metabotropic GABA receptor subunits GABAB1 and GABAB2 relative to synaptic sites in the rat developing cerebellum. *Eur J Neurosci* 23: 1479-1490, 2006.

Lujan R, Shigemoto R, Kulik A, and Juiz JM. Localization of the GABAB receptor 1a/b subunit relative to glutamatergic synapses in the dorsal cochlear nucleus of the rat. *J Comp Neurol* 475: 36-46, 2004.

Luscher C, Jan LY, Stoffel M, Malenka RC, and Nicoll RA. G protein-coupled inwardly rectifying K+ channels (GIRKs) mediate postsynaptic but not presynaptic transmitter actions in hippocampal neurons. *Neuron* 19: 687-695, 1997.

Luthi A, and McCormick DA. H-current: properties of a neuronal and network pacemaker. *Neuron* 21: 9-12, 1998a.

Luthi A, and McCormick DA. Periodicity of thalamic synchronized oscillations: the role of Ca2+-mediated upregulation of Ih. *Neuron* 20: 553-563, 1998b.

MacLean JN, Zhang Y, Johnson BR, and Harris-Warrick RM. Activity-independent homeostasis in rhythmically active neurons. *Neuron* 37: 109-120, 2003.

Magee JC. Dendritic hyperpolarization-activated currents modify the integrative properties of hippocampal CA1 pyramidal neurons. *J Neurosci* 18: 7613-7624, 1998.

Magee JC. Dendritic Ih normalizes temporal summation in hippocampal CA1 neurons. *Nat Neurosci* 2: 848, 1999.

Magnusson AK, Kapfer C, Grothe B, and Koch U. Maturation of glycinergic inhibition in the gerbil medial superior olive after hearing onset. *J Physiol* 568: 497-512, 2005.

Magnusson AK, Park TJ, Pecka M, Grothe B, and Koch U. Retrograde GABA signaling adjusts sound localization by balancing excitation and inhibition in the brainstem. *Neuron* 59: 125-137, 2008.

Malenka RC. Synaptic plasticity in the hippocampus: LTP and LTD. *Cell* 78: 535-538, 1994.

Malenka RC, and Nicoll RA. NMDA-receptor-dependent synaptic plasticity: multiple forms and mechanisms. *Trends Neurosci* 16: 521-527, 1993.

Manis PB, and Marx SO. Outward currents in isolated ventral cochlear nucleus neurons. *J Neurosci* 11: 2865-2880, 1991.

Manis PB, Spirou GA, Wright DD, Paydar S, and Ryugo DK. Physiology and morphology of complex spiking neurons in the guinea pig dorsal cochlear nucleus. *J Comp Neurol* 348: 261-276, 1994.

Manley GA. Cochlear mechanisms from a phylogenetic viewpoint. *Proc Natl Acad Sci U S A* 97: 11736-11743, 2000.

Mann-Metzer P, and Yarom Y. Pre- and postsynaptic inhibition mediated by GABA(B) receptors in cerebellar inhibitory interneurons. *J Neurophysiol* 87: 183-190, 2002.

Mapelli L, Rossi P, Nieus T, and D'Angelo E. Tonic activation of GABAB receptors reduces release probability at inhibitory connections in the cerebellar glomerulus. *J Neurophysiol* 101: 3089-3099, 2009.

Marcotti W, Johnson SL, Rusch A, and Kros CJ. Sodium and calcium currents shape action potentials in immature mouse inner hair cells. *J Physiol* 552: 743-761, 2003.

Markovitz NS, and Pollak GD. Binaural processing in the dorsal nucleus of the lateral lemniscus. *Hear Res* 73: 121-140, 1994.

Markram H, Lubke J, Frotscher M, and Sakmann B. Regulation of synaptic efficacy by coincidence of postsynaptic APs and EPSPs. *Science* 275: 213-215, 1997.

Masterton B, Diamond IT, Harrison JM, and Beecher MD. Medial Superior Olive and Sound Localization. *Science* 155: 1696-1697, 1967.

May BJ. Role of the dorsal cochlear nucleus in the sound localization behavior of cats. *Hear Res* 148: 74-87, 2000.

McAlpine D, Jiang D, and Palmer AR. A neural code for low-frequency sound localization in mammals. *Nat Neurosci* 4: 396-401, 2001.

McAlpine D, Jiang D, Shackleton TM, and Palmer AR. Convergent input from brainstem coincidence detectors onto delay-sensitive neurons in the inferior colliculus. *J Neurosci* 18: 6026-6039, 1998.

McLean HA, Caillard O, Khazipov R, Ben-Ari Y, and Gaiarsa JL. Spontaneous release of GABA activates GABAB receptors and controls network activity in the neonatal rat hippocampus. *J Neurophysiol* 76: 1036-1046, 1996.

Miko IJ, Nakamura PA, Henkemeyer M, and Cramer KS. Auditory brainstem neural activation patterns are altered in EphA4- and ephrin-B2-deficient mice. *J Comp Neurol* 505: 669-681, 2007.

Miller KD. Synaptic economics: competition and cooperation in synaptic plasticity. *Neuron* 17: 371-374, 1996.

Misgeld U, Bijak M, and Jarolimek W. A physiological role for GABAB receptors and the effects of baclofen in the mammalian central nervous system. *Prog Neurobiol* 46: 423-462, 1995.

Mitchell SJ, and Silver RA. GABA spillover from single inhibitory axons suppresses low-frequency excitatory transmission at the cerebellar glomerulus. *J Neurosci* 20: 8651-8658, 2000.

Morest DK. The growth of synaptic endings in the mammalian brain: a study of the calyces of the trapezoid body. *Z Anat Entwicklungsgesch* 127: 201-220, 1968.

Mouginot D, Kombian SB, and Pittman QJ. Activation of presynaptic GABAB receptors inhibits evoked IPSCs in rat magnocellular neurons in vitro. *J Neurophysiol* 79: 1508-1517, 1998.

Mugnaini E, Warr WB, and Osen KK. Distribution and light microscopic features of granule cells in the cochlear nuclei of cat, rat, and mouse. *J Comp Neurol* 191: 581-606, 1980.

Mulkey RM, and Malenka RC. Mechanisms underlying induction of homosynaptic long-term depression in area CA1 of the hippocampus. *Neuron* 9: 967-975, 1992.

Muller J, and Tsuji LA. Impedance-matching hearing in Paleozoic reptiles: evidence of advanced sensory perception at an early stage of amniote evolution. *PLoS One* 2: e889, 2007.

Musicant AD, Chan JC, and Hind JE. Direction-dependent spectral properties of cat external ear: new data and cross-species comparisons. *J Acoust Soc Am* 87: 757-781, 1990.

Nabekura J, Katsurabayashi S, Kakazu Y, Shibata S, Matsubara A, Jinno S, Mizoguchi Y, Sasaki A, and Ishibashi H. Developmental switch from GABA to glycine release in single central synaptic terminals. *Nat Neurosci* 7: 17-23, 2004.

Nakamura Y, and Takahashi T. Developmental changes in potassium currents at the rat calyx of Held presynaptic terminal. *J Physiol* 581: 1101-1112, 2007.

Nakanishi S. Metabotropic glutamate receptors: synaptic transmission, modulation, and plasticity. *Neuron* 13: 1031-1037, 1994.

Nelken I. Processing of complex sounds in the auditory system. *Curr Opin Neurobiol* 18: 413-417, 2008.

Nelken I, and Bar-Yosef O. Neurons and objects: the case of auditory cortex. *Front Neurosci* 2: 107-113, 2008.

Nicoll RA. My close encounter with GABA(B) receptors. *Biochem Pharmacol* 68: 1667-1674, 2004.

Nishimaki T, Jang IS, Ishibashi H, Yamaguchi J, and Nabekura J. Reduction of metabotropic glutamate receptor-mediated heterosynaptic inhibition of developing MNTB-LSO inhibitory synapses. *Eur J Neurosci* 26: 323-330, 2007.

Noh J, Seal RP, Garver JA, Edwards RH, and Kandler K. Glutamate co-release at GABA/glycinergic synapses is crucial for the refinement of an inhibitory map. *Nat Neurosci* 13: 232-238, 2010.

Nolan MF, Dudman JT, Dodson PD, and Santoro B. HCN1 channels control resting and active integrative properties of stellate cells from layer II of the entorhinal cortex. *J Neurosci* 27: 12440-12451, 2007.

Nolan MF, Malleret G, Dudman JT, Buhl DL, Santoro B, Gibbs E, Vronskaya S, Buzsaki G, Siegelbaum SA, Kandel ER, and Morozov A. A behavioral role for dendritic integration:

HCN1 channels constrain spatial memory and plasticity at inputs to distal dendrites of CA1 pyramidal neurons. *Cell* 119: 719-732, 2004.

Nordeen KW, Killackey HP, and Kitzes LM. Ascending auditory projections to the inferior colliculus in the adult gerbil, Meriones unguiculatus. *J Comp Neurol* 214: 131-143, 1983.

Notomi T, and Shigemoto R. Immunohistochemical localization of Ih channel subunits, HCN1-4, in the rat brain. *J Comp Neurol* 471: 241-276, 2004.

Oertel D, and Young ED. What's a cerebellar circuit doing in the auditory system? *Trends Neurosci* 27: 104-110, 2004.

Oleskevich S, and Walmsley B. Synaptic transmission in the auditory brainstem of normal and congenitally deaf mice. *J Physiol* 540: 447-455, 2002.

Oleskevich S, Youssoufian M, and Walmsley B. Presynaptic plasticity at two giant auditory synapses in normal and deaf mice. *J Physiol* 560: 709-719, 2004.

Oliver DL. Ascending efferent projections of the superior olivary complex. *Microsc Res Tech* 51: 355-363, 2000.

Osen KK. Cytoarchitecture of the cochlear nuclei in the cat. *J Comp Neurol* 136: 453-484, 1969.

Oswald AM, Doiron B, Rinzel J, and Reyes AD. Spatial profile and differential recruitment of GABAB modulate oscillatory activity in auditory cortex. *J Neurosci* 29: 10321-10334, 2009.

Otmakhova NA, Otmakhov N, and Lisman JE. Pathway-specific properties of AMPA and NMDA-mediated transmission in CA1 hippocampal pyramidal cells. *J Neurosci* 22: 1199-1207, 2002.

Overholt EM, Rubel EW, and Hyson RL. A circuit for coding interaural time differences in the chick brainstem. *J Neurosci* 12: 1698-1708, 1992.

Pan BX, Dong Y, Ito W, Yanagawa Y, Shigemoto R, and Morozov A. Selective gating of glutamatergic inputs to excitatory neurons of amygdala by presynaptic GABAb receptor. *Neuron* 61: 917-929, 2009.

Pape HC, and McCormick DA. Noradrenaline and serotonin selectively modulate thalamic burst firing by enhancing a hyperpolarization-activated cation current. *Nature* 340: 715-718, 1989.

Parks TN, and Rubel EW. Organization and development of brain stem auditory nuclei of the chicken: organization of projections from n. magnocellularis to n. laminaris. *J Comp Neurol* 164: 435-448, 1975.

Pecka M, Brand A, Behrend O, and Grothe B. Interaural time difference processing in the mammalian medial superior olive: the role of glycinergic inhibition. *J Neurosci* 28: 6914-6925, 2008.

Pecka M, Zahn TP, Saunier-Rebori B, Siveke I, Felmy F, Wiegrebe L, Klug A, Pollak GD, and Grothe B. Inhibiting the inhibition: a neuronal network for sound localization in reverberant environments. *J Neurosci* 27: 1782-1790, 2007.

Penzo MA, and Pena JL. Endocannabinoid-mediated long-term depression in the avian midbrain expressed presynaptically and postsynaptically. *J Neurosci* 29: 4131-4139, 2009.

Perez-Otano I, and Ehlers MD. Homeostatic plasticity and NMDA receptor trafficking. *Trends Neurosci* 28: 229-238, 2005.

Petralia RS, Wang YX, Niedzielski AS, and Wenthold RJ. The metabotropic glutamate receptors, mGluR2 and mGluR3, show unique postsynaptic, presynaptic and glial localizations. *Neuroscience* 71: 949-976, 1996.

Pitler TA, and Alger BE. Differences between presynaptic and postsynaptic GABAB mechanisms in rat hippocampal pyramidal cells. *J Neurophysiol* 72: 2317-2327, 1994.

Pollak GD. Roles of GABAergic inhibition for the binaural processing of multiple sound sources in the inferior colliculus. *Ann Otol Rhinol Laryngol Suppl* 168: 44-54, 1997.

Pollak GD. Time is traded for intensity in the bat's auditory system. *Hear Res* 36: 107-124, 1988.

Pollak GD, Burger RM, and Klug A. Dissecting the circuitry of the auditory system. *Trends Neurosci* 26: 33-39, 2003.

Popescu MV, and Polley DB. Monaural deprivation disrupts development of binaural selectivity in auditory midbrain and cortex. *Neuron* 65: 718-731, 2010.

Rautenberg PL, Grothe B, and Felmy F. Quantification of the three-dimensional morphology of coincidence detector neurons in the medial superior olive of gerbils during late postnatal development. *J Comp Neurol* 517: 385-396, 2009.

Rayleigh L. On our perception of sound direction. *Philos Mag* 13: 214-232, 1907.

Redburn DA. Development of GABAergic neurons in the mammalian retina. *Prog Brain Res* 90: 133-147, 1992.

Rees A, and Moller AR. Responses of neurons in the inferior colliculus of the rat to AM and FM tones. *Hear Res* 10: 301-330, 1983.

Rees A, and Moller AR. Stimulus properties influencing the responses of inferior colliculus neurons to amplitude-modulated sounds. *Hear Res* 27: 129-143, 1987.

Reichling DB, Kyrozis A, Wang J, and MacDermott AB. Mechanisms of GABA and glycine depolarization-induced calcium transients in rat dorsal horn neurons. *J Physiol* 476: 411-421, 1994.

Represa A, and Ben-Ari Y. Trophic actions of GABA on neuronal development. *Trends Neurosci* 28: 278-283, 2005.

Richichi C, Brewster AL, Bender RA, Simeone TA, Zha Q, Yin HZ, Weiss JH, and Baram TZ. Mechanisms of seizure-induced 'transcriptional channelopathy' of hyperpolarization-activated cyclic nucleotide gated (HCN) channels. *Neurobiol Dis* 29: 297-305, 2008.

Roberts RC, and Ribak CE. GABAergic neurons and axon terminals in the brainstem auditory nuclei of the gerbil. *J Comp Neurol* 258: 267-280, 1987.

Robinson RB, and Siegelbaum SA. Hyperpolarization-activated cation currents: from molecules to physiological function. *Annu Rev Physiol* 65: 453-480, 2003.

Rose JE, Kitzes LM, Gibson MM, and Hind JE. Observations on phase-sensitive neurons of anteroventral cochlear nucleus of the cat: nonlinearity of cochlear output. *J Neurophysiol* 37: 218-253, 1974.

Russell FA, and Moore DR. Effects of unilateral cochlear removal on dendrites in the gerbil medial superior olivary nucleus. *Eur J Neurosci* 11: 1379-1390, 1999.

Ryan A. Hearing sensitivity of the mongolian gerbil, Meriones unguiculatis. *J Acoust Soc Am* 59: 1222-1226, 1976.

Sakaba T, and Neher E. Direct modulation of synaptic vesicle priming by GABA(B) receptor activation at a glutamatergic synapse. *Nature* 424: 775-778, 2003.

Sanes DH, Markowitz S, Bernstein J, and Wardlow J. The influence of inhibitory afferents on the development of postsynaptic dendritic arbors. *J Comp Neurol* 321: 637-644, 1992.

Sanes DH, McGee J, and Walsh EJ. Metabotropic glutamate receptor activation modulates sound level processing in the cochlear nucleus. *J Neurophysiol* 80: 209-217, 1998.

Sanes DH, Merickel M, and Rubel EW. Evidence for an alteration of the tonotopic map in the gerbil cochlea during development. *J Comp Neurol* 279: 436-444, 1989.

Sanes DH, and Rubel EW. The ontogeny of inhibition and excitation in the gerbil lateral superior olive. *J Neurosci* 8: 682-700, 1988.

Sanes DH, and Siverls V. Development and specificity of inhibitory terminal arborizations in the central nervous system. *J Neurobiol* 22: 837-854, 1991.

Sanes DH, and Takacs C. Activity-dependent refinement of inhibitory connections. *Eur J Neurosci* 5: 570-574, 1993.

Santoro B, Liu DT, Yao H, Bartsch D, Kandel ER, Siegelbaum SA, and Tibbs GR. Identification of a gene encoding a hyperpolarization-activated pacemaker channel of brain. *Cell* 93: 717-729, 1998.

Scanziani M. GABA spillover activates postsynaptic GABA(B) receptors to control rhythmic hippocampal activity. *Neuron* 25: 673-681, 2000.

Schnupp JW, and Carr CE. On hearing with more than one ear: lessons from evolution. *Nat Neurosci* 12: 692-697, 2009.

Schuller G. Coding of small sinusoidal frequency and amplitude modulations in the inferior colliculus of 'CF-FM' bat, Rhinolophus ferrumequinum. *Exp Brain Res* 34: 117-132, 1979.

Schwartz IR, and Wittebort AZ. Axon terminals in the cat medial superior olivary nucleus. *Anat Rec* 184: 1976.

Scott LL, Hage TA, and Golding NL. Weak action potential backpropagation is associated with high-frequency axonal firing capability in principal neurons of the gerbil medial superior olive. *J Physiol* 583: 647-661, 2007.

Scott LL, Mathews PJ, and Golding NL. Posthearing developmental refinement of temporal processing in principal neurons of the medial superior olive. *J Neurosci* 25: 7887-7895, 2005.

Seidl AH, and Grothe B. Development of sound localization mechanisms in the mongolian gerbil is shaped by early acoustic experience. *J Neurophysiol* 94: 1028-1036, 2005.

Shah MM, Anderson AE, Leung V, Lin X, and Johnston D. Seizure-induced plasticity of h channels in entorhinal cortical layer III pyramidal neurons. *Neuron* 44: 495-508, 2004.

Shaikh AG, and Finlayson PG. Excitability of auditory brainstem neurons, in vivo, is increased by cyclic-AMP. *Hear Res* 201: 70-80, 2005.

Shaikh AG, and Finlayson PG. Hyperpolarization-activated (I(h)) conductances affect brainstem auditory neuron excitability. *Hear Res* 183: 126-136, 2003.

Shibata S, Kakazu Y, Okabe A, Fukuda A, and Nabekura J. Experience-dependent changes in intracellular Cl- regulation in developing auditory neurons. *Neurosci Res* 48: 211-220, 2004.

Shigemoto R, Nomura S, Ohishi H, Sugihara H, Nakanishi S, and Mizuno N. Immunohistochemical localization of a metabotropic glutamate receptor, mGluR5, in the rat brain. *Neurosci Lett* 163: 53-57, 1993.

Shinn-Cunningham BG, Santarelli S, and Kopco N. Tori of confusion: binaural localization cues for sources within reach of a listener. *J Acoust Soc Am* 107: 1627-1636, 2000.

Shinonaga Y, Takada M, and Mizuno N. Direct projections from the non-laminated divisions of the medial geniculate nucleus to the temporal polar cortex and amygdala in the cat. *J Comp Neurol* 340: 405-426, 1994.

Shore SE. Multisensory integration in the dorsal cochlear nucleus: unit responses to acoustic and trigeminal ganglion stimulation. *Eur J Neurosci* 21: 3334-3348, 2005.

Siveke I, Pecka M, Seidl AH, Baudoux S, and Grothe B. Binaural response properties of low-frequency neurons in the gerbil dorsal nucleus of the lateral lemniscus. *J Neurophysiol* 96: 1425-1440, 2006.

Skottun BC. Sound localization and neurons. *Nature* 393: 531, 1998.

Smith AJ, Owens S, and Forsythe ID. Characterisation of inhibitory and excitatory postsynaptic currents of the rat medial superior olive. *J Physiol* 529 Pt 3: 681-698, 2000.

Smith PH, Joris PX, Carney LH, and Yin TC. Projections of physiologically characterized globular bushy cell axons from the cochlear nucleus of the cat. *J Comp Neurol* 304: 387-407, 1991.

Smith PH, Joris PX, and Yin TC. Projections of physiologically characterized spherical bushy cell axons from the cochlear nucleus of the cat: evidence for delay lines to the medial superior olive. *J Comp Neurol* 331: 245-260, 1993.

Snyder RL, and Leake PA. Topography of spiral ganglion projections to cochlear nucleus during postnatal development in cats. *J Comp Neurol* 384: 293-311, 1997.

Sonntag M, Englitz B, Kopp-Scheinpflug C, and Rubsamen R. Early postnatal development of spontaneous and acoustically evoked discharge activity of principal cells of the medial nucleus of the trapezoid body: an in vivo study in mice. *J Neurosci* 29: 9510-9520, 2009.

Spirou GA, Rowland KC, and Berrebi AS. Ultrastructure of neurons and large synaptic terminals in the lateral nucleus of the trapezoid body of the cat. *J Comp Neurol* 398: 257-272, 1998.

Spitzer MW, and Semple MN. Neurons sensitive to interaural phase disparity in gerbil superior olive: diverse monaural and temporal response properties. *J Neurophysiol* 73: 1668-1690, 1995.

Steinert JR, Kopp-Scheinpflug C, Baker C, Challiss RA, Mistry R, Haustein MD, Griffin SJ, Tong H, Graham BP, and Forsythe ID. Nitric oxide is a volume transmitter regulating postsynaptic excitability at a glutamatergic synapse. *Neuron* 60: 642-656, 2008.

Stieber J, Stockl G, Herrmann S, Hassfurth B, and Hofmann F. Functional expression of the human HCN3 channel. *J Biol Chem* 280: 34635-34643, 2005.

Stieber J, Thomer A, Much B, Schneider A, Biel M, and Hofmann F. Molecular basis for the different activation kinetics of the pacemaker channels HCN2 and HCN4. *J Biol Chem* 278: 33672-33680, 2003.

Stotler WA. An experimental study of the cells and connections of the superior olivary complex of the cat. *J Comp Neurol* 98: 401-431, 1953.

Suga N. The Cognitive Neurosciences. *MIT Press* 295-318, 1994.

Suga N, and Ma X. Multiparametric corticofugal modulation and plasticity in the auditory system. *Nat Rev Neurosci* 4: 783-794, 2003.

Sun H, Ma CL, Kelly JB, and Wu SH. GABAB receptor-mediated presynaptic inhibition of glutamatergic transmission in the inferior colliculus. *Neurosci Lett* 399: 151-156, 2006.

Surges R, Brewster AL, Bender RA, Beck H, Feuerstein TJ, and Baram TZ. Regulated expression of HCN channels and cAMP levels shape the properties of the h current in developing rat hippocampus. *Eur J Neurosci* 24: 94-104, 2006.

Takahashi T, Kajikawa Y, and Tsujimoto T. G-Protein-coupled modulation of presynaptic calcium currents and transmitter release by a GABAB receptor. *J Neurosci* 18: 3138-3146, 1998.

Tan ML, Theeuwes HP, Feenstra L, and Borst JG. Membrane properties and firing patterns of inferior colliculus neurons: an in vivo patch-clamp study in rodents. *J Neurophysiol* 98: 443-453, 2007.

Tang ZQ, Gao H, and Lu Y. Control of a depolarizing GABAergic input in an auditory coincidence detection circuit. *J Neurophysiol* 2009.

Taschenberger H, Leao RM, Rowland KC, Spirou GA, and von Gersdorff H. Optimizing synaptic architecture and efficiency for high-frequency transmission. *Neuron* 36: 1127-1143, 2002.

Thompson AM, and Lauder JM. Postnatal expression of the serotonin transporter in auditory brainstem neurons. *Dev Neurosci* 27: 1-12, 2005.

Thompson AM, and Thompson GC. Efferent projections from posteroventral cochlear nucleus to lateral superior olive in guinea pig. *Brain Res* 421: 382-386, 1987.

Tollin DJ. The lateral superior olive: a functional role in sound source localization. *Neuroscientist* 9: 127-143, 2003.

Tollin DJ, and Yin TC. Interaural phase and level difference sensitivity in low-frequency neurons in the lateral superior olive. *J Neurosci* 25: 10648-10657, 2005.

Trussell LO. Synaptic mechanisms for coding timing in auditory neurons. *Annu Rev Physiol* 61: 477-496, 1999.

Tsuchitani C, and Boudreau JC. Stimulus level of dichotically presented tones and cat superior olive S-segment cell dcharge. *J Acoust Soc Am* 46: 979-988, 1969.

Tucci DL, Cant NB, and Durham D. Conductive hearing loss results in a decrease in central auditory system activity in the young gerbil. *Laryngoscope* 109: 1359-1371, 1999.

Turrigiano G, LeMasson G, and Marder E. Selective regulation of current densities underlies spontaneous changes in the activity of cultured neurons. *J Neurosci* 15: 3640-3652, 1995.

Turrigiano GG, and Nelson SB. Homeostatic plasticity in the developing nervous system. *Nat Rev Neurosci* 5: 97-107, 2004.

Tzounopoulos T, Kim Y, Oertel D, and Trussell LO. Cell-specific, spike timing-dependent plasticities in the dorsal cochlear nucleus. *Nat Neurosci* 7: 719-725, 2004.

Tzounopoulos T, Rubio ME, Keen JE, and Trussell LO. Coactivation of pre- and postsynaptic signaling mechanisms determines cell-specific spike-timing-dependent plasticity. *Neuron* 54: 291-301, 2007.

Ulens C, and Tytgat J. Gi- and Gs-coupled receptors up-regulate the cAMP cascade to modulate HCN2, but not HCN1 pacemaker channels. *Pflugers Arch* 442: 928-942, 2001.

Vaca L, Stieber J, Zong X, Ludwig A, Hofmann F, and Biel M. Mutations in the S4 domain of a pacemaker channel alter its voltage dependence. *FEBS Lett* 479: 35-40, 2000.

Vale C, Juiz JM, Moore DR, and Sanes DH. Unilateral cochlear ablation produces greater loss of inhibition in the contralateral inferior colliculus. *Eur J Neurosci* 20: 2133-2140, 2004.

Van Bergeijk WA. Evolution of the sense of hearing in vertebrates. *Am Zool* 6: 371-377, 1966.

van Welie I, van Hooft JA, and Wadman WJ. Background activity regulates excitability of rat hippocampal CA1 pyramidal neurons by adaptation of a K+ conductance. *J Neurophysiol* 95: 2007-2012, 2006.

van Welie I, van Hooft JA, and Wadman WJ. Homeostatic scaling of neuronal excitability by synaptic modulation of somatic hyperpolarization-activated Ih channels. *Proc Natl Acad Sci U S A* 101: 5123-5128, 2004.

Varela JA, Sen K, Gibson J, Fost J, Abbott LF, and Nelson SB. A quantitative description of short-term plasticity at excitatory synapses in layer 2/3 of rat primary visual cortex. *J Neurosci* 17: 7926-7940, 1997.

Vargas KJ, Terunuma M, Tello JA, Pangalos MN, Moss SJ, and Couve A. The availability of surface GABA B receptors is independent of gamma-aminobutyric acid but controlled by glutamate in central neurons. *J Biol Chem* 283: 24641-24648, 2008.

Vasilyev DV, and Barish ME. Postnatal development of the hyperpolarization-activated excitatory current Ih in mouse hippocampal pyramidal neurons. *J Neurosci* 22: 8992-9004, 2002.

Von Bekesy G. Current status of theories of hearing. *Science* 123: 779-783, 1956a.

von Bekesy G. Simplified Model to Demonstrate the Energy Flow and Formation of Traveling Waves Similar to Those Found in the Cochlea. *Proc Natl Acad Sci U S A* 42: 930-944, 1956b.

Wagner JJ, and Alger BE. GABAergic and developmental influences on homosynaptic LTD and depotentiation in rat hippocampus. *J Neurosci* 15: 1577-1586, 1995.

Wahl-Schott C, and Biel M. HCN channels: structure, cellular regulation and physiological function. *Cell Mol Life Sci* 66: 470-494, 2009.

Wainger BJ, DeGennaro M, Santoro B, Siegelbaum SA, and Tibbs GR. Molecular mechanism of cAMP modulation of HCN pacemaker channels. *Nature* 411: 805-810, 2001.

Wang J, Reichling DB, Kyrozis A, and MacDermott AB. Developmental loss of GABA- and glycine-induced depolarization and Ca2+ transients in embryonic rat dorsal horn neurons in culture. *Eur J Neurosci* 6: 1275-1280, 1994.

Wang X, and Robertson D. Effects of bioamines and peptides on neurones in the ventral nucleus of trapezoid body and rostral periolivary regions of the rat superior olivary complex: an in vitro investigation. *Hear Res* 106: 20-28, 1997.

Warr WB. Fiber degeneration following lesions in the multipolar and globular cell areas in the ventral cochlear nucleus of the cat. *Brain Res* 40: 247-270, 1972.

Warr WB. Fiber degeneration following lesions in the posteroventral cochlear nucleus of the cat. *Exp Neurol* 23: 140-155, 1969.

Webb JF. Gross morphology and evolution of the mechanoreceptive lateral-line system in teleost fishes. *Brain Behav Evol* 33: 34-53, 1989.

Webster DB, and Trune DR. Cochlear nuclear complex of mice. *Am J Anat* 163: 103-130, 1982.

Wehr M, and Zador AM. Synaptic mechanisms of forward suppression in rat auditory cortex. *Neuron* 47: 437-445, 2005.

Weinberger NM. Specific long-term memory traces in primary auditory cortex. *Nat Rev Neurosci* 5: 279-290, 2004.

Wenthold RJ, Huie D, Altschuler RA, and Reeks KA. Glycine immunoreactivity localized in the cochlear nucleus and superior olivary complex. *Neuroscience* 22: 897-912, 1987.

Werthat F, Alexandrova O, Grothe B, and Koch U. Experience-dependent refinement of the inhibitory axons projecting to the medial superior olive. *Dev Neurobiol* 68: 1454-1462, 2008.

Wightman FL, and Kistler DJ. The dominant role of low-frequency interaural time differences in sound localization. *J Acoust Soc Am* 91: 1648-1661, 1992.

Wightman FL, and Kistler DJ. Monaural sound localization revisited. *J Acoust Soc Am* 101: 1050-1063, 1997.

Winer JA, and Lee CC. The distributed auditory cortex. *Hear Res* 229: 3-13, 2007.

Wojcik WJ, and Neff NH. gamma-aminobutyric acid B receptors are negatively coupled to adenylate cyclase in brain, and in the cerebellum these receptors may be associated with granule cells. *Mol Pharmacol* 25: 24-28, 1984.

Wu SH, and Oertel D. Intracellular injection with horseradish peroxidase of physiologically characterized stellate and bushy cells in slices of mouse anteroventral cochlear nucleus. *J Neurosci* 4: 1577-1588, 1984.

Wu Y, Wang W, Diez-Sampedro A, and Richerson GB. Nonvesicular inhibitory neurotransmission via reversal of the GABA transporter GAT-1. *Neuron* 56: 851-865, 2007.

Xie R, Gittelman JX, Li N, and Pollak GD. Whole cell recordings of intrinsic properties and sound-evoked responses from the inferior colliculus. *Neuroscience* 154: 245-256, 2008.

Yamada K, Kaga K, Uno A, and Shindo M. Sound lateralization in patients with lesions including the auditory cortex: comparison of interaural time difference (ITD) discrimination and interaural intensity difference (IID) discrimination. *Hear Res* 101: 173-180, 1996.

Yamada K, Yu B, and Gallagher JP. Different subtypes of GABAB receptors are present at pre- and postsynaptic sites within the rat dorsolateral septal nucleus. *J Neurophysiol* 81: 2875-2883, 1999.

Yamada R, Kuba H, Ishii TM, and Ohmori H. Hyperpolarization-activated cyclic nucleotide-gated cation channels regulate auditory coincidence detection in nucleus laminaris of the chick. *J Neurosci* 25: 8867-8877, 2005.

Yamauchi T, Hori T, and Takahashi T. Presynaptic inhibition by muscimol through GABAB receptors. *Eur J Neurosci* 12: 3433-3436, 2000.

Yevenes GE, Moraga-Cid G, Guzman L, Haeger S, Oliveira L, Olate J, Schmalzing G, and Aguayo LG. Molecular determinants for G protein betagamma modulation of ionotropic glycine receptors. *J Biol Chem* 281: 39300-39307, 2006.

Yevenes GE, Peoples RW, Tapia JC, Parodi J, Soto X, Olate J, and Aguayo LG. Modulation of glycine-activated ion channel function by G-protein betagamma subunits. *Nat Neurosci* 6: 819-824, 2003.

Yin TC, and Chan JC. Interaural time sensitivity in medial superior olive of cat. *J Neurophysiol* 64: 465-488, 1990.

Young ED, Nelken I, and Conley RA. Somatosensory effects on neurons in dorsal cochlear nucleus. *J Neurophysiol* 73: 743-765, 1995.

Young SR, and Rubel EW. Embryogenesis of arborization pattern and topography of individual axons in N. laminaris of the chicken brain stem. *J Comp Neurol* 254: 425-459, 1986.

Young SR, and Rubel EW. Frequency-specific projections of individual neurons in chick brainstem auditory nuclei. *J Neurosci* 3: 1373-1378, 1983.

Youssoufian M, Couchman K, Shivdasani MN, Paolini AG, and Walmsley B. Maturation of auditory brainstem projections and calyces in the congenitally deaf (dn/dn) mouse. *J Comp Neurol* 506: 442-451, 2008.

Yu LM, and Goda Y. Dendritic signalling and homeostatic adaptation. *Curr Opin Neurobiol* 19: 327-335, 2009.

Zha Q, Brewster AL, Richichi C, Bender RA, and Baram TZ. Activity-dependent heteromerization of the hyperpolarization-activated, cyclic-nucleotide gated (HCN) channels: role of N-linked glycosylation. *J Neurochem* 105: 68-77, 2008.

Zhang LI, Tao HW, Holt CE, Harris WA, and Poo M. A critical window for cooperation and competition among developing retinotectal synapses. *Nature* 395: 37-44, 1998.

Zhang S, and Oertel D. Cartwheel and superficial stellate cells of the dorsal cochlear nucleus of mice: intracellular recordings in slices. *J Neurophysiol* 69: 1384-1397, 1993.

Zhang W, and Linden DJ. The other side of the engram: experience-driven changes in neuronal intrinsic excitability. *Nat Rev Neurosci* 4: 885-900, 2003.

Zhao Y, Rubio ME, and Tzounopoulos T. Distinct functional and anatomical architecture of the endocannabinoid system in the auditory brainstem. *J Neurophysiol* 101: 2434-2446, 2009.

Zirpel L, Lachica EA, and Rubel EW. Activation of a metabotropic glutamate receptor increases intracellular calcium concentrations in neurons of the avian cochlear nucleus. *J Neurosci* 15: 214-222, 1995.

Zook JM, and Casseday JH. Origin of ascending projections to inferior colliculus in the mustache bat, Pteronotus parnellii. *J Comp Neurol* 207: 14-28, 1982.

7 LIST OF ABBREVIATIONS

4-AP	4-aminopyridine
5-HT	serotonin
τ	activation time constant
AC	auditory cortex
aCSF	artificial cerebrospinal fluid
AFN	Atipamezol-Flumazenil-Naloxon
AMPA	α-amino-3-hydroxy-5-methyl-4-isoxazolepropionic acid
AP	action potential
ATP	adenosine triphosphate
AVCN	anteroventral cochlear nucleus
BAC	Baclofen
BS	blocking solution
CA	cochlear ablations
cAMP	cyclic adenosine monophosphate
CB1R	Cannabinoid receptor
CN	cochlear nucleus
CV	coefficient of variation
DCN	dorsal cochlear nucleus
DL-APV	DL-2-amino-5-phosphonopentanoic acid
DNLL	dorsal nucleus of the lateral lemniscus
DNQX	6,7-dinitroquinoxaline-2,3-dione
E_{Cl^-}	chloride reversal potential
EPSC	excitatory postsynaptic current
EPSP	excitatory postsynaptic potential
GABA	γ-Aminobutyric acid
$GABA_AR$	γ-Aminobutyric acid A receptor
$GABA_BR$	γ-Aminobutyric acid B receptor
GAD65	glutamate decarboxylase 65
GAT	γ-Aminobutyric acid transporter
GBC	globular bushy cell
GlyR	glycine receptor
GlyT2	glycine transporter 2
G protein	guanine nucleotide-binding protein
GIRK channel	G-protein coupled inwardly rectifying potassium channel
GPCR	G-protein-coupled receptor

HCN	hyperpolarization-activated and cyclic nucleotide-gated cation channel
IC	inferior colliculus
IC_{50}	half maximal inhibitory concentration
I_h	HCN-mediated current
I_{KLT}	low-threshold-activated potassium current
IHC	inner hair cell
ILD	interaural level difference
IPSC	inhibitory postsynaptic current
IPSP	inhibitory postsynaptic potential
ITD	interaural time difference
K	slope of the Boltzmann function
K_{LT}	low-threshold potassium channels
K_v channels	voltage-gated potassium channel
KCC2	K-Cl cotransporter 2
LNTB	lateral and medial nucleus of the trapezoid body
LSO	lateral superior olive
LTD	long-term depression
LTP	long-term potentiation
MAP2	microtubule associated protein 2
mGluR	metabotropic glutamate receptor
MGN	medial geniculate body
mIPSC	miniature inhibitory postsynaptic current
MNTB	medial nucleus of the trapezoid body
Na_v channels	voltage-gated sodiumchannel
NL	nucleus laminaris
NLL	nucleus of the lateral lemniscus
NM	nucleus magnocellularis
NMDA	*N*-methyl *D*-aspartate
OHC	outer hair cell
P	postnatal day
PBS	phosphate buffered saline
PFA	paraformaldehyd
PPR	paired pulse ratio
PVCN	posteroventral cochlear nucleus
SBC	spherical bushy cell
SAM	sinusoidally amplitude modulated sound
SFM	sinusoidally frequency modulated sound

SOC	superior olivary complex
SPN	superior periolivary nucleus
STDP	spike-timing dependent plasticity
TTX	tetrodotoxin
R_{in}	input resistance
VGIC	voltage-gated ion channel

8 ACKNOWLEDGEMENTS

First and foremost, I wish to thank PD Dr. Ursula Koch for guiding me through a demanding and exciting time during my PhD thesis. I am deeply grateful for your enduring support and the long time you spent explaining the “basics of neurobiology” to me! You cannot imagine how exceptionally helpful it was being supervised by someone who, whenever I asked for it, found the time for discussions and explanations. Thank you very much for challenging and supporting me, Ursula.

Of course, I also want to thank Prof. Benedikt Grothe for accepting me as a PhD student in his lab. I know you have a tight schedule by definition, nevertheless, proof-reading my manuscript and helpful advice on the first version happened within no time. Thank you for that! By the way, without your lab, I possibly wouldn’t be married yet.

I would like to thank the further members of my TAC, Prof. Christian Leibold and Dr. Valentin Stein, for helpful comments during long data presentations.

For the nice time in Martinsried, I thank all members and former members of the numerous groups and subdivisions associated with the Grothe lab. To me, it’s all Neurobiology! In particular, I would like to thank Kiri Couchman for her native (and sometime untamable) tongue and heated discussions about the role of GABA in the brainstem. Furthermore, I am thankful for the initial introduction into SOC electrophysiology I received from Dr. Anna Magnusson. Moreover, I thank Prof. Mario Wullimann for giving me a rough overview on the evolution of hearing. I know that I stopped you! Additionally, I thank Dr. Michael Pecka who had a helping hand explaining me “the *in vivo* stuff” and Dr. Olga Alexandrova for introducing me to focal microscopy. Claudia Aerdker was extremely helpful with carrying out the immunohistochemistry and Dieter Leippert did his best to take care of our gerbils. By the way, thanks to the “Tierstallmädls”! I must not forget Dr. Sven Schörnich who pretends to refuse but in the end always fixed my computer problems.

I thank my parents for supporting me all the years and for helping me overcome some hard times.

My deepest gratitude goes to my wife Aurelia.

EHRENWÖRTLICHE ERKLÄRUNG

Hiermit versichere ich, Benjamin Haßfurth, dass die vorliegende Arbeit von mir selbstständig und nur unter Verwendung der angegebenen Hilfsmittel angefertigt wurde.

Benjamin Haßfurth

Martinsried, 27.05.2010